Mechanical Vibration Characteristics of Bell-type Pump Mountings

by

SAID ALY MOHAMED SHEBAK

B.Sc., M.Sc.

A thesis submitted for the degree

of Doctor of Philosophy

Mechanical Engineering Department

The University of Aston in Birmingham

June, 1981

supervisor

T.H. Richards

Name: Said Aly Mohamed Shebak Date: June, 1981

Title of Study: Mechanical vibration characteristics of bell-type pump mountings

Candidate for Degree of Doctor of Philosophy

Summary:

This thesis describes an analytical and experimental study to determine the mechanical characteristics of the pump mounting, bell housing type. For numerical purposes, the mount was modelled as a thin circular cylindrical shell with cutouts, stiffened with rings and stringers; the boundary conditions were considered to be either clamped-free or clamped-supporting rigid heavy mass. The theoretical study was concerned with both the static response and the free vibration characteristics of the mount. The approach was based on the Rayleigh-Ritz approximation technique using beam characteristic (axial) and trigonometric (circumferential) functions in the displacement series, in association with the Love - Timoshenko thin shell theory. Studies were carried out to determine the effect of the supported heavy mass on the static response, frequencies and mode shapes; in addition, the effects of stringers, rings and cutouts on vibration characteristics were investigated. The static and dynamic formulations were both implemented on the Hewlett Packard 9845 computer. The experimental study was conducted to evaluate the results of the natural frequencies and mode shapes, predicted numerically. In the experimental part, a digital computer was used as an experiment controller, which allowed accurate and quick results.

The following observations were made:

1. Good agreements were obtained with the results of other investigators.
2. Satisfactory agreement was achieved between the theoretical and experimental results.
3. Rings coupled the axial modal functions of the plain cylinder and tended to increase frequencies, except for the torsion modes where frequencies were reduced. Stringers coupled the circumferential modal functions and tended to decrease frequencies. The effect of rings was stronger than that of stringers.
4. Cutouts tended to reduce frequencies; in general, but this depends on the location of the cutouts; if they are near the free edge then an increase in frequencies is obtained. Cutouts coupled both axial and circumferential modal functions.
5. The supported heavy mass had similar effects to those of the rings, but in an exaggerated manner, particularly in the reduction of torsion frequencies.
6. The method of analysis was found to be a convenient analytical tool for estimating the overall behaviour of the shell with cutouts.

Proposals are offered regarding further relating work.

Key words: Pump mounting , Shells , Rayleigh-Ritz , C.A.D.

ACKNOWLEDGEMENTS

The author wishes to express his sincere appreciation and indebtedness to all who have helped in any way to make this study possible. He owes a special word of gratitude to the following:

To Mr. T.H. Richards, Reader in Mechanical Engineering, who served as my supervisor, for his instruction, advice, patient and personal guidance, encouragement and inspiration;

To Professor K. Foster, the Head of the Mechanical Engineering Department for offering the grant to perform this study and his personal interest in the progress made;

To Dr. J. Penny and Dr. R. Taylor for their help and suggestions in experimental work;

To Mr. A. Clark and Mr. A. Youssefi for their useful discussions during this research;

To the technical staff in the Mechanical Engineering Department for their help in building the experimental rig;

To Mrs. C. Taylor for her co-operation and typing of this thesis;

To my family in Egypt who gave a substantial encouragement throughout this study.

LIST OF CONTENTS

LIST OF TABLES

LIST OF FIGURES

LIST OF SYMBOLS

L	length of the cylinder
L_c	length of cutout
A	action integral
D	cylinder flexural stiffness
E	Young's modulus of elasticity
G	Modulus of rigidity
h	thickness of the shell
CCI1, CCI2	circumferential integrals of cutout
IX1 to IX5	longitudinal integrals in the shell and stringer equations
IX1c to IX5c	corresponding to IX1 to IX5, for cutout
SCF1, SCF2	Stringer circumferential functions
RLF1, RLF2	Ring longitudinal Functions
$(GJ)_{sl}$, $(GJ)_{rk}$	torsional stiffness of the lth stringer, kth ring
$I_{yy_{sl}}$, $I_{xx_{rk}}$	moment of inertia of the lth stringer, kth ring cross-sectional area about y'_s and x'_r axes, respectively
$I_{zz_{sl}}$, $I_{zz_{rk}}$	moment of inertia of the lth stringer, kth ring cross-sectional area about z' axis
$K11_{mn,\bar{m}\bar{n}}$ to $K33_{mn,\bar{m}\bar{n}}$	elements of the generalized stiffness matrix
m	integer index associated with the longitudinal factor of a term in the assumed displacement series
$\bar{m}$	same as "m", but associated with a virtual displacement
$m1$	number of dominant longitudinal half waves in a vibration mode of the shell

$M11_{mn,\bar{m}\bar{n}}$ to $M33_{mn,\bar{m}\bar{n}}$	elements of the generalized mass matrix
n	integer index associated with the circumferential factor of a term in the assumed displacement series.
$\bar{n}$	same as "n" but associated with virtual displacement
nl	number of dominant circumferential waves in a vibration mode of the shell
Nc	total number of cutouts
Nr	total number of rings
Ns	total number of stringers
R	radius of the cylinder
Rc_k	radius of the centroid of the kth ring
T	kinetic energy
u,v,w	longitudinal, circumferential and radial displacements, respectively, of the shell median surface
q_{mn}^{us}, q_{mn}^{vs}, q_{mn}^{ws}	time-dependent generalized coordinates for the symmetric mode displacements, u, v and w respectively
q_{mn}^{ua}, q_{mn}^{va}, q_{mn}^{wa}	same as "q^{us}, q^{vs}, q^{ws}" but for the antisymmetric mode
U	strain energy
x,θ,z	longitudinal, circumferential and radial coordinate system of the shell
$\grave{x},\grave{y},\grave{z}$	longitudinal, circumferential and radial coordinates of the stiffeners
$\bar{x}_{rk}$, $\bar{y}_{sl}$	x distance of the centroid of the kth ring, y distance of the centroid of the lth stringer from the z axis passing through its point of attachment to the shell surface
$\bar{z}_{sl}$, $\bar{z}_{rk}$	z distance of the centroid of the lth stringer, kth ring from the middle surface of the shell

δ	variational operator
θ_c	angle subtending the cutout
ν	Poisson's ratio
ρ	mass density
ω	circular frequency (rad/sec)
X,Y,Z	coordinate axes associated with centre of gravity of the pump
M_p	mass of the pump
l	x distance of the centre of gravity of the pump from cylinder "free" face
I_{XX_p}, I_{YY_p}, I_{ZZ_p}	pump mass moment of inertia about X,Y and Z axis respectively
e_{xx}, $e_{\theta\theta}$, $e_{x\theta}$	axial circumferential and shear strain of a shell element
σ_{xx}, $\sigma_{\theta\theta}$, $\sigma_{x\theta}$	axial, circumferential and shear stress of a shell element

Square Matrices:

$[K]$	generalized stiffness matrix
$[M]$	generalized mass matrix

Column Matrices:

$\{q\}$	vector of time-dependent generalized coordinates

Subscripts:

c	cutout if associated with shell element centroid if associated with stiffeners
k	kth ring
l	lth stringer
o	shell
r	ring
s	stringer

Superscripts:

u, v, w	associated with the shell u-displacement, v-displacement and w-displacement respectively
s, a	associated with the θ-symmetric mode, θ-antisymmetric mode, respectively
A	associated with u axial mode
R	associated with u rotation mode
T	associated with torsion mode transpose if associated with matrices.

CHAPTER ONE

INTRODUCTION

Noise may be regarded, generally, as any undesired signal, although it is usually interpreted as an unwanted type of sound. The source of noise is vibration and in mechanical systems it may imply undesirable behaviour, perhaps resulting in malfunction of machinery. In modern society, noise has also come to be regarded as a form of pollution so that there is increasing attention paid to controlling the problem.

Man has been concerned with noise since his first steps on this planet, annoyed with the noise from many sources; thus, nature itself can produce noise with very high levels such as those sound disturbances associated with waves beating on rocks, wind howling through trees, thunder in the sky or the eruption of volcanos. Besides these natural sources of noise, man himself created a lot of noise and began to pollute his surroundings when he started to manufacture his primitive tools and weapons for hunting and other purposes. But the industrial revolution heralded the start of the present noise age!

The new revolution brought about all kinds of pollution; smell, smoke, eye sores in the landscape and noise. These problems were associated with all stages of the industrial revolution from the steam engine, railway locomotives, internal combustion engine to the diesel and jet engines. All these and others add to the noise

problem, and many people are disturbed and suffer because of the problem. With more complicated built machines, the problem has grown to such an extent that noise reduction and control has become the exact science of today.

The problem of sound and vibration had a great attention from the early days of the ancient Greek scientists. Pythagoras experimented with the vibration of a stretched string, Aristotle, Euclid and Ptolemy produced some theories, but not directly relating to the physical aspect of sound. The foundations of acoustics were laid by Galileo Galilei, 2000 years after Pythagoras, but the fathers of the modern science of acoustics are usually regarded as having been Hermann Helmholtz and Lord Rayleigh who, in the later half of the 19th century, developed many fundamental theories. While Helmholtz was concerned with the theory of resonators, Rayleigh produced a more general concept in his publication, The Theory of Sound (1).

Because of the health hazards due to high noise level, people are now more concerned about the problem than previously and more researches about the subject, in general, are available in the literatures, dealing with noise sources, reduction and control (2, 3, 4, 5). The author is concerned here with the noise problem in hydraulic systems.

The higher speeds and pressures employed in modern hydraulic systems create significant problems in noise production and radiation and this at a time when legislation is becoming increasingly stringent in its objectives of controlling industrial noise levels. The

noise problem in hydraulic systems is a complicated one due to the mechanism of operation and the pump function. In operation, the pumping action and the movement of the mechanical parts inside the pump casing generate pressure pulsations in the fluid and mechanical vibrations. These vibrations give rise to movement of the pump casing, which in turn is in mechanical contact with other parts of the system, e.g. mount, valves and pipes. Some of the produced vibrations are transmitted to other parts and they, in turn, radiate noise and transmit vibration.

In general, the noise in a fluid power system is produced as mechanical vibration of the structure, known as structure borne noise (S.B.N.) and as pressure fluctuations in the fluid, known as liquid borne noise (L.B.N.). The S.B.N. and L.B.N. produce what is known as air borne noise (A.B.N.), the audible sound radiated through the surrounding medium. The airborne noise due to the liquid borne noise is discussed in (6, 7, 8). Experimental work was reported in (9) to measure the air borne noise due to the structure borne noise in the system, but no theoretical studies were mentioned.

The main object of the present work is to study the vibration characteristics of pump mountings as a first step towards the understanding of the structural borne noise of that part in the hydraulic system.

All the fluid power system components, in particular, the pump mount - which links the pump to the motor or to the foundation - have a marked influence on noise due to radiation from its surface brought about by structural vibration transmission from

the pump and other components and also the part transmitted to the motor casing. Due to its compact construction, the pump itself is not a strong radiator of noise even though it is a powerful generator.

Also the pump mount, especially of the flanged bell housing type, has a strong influence on the noise that radiates from the pump casing. That is because it alters the effective stiffness and mass of the casing. This effect could be minimized if there were a substantial mis-match of the mechanical impedance between the case and the mount, which results in reducing the energy flow between the pump and its mount.

The techniques used to reduce noise in the hydraulic systems can be classified as:-

1. Reduction of noise at sources (pump construction, valves)
2. Interrupt the transmission path with damping and isolating materials.
3. Reduce the fluid borne vibration by damping out the pressure ripple with an acoustic silencer.
4. Interrupt the pipe transmission paths with flexible hose.
5. Acoustic cladding (masking).

The problem under investigation here, namely the reduction of the effect of the mounting, may suggest that technique 2 is suitable to be used in order to isolate the pump generated noise. In practice however, the bell housing is bolted onto a motor and the pump is bolted to the bell housing, usually, or preferably, rigidly connected to minimise the misalignment due to the over hung weight and torque deflection. Unfortunately using an isolating material might increase

the possibility of misalignment. In addition, the properties of the isolator material are highly affected by temperature variations and the other environmental operating conditions, hydraulic fluids, hydrocarbons, ozone...etc. Furthermore, it is difficult to be sure of a complete metal to metal isolation, especially in awkward places. The high expenses of the isolator materials add to these disadvantages.

With these facts in mind, the noise problems associated with the bell housing can be controlled by reducing its response to the exciting forces. So far, the pump mount should be designed to minimise its influence on the whole system generated noise by:-

1. Reducing the mount capability for radiating noise.
2. Reducing its capability for transmitting mechanical vibrations between the various parts it connects.

These goals can be achieved through the following considerations:-

1. Mount to have the minimum dimensions necessary to support the pump adequately.
2. Mount natural frequencies to be well removed - if possible - from the forcing frequencies imposed upon it, to reduce the possibility of exciting the mount at its own natural modes of vibrations (i.e. prevent or reduce the resonance effects).

Since the natural frequencies of any structure are functions of its material constants, relative dimensions and the geometric arrangement of its built up components, these facts provide numerous parameters to be tested from the vibration point of view.

The type of the pump mounting investigated here is the bell housing one. In its most complex geometrical shape, the bell housing mount consists of a cylindrical thin wall shell stiffened with longitudinal stringers (ribs), circular flanges and containing some cutouts to observe and allow the coupling of the driving shaft. The main objective of this thesis is to present analytical and experimental methods for determining the mechanical characteristics of the pump mounting - bell housing type. In a more precise way, to provide a comprehensive technique to study both the static and dynamic characteristics of such components and so assist in their design. This main objective is achieved through the following sub-objectives:-

1. To develop a mathematical model of the bell housing mount to determine the elements of the mechanical problems, namely the stiffness and force matrices for the static part and the stiffness and mass matrices for the free vibration (dynamic part).
2. To develop a computer program to generate the elements based on the theory developed.
3. To solve the formulated problem:

   a) Equations of equilibrium in the static case.

   b) Eigen value problem in the dynamic case.

   in order to obtain the stress distribution forms and also the natural frequencies with their associated mode shapes.
4. To build a test rig to study experimentally the vibration behaviour of the model.

5. To test the theoretical method against other methods available in the literature.
6. To compare the experimental test results with the predicted computational results.
7. To study the effects,on the frequencies and mode shapes, of varying parameters such as size and locations of cutouts, the supported pump inertia...etc.

In chapter two, a survey of the literature on the vibration of stiffened or unstiffened cylindrical shells is given with an indication of its deficiencies in relation to the present problem. Chapter three is concerned with the developed theory which will handle the actual model with a variety of conditions. Chapter four is a description of the computer program built up, the required input data, generation of mass, stiffness and force matric es, solution of the problem and finally the output formats. In chapter five, a description of the experimental test rig is given, test procedures are explained, with the associated precautions to be considered for instrumentation arrangements and measurement technique. Chapter six is concerned with the results.

First the predictions of the presently developed model are compared with known related results; such tests were required to ascertain that the modelling and associated rather elaborate computer programs were functioning. Next, the influence of varying relevant system parameters is reported. Finally the computer predictions were compared with experimental data produced in the tests carried out. Chapter seven

presents the conclusions and suggestions for further investigations. If the mathematical expressions of the theoretical part are interrupting the flow of the theory, then such expressions are presented in the relevant Appendices.

CHAPTER TWO

REVIEW OF LITERATURE RELATING TO SHELL DYNAMICS

2.1 Introduction

Geometrically, the bell housing pump mounting is essentially a cylindrical shell stiffened with longitudinal stringers (ribs), two end ring flanges and, perhaps, some intermediate ring stiffeners. To provide access to the driving shaft and coupling, there may be one or more cutouts. This configuration represents the utmost complications that may occur in a bell housing mount, it could be found in a more simplified form.

In view of this described geometry, it was decided that this class of pump mountings would be modelled as a thin walled stringer-ring reinforced cylindrical shell in which one or more cutouts may be present. Although this represents a significant simplification compared with treating the mounting as a three dimensional object, the static and dynamic problems are still extremely complicated so that some approximation techniques are required to effect a solution. In this chapter, we discuss some of the approaches which have previously been applied to this type of problem.

2.2 Approximation Methods

It has been pointed out that the model under investigation is quite complex structure, so some approximate technique should be called in to find the stress levels and the vibration characteristics associated with it.

The approximate techniques are used either to formulate the elasticity partial differential equations in an approximate manner, then solving the set of resultant equations in exact form, or solving the exact partial differential equations in an approximate manner. In other words, methods of approximations in general, may be classified into two categories:-

(i) Approximate treatment of an exact differential equations set, such as finite difference method.

(ii) Exact treatment of an approximate system, such as Rayleigh-Ritz and finite element methods.

In the finite difference method, the set of governing differential equations, as well as the equations defining the boundary conditions are replaced by the corresponding finite difference equations. This, then, reduces the problem to a set of simultaneous algebraic equations. The accuracy of the method depends upon the size of the intervals, or the mesh size. The finer mesh increases the accuracy, but on the other hand, the resulting equations are increased and hence the amount of work required for solution increased materially, with higher round off errors.

In the second group of methods, which are called energy or variational methods, the governing differential equations of an elasticity problem can be obtained as a direct consequence of the minimisation of a certain energy expression. Instead of solving the differential equations, we may therefore seek a solution which will minimise the energy expression and may thereby avoid the mathematical difficulty in the solution of such partial differential equations.

In the case of static problems, the starting point may be taken to be the potential energy principle. Here with the aid of the assumed displacement pattern, we may proceed to the classical Rayleigh-Ritz and other methods, or more recently developed finite element method. Indeed the latter technique may be viewed as a piecewise Ritz method. The significant factor is that such methods generate the static equilibrium equations in the form

$$[K] \{q\} = \{Q\} \qquad 2.1.$$

In the case of free vibration, the starting point is the Hamilton's principle, which in turn, gives the linear eigen value problem in the form

$$([K] - \lambda [M]) \{q\} = \{0\} \qquad 2.2.$$

The detailed contents of $[K]$ and $[M]$ depends on which particular method and displacement model is assumed, but in any case, use of computer is essential.

The Rayleigh-Ritz method may be carried out as follows: First assume the solution in the form of a series which satisfies the boundary conditions, but with undetermined parameters, q_i. Second, insert these functions into the expression of the potential energy in static case, or the potential and kinetic energies in the dynamic case, and carry out any required integration. The resulting expressions are functions of the undetermined parameters, q_i, where i = 1, 2.., n. Since the potential energy must be minimum at equilibrium, in the static case, the q's can be determined from the minimising conditions:

$$\frac{\partial \Pi}{\partial q_i} = 0 \qquad i = 1, 2.., n \qquad 2.3.$$

where Π is the total potential energy of the system, including the strain energy of the deformed body, and the potential energy of the external forces. With some mathematical manipulations, equation 2.3 takes the form 2.1, from which the values of q's may be found. Substituting these values of q's into the assumed form of the functions, we have an approximate solution of the given problem. The accuracy of the solution improves when more undetermined parameters are taken. One way to get an idea of the accuracy of the solution is to solve the problem by successively taking more q's and comparing the final results.

If the results converge rapidly, then we may conclude that the approximation is good. The same process is performed in the dynamic case, which in turn yields the eigen value problem in the form 2.2.

In the finite element technique, the solid body is imagined as divided into a finite number of elements, connected with each other through nodal points. Within each element, the distribution of the displacements are assumed in a suitable form with some associated parameter, which may be identified with nodal values of the wanted displacement functions and their derivatives. Then, on the basis of these assumed displacements, the strain and kinetic energies of an element may be computed in a similar manner as previously discussed in Rayleigh-Ritz method. Summation over all the elements yield the total energies of the whole structure. In the static case, the actions of the applied loads are taken into account. The overall assembled structure yields the equations of equilibrium in the form 2.1 for the static case, or the eigen value problem in the form 2.2 for free vibration case. The accuracy of the technique can be improved by using a more fine mesh, but the preparation of the input data for the computer solution is indeed a tedious and time consuming job, and also the round off errors associated with large size matrix manipulations always occurred. Further, if a new kind of finite element is to be developed to achieve more convergence, one has to reformulate the whole mass and stiffness properties of the new element. But from the designers point of view, a desirable analysis technique is that which gives an adequate solution with the greatest ease. In the context of the present work, the finite difference approach result in large round off errors and large computer storage. Also the

finite element approach requires a substantial amount of data preparation for each candidate design solution considered: in contrast this is far simpler for a Rayleigh-Ritz approach. As will be seen later, this does not imply that the development of a computer program is a simple task in the Ritz case, but, then the user is not concerned with such details. A comprehensive account of the energy method is given by Richards in reference (10).

2.3 Historical literature survey on shell vibration

A thin shell is a three dimensional body which is bounded by two closely spaced curved surfaces, the distance between the surfaces being small in comparison with the other dimensions. As a construction element, the thin shell has been used since the time of the ancient Greeks, who used shells as part of their architecture. One of the main reasons of using shells rather than the plates (which are considered as a special limiting case of shells, having no curvatures) is that while the plate can support the lateral load by the action of bending and twisting moments - except for large deflexions - a shell supports the applied load by in-plane (membrane stresses) as well as bending and twisting stresses. This difference in properties makes a shell much stiffer and more economical structure than a plate under the same conditions. The penalty for this advantage in application is that the theory of the shell behaviour is far more complicated than that for plates.

In the case of plate problems, for small deflections, the actions of the bending and membrane stresses are uncoupled, resulting, in separate bending and membrane theories. In the former case, the governing partial differential equation, in the cartezian co-ordinates x, y (12) is

$$\frac{\partial^4 w}{\partial x^4} + 2 \frac{\partial^4 w}{\partial x^2 \partial y^2} + \frac{\partial^4 w}{\partial y^4} = q/D \qquad 2.4$$

where w is the lateral deflection

q is load density (load/area)

D is plate flexural rigidity $= \frac{Eh^3}{12(1-\nu^2)}$

In the second theory - plane stress situation, (13) - the governing partial differential equation in the x-y co-ordinates is

$$\frac{\partial^4 \Phi}{\partial x^4} + 2 \frac{\partial^4 \Phi}{\partial x^2 \partial y^2} + \frac{\partial^4 \Phi}{\partial y^4} = 0 \qquad 2.5$$

where Φ is the stress function, defined to satisfy:

$$\sigma_{xx} = \frac{\partial^2 \Phi}{\partial y^2} \qquad 2.6.a$$

$$\sigma_{yy} = \frac{\partial^2 \Phi}{\partial x^2} \qquad 2.6.b$$

$$\sigma_{xy} = -\frac{\partial^2 \Phi}{\partial x \partial y} \qquad 2.6.c$$

in the absence of the body forces.

All academics agree on these forms of the classical fourth order partial differential equations in the case of plates. Such agreement does not exist in the shell theory. Thus because of the combination of both bending and membrane actions, the classical theory of shells is governed by an eighth order system of governing partial differential equations. Numerous different shell theories have been derived and used, differences being due to various basic assumptions about shell behaviour, particularly the strain-displacement relations. Therefore, if analytical results for stresses or frequencies of a given shell are presented, the corresponding shell theory used in the analysis must be specified.

Modern theoretical and experimental studies on thin shells began in the 1820's, in order to solve the problems associated with shell applications in pressure vessels, piping, roof building...etc. Since starting to investigate the problems associated with shells, about 5000 papers, (14) have been published. Also, reference (14) gives an approximate expression for the number of papers published each year as an exponential function of the form

$$N = e^{0.074\, n} - 1 \qquad 2.7$$

where N = number of papers produced in the nth year

n = number of years taken from an arbitrary origin of 1886.

Since the author is concerned with shell vibration, the next section will deal with some of the fundamental theories associated with his purpose.

2.3.1 Notes on the fundamental theories of shell vibration

The main purpose of this section is briefly to review some of the fundamental theories used to describe shell vibrations, particularly the thin cylindrical shell, which is considered to be appropriate idealisation of the pump bell housing mount. All the following theories derive from Love's postulates. The following assumptions were made by Love (15).

1. The thickness of the shell is small compared with the other dimensions.
2. Strains and displacements are sufficiently small so that the higher order magnitudes in the strain-displacement relations, except the first order, may be neglected.
3. The transverse normal stress is small in comparison with the other two normal stresses and may be neglected.
4. The normals to the undeformed middle surface remain straight and normal to the deformed middle surface and suffer no extension (Kirchhoff's hypothesis)

These approximations are universally accepted by others to develop their own shell theories. No attempt will be made to derive these theories in detail, but they can be found in the relevant references.

The earliest study on the vibration of cylindrical circular shells was made by Rayleigh (1); he investigated both the extensional and in-extensional vibration. For the first category, he deduced the frequency equation:

$$\omega^4 - \omega^2 \frac{E}{\rho(1-\nu^2)} \left(\frac{1}{a^2} + \frac{n\pi^2}{l^2}\right) + \frac{E^2 n^2 \pi^2}{\rho^2 (1-\nu^2) a^2 l^2} = 0 \qquad 2.8$$

where ω is the angular frequency, n is the circumferential wave number, a is the radius of the middle surface, l is the half length of the cylinder. If the length is large with respect to the radius, one can distinguish between two types of vibration: almost purely radial motion with frequency:

$$\omega^2 = \frac{E}{\rho(1-\nu^2)a^2} \qquad 2.9.a$$

and almost purely longitudinal motion with frequency:

$$\omega^2 = \frac{n^2 E \pi^2}{\rho l^2} \qquad 2.9.b$$

For the second category, he derived the following equation:

$$\omega^2 = \frac{Eh^2}{12\rho(1-\nu^2)a^4} \frac{n^2(n^2-1)^2}{n^2+1} \frac{1 + 6(1-\nu)a^2/n^2 l^2}{1 + 3a^2/n^2(n^2+1) l^2} \qquad 2.10$$

for the natural frequency.

It has been pointed out by Love (15) that the inextensional displacements, used by Rayleigh, fail to satisfy the equations of motion and the boundary conditions, and in general, these results are only approximate, because the bending stiffness had been neglected in the extensional motion.

Donnell and Mushtari, (16, 17), developed a more advanced theory. They derived the following equations of motion

$$\begin{bmatrix} \frac{\partial^2}{\partial s^2} + \frac{(1-\nu)}{2}\frac{\partial^2}{\partial \theta^2} - \frac{\gamma^2\partial^2}{\partial t^2} & \frac{1+\nu}{2}\frac{\partial^2}{\partial s \partial \theta} & \frac{\nu\partial}{\partial s} \\ \frac{1+\nu}{2}\frac{\partial^2}{\partial s \partial \theta} & \frac{1-\nu}{2}\frac{\partial^2}{\partial s^2} + \frac{\partial^2}{\partial \theta^2} - \frac{\gamma^2\partial^2}{\partial t^2} & \frac{\partial}{\partial \theta} \\ \frac{\nu\partial}{\partial s} & \frac{\partial}{\partial \theta} & 1+k\nabla^4+\frac{\gamma^2\partial^2}{\partial t^2} \end{bmatrix} \begin{Bmatrix} u \\ v \\ w \end{Bmatrix}$$

$$= \{0\} \qquad 2.11$$

where $\gamma^2 = \frac{\rho(1-\nu^2)R^2}{E}$, $k = \frac{h^2}{12R^2}$, $\nabla^2 = \frac{\partial^2}{\partial s^2} + \frac{\partial^2}{\partial \theta^2}$

and $s = \frac{x}{R}$

Equations 2.11 imply neglect of the effect of the tangential displacements (u and v), and their derivatives on the midsurface changes in curvatures and twist. They are accurate as far as the factor k is small.

Love (15) and Timoshenko (13), in their formulations, retained the tangential displacements and their derivatives, but neglected the terms in z/R in the strain-displacement relations. Their equations of motion are similar to those in 2.11, with addition of the following term to the left hand side of 2.11:

$$k \begin{bmatrix} 0 & 0 & 0 \\ 0 & (1-\nu)\frac{\partial^2}{\partial s^2} + \frac{\partial^2}{\partial \theta^2} & -\frac{\partial^3}{\partial s^2 \partial \theta} - \frac{\partial^3}{\partial \theta^3} \\ 0 & -(2-\nu)\frac{\partial^3}{\partial s^2 \partial \theta} - \frac{\partial^3}{\partial \theta^3} & 0 \end{bmatrix} \begin{Bmatrix} u \\ v \\ w \end{Bmatrix}$$

Flügge (18) and Novozhilov (19) used similar strain-displacement relations, but by keeping a higher order of z/R terms, they obtained different force and moment resultant expressions; these differences were reflected in the corresponding equations of motion. In the case of Flügge's theory, the following terms should be added to the left hand side of 2.11:

$$k\begin{bmatrix} \frac{1-\nu}{2}\frac{\partial^2}{\partial\theta^2} & 0 & -\frac{\partial^3}{\partial s^3}+\frac{(1-\nu)}{2}\frac{\partial^3}{\partial s\partial\theta^2} \\ 0 & \frac{3(1-\nu)}{2}\frac{\partial^2}{\partial s^2} & -\frac{(3-\nu)}{2}\frac{\partial^3}{\partial s^2\partial\theta} \\ -\frac{\partial^3}{\partial s^3}+\frac{(1-\nu)}{2}\frac{\partial^3}{\partial s\partial\theta^2} & -\frac{(3-\nu)}{2}\frac{\partial^3}{\partial s^2\partial\theta} & 1+2\frac{\partial^2}{\partial\theta^2} \end{bmatrix}\begin{Bmatrix} u \\ v \\ w \end{Bmatrix}$$

The corresponding expression due to the Novozhilov theory takes the form

$$k\begin{bmatrix} 0 & 0 & 0 \\ 0 & 2(1-\nu)\frac{\partial^2}{\partial s^2}+\frac{\partial^2}{\partial\theta^2} & -(2-\nu)\frac{\partial^3}{\partial s^2\partial\theta}-\frac{\partial^3}{\partial\theta^3} \\ 0 & -2(1-\nu)\frac{\partial^3}{\partial s^2\partial\theta}-\frac{\partial^3}{\partial\theta^3} & 0 \end{bmatrix}\begin{Bmatrix} u \\ v \\ w \end{Bmatrix}$$

In the Sander's theory (20) - sometimes described as the "exact" theory - the strain-displacement relations were developed from the principle of virtual work. Sanders approach led to the addition of the following term to the equation 2.11

$$k \begin{bmatrix} \frac{(1-\nu)}{8}\frac{\partial^2}{\partial\theta^2} & \frac{-3(1-\nu)}{8}\frac{\partial^2}{\partial s\partial\theta} & \frac{(1-\nu)}{2}\frac{\partial^3}{\partial s\partial\theta^2} \\ \frac{-3(1-\nu)}{8}\frac{\partial^2}{\partial s\partial\theta} & \frac{9(1-\nu)}{8}\frac{\partial^2}{\partial s^2}+\frac{\partial^2}{\partial\theta^2} & -\frac{(3-\nu)}{2}\frac{\partial^3}{\partial s^2\partial\theta}-\frac{\partial^3}{\partial\theta^3} \\ \frac{(1-\nu)}{2}\frac{\partial^3}{\partial s\partial\theta^2} & -\frac{(3-\nu)}{2}\frac{\partial^3}{\partial s^2\partial\theta}-\frac{\partial^3}{\partial\theta^3} & 0 \end{bmatrix} \begin{Bmatrix} u \\ v \\ w \end{Bmatrix}$$

A more detailed discussion of the subject can be found in (21, 22, 23).

Nevertheless, one may say that the differences in the equations arises basically from small differences in the formulation of the strain-displacement relations and the expressions for force and moment resultants. The discrepancies occur only in terms which, numerically, have little significance, as long as the limitations of thin shell theory are observed.

In many cases, the results of the various formulations are very close or even identical as demonstrated by Kadi in a very comprehensive study (24). The same conclusions were reported by Warburton (26).

2.3.2. Boundary Conditions:

The boundary conditions associated with either the equations of equilibrium in the static case, or the equations of motion in the dynamic case may be derived from the fact

that the work done by the reactions at the boundaries is zero. In the case of the cylindrical circular shell, these simple boundary conditions may be listed as follows:-

at $x = 0$ and $x = L$

either $N_x = 0$ or $u = 0$ 2.12.a

, $N_{x\theta} + \frac{M_{x\theta}}{R} = 0$ or $v = 0$ 2.12.b

, $Q_x + \frac{1}{R}\frac{\partial M_{x\theta}}{\partial \theta} = 0$ or $w = 0$ 2.12.c

and $M_x = 0$ or $\frac{\partial w}{\partial x} = 0$ 2.12.d

Since the partial differential equations governing the shell theory are of eighth order, this gives a 136 possible combinations of these simple conditions. In other words, there are 136 distinct possible classes of problems. Some of them were discussed in (25). From these 136 problems, there are 16 cases where the shell has identical boundary conditions at both ends; i.e. simply supported-simply supported, free-free, clamped-clamped...etc.

The problem of circular cylindrical shell with simply supported conditions at both ends has received the most attention in the literature; this is due to the fact that a simple form of solution to the eighth order differential equations can

satisfy these boundary conditions exactly. Next to the simply supported end conditions, the problems with identical boundary conditions at both ends, in general, have received a reasonable attention. This is because in the case of identical boundary conditions, the problem can split up into two: concerned with the modes symmetric and antisymmetric with respect to the middle section of the shell. Separately, each yields a fourth order characteristic determinant instead of the original eighth order one. Unfortunately, few papers are available, concerning cylinders with different boundary conditions at the two ends, from which the clamped-free case is chosen to idealise the problem under consideration, in the intermediate analysis stage.

Forsberg (27) gave a method for determination of the natural frequencies of a cylindrical shell with any prescribed end conditions. Instead of using the usual procedure of finding the natural frequency for a shell of given length, Forsberg, starting from the equations of motion, reversed the process, i.e. first he assumed the natural frequency, then the equivalent length of the shell can be found exactly for these prescribed natural frequency and boundary conditions. Doing such process for many frequencies, the corresponding lengths may be calculated and a relation between frequency and length may be drawn. From such relation, the natural frequency of a shell with given length can be estimated. The solution is exact, but the computation required for the method is considerably greater than that for standard approximate methods.

2.3.3. Unstiffened clamped-free cylindrical shell

Sewall and Naumann (53) used the Rayleigh-Ritz technique with Novozhilov's theory (19) to obtain the natural frequencies of a clamped-free cylindrical shell. They reported a good agreement between the predicted results and the experimental ones. Resnick and Dugundji (28) used beam functions in their energy method with Sanders theory (20) to solve the same problem, but disagreements between theoretical and experimental results were reported, particularly for lower mode numbers. Ramamurti and Pattabiramm (29) and Ucmaklioglu (47) used the finite element method to study the problem, and comparisons of their results with other simpler methods showed small discrepancies. Sharma and Johns (49, 52) presented extensive numerical results, using the Rayleigh-Ritz technique in conjunction with the Flügge theory. But imposing the conditions of zero hoop and shear strain in the median plane limited the application of their method to a quite high length to radius ratio, as in the case of tall slender chimney stacks.

2.3.4. Stiffened Cylindrical shell

The vibration problem of stiffened cylindrical shells has been studied in the aero-space field. In general, the stiffeners were treated either by averaging their properties over the shell surface or treating them as discrete elements. In the former "smearing" technique, the orthotropic circular cylindrical shell equations were used. The method gives a good result if the stiffening elements are relatively closely

spaced. When the distance of separation is large then the structure must be represented as a combination of shell elements and stiffener elements, each having its own equation of motion, and coupled to each other through equations of continuity (compatibility).

The second technique is regarded as more general in the sense that the stiffeners may be few in number, nonuniform in shape and nonuniformly spaced.

Sewall and Naumann (53) investigated the effect of longitudinal stiffeners on the vibration of thin cylindrical shells with different end conditions, using the smearing technique. The same technique was utilized by Sewall et al (50) to study the effect of rings on the vibration of ring-stiffened cylinders.

Mikulas and McElman (30) established the equations of motion for ring-stringer stiffened cylindrical shells, using Donnell-Mushtari equations.

Egle and Sewall (31) gave an analytical method to treat the stiffeners as discrete elements, but the results they presented were only for cylinders with simply supported end conditions and longitudinal stiffeners. Forsberg (51) developed an exact solution for the equations of motion for ring-stiffened cylinders, treating rings as discrete elements. A comparison of his results and those of the present analysis are given in chapter six. A similar method was developed by Wah and Hu (32) to solve the vibration problem for ring-stiffened

cylinders, but the results given therein are only for simply supported shells. Sharma and Johns (49, 52) also treated the same problem, but once more, their solution is only accurate for tall cylinders.

Egle and Soder (54) gave an extensive study of a cylindrical shell stiffened by rings and stringers, using the discrete analysis approach with arbitrary end conditions. They used Flügge strain-displacement relations in the analysis. A comparison of their results and those of the present method is shown in chapter six. Boyd and Rao (46) solve the same problem, treating the stiffeners as discrete elements in conjunction with Flügge theory and Rayleigh-Ritz approximation technique.

2.3.5. Cylindrical shell with cutouts

The problem of vibration of shells with cutouts is of special interest. The cutout may be introduced in the structure for purposes of access and visibility - for instance as in the case of the present problem. However, the published results are indeed very limited. Pattabiraman et al (33) in their review, were concerned only with different methods of investigating the effect of static and dynamic loading on stress concentrations around holes. Brogan et al (34, 58) appear to be the first to investigate - experimentally and analytically - the effect of cutouts on the natural frequencies and mode shapes of a cylindrical shell with integral end rings. They employed the

finite difference method with up to 4200 degrees of freedom. The fundamental natural frequency decreased by less than 7% for a considerable cutout size (120 degree arc, 0.3 L span) - L is the cylinder length. The method used required a complicated difference grid and suffered from large round off errors due to the high order of the differential equations always associated with shell theory.

Mahabaliraja and Boyd (55), using the Rayleigh-Ritz technique, solved the problem in an approximate manner, but their results did not include the fixed-free boundary condition. In contradiction to the results of (34, 58), Mahabaliraja and Boyd reported a substantial reduction in the fundamental frequency, of the order of 56% compared with a complete cylinder. This reduction occurred when using two rectangular cutouts, diametrically opposed, 90 degree arc and 0.3 L span length.

Toda and Komatsu (56) reported a reduction of up to 22% in the fundamental frequency of a clamped-free cylindrical shell, with two circular holes of diameters 0.5 of the shell radius. Ramamurti and Pattabiraman (57) have shown a reduction of about 11% in the fundamental frequency for a rectangular cutout of size 120 degrees arc and 0.143 L span, compared with the complete cylinder. They employed the finite element method due to Olson and Lindberg (35), with 28 degrees of freedom per element, and of total 412 degrees of freedom for one half the length of the shell, due to symmetry of the structure, in axial direction. They used the same boundary

conditions as (34, 58). The above survey about the effect of the cutout on the fundamental frequency may be summarized in Table 2.1

Ref.	Shell parameters			Cutout configuration	Freq. change
	h/R	L/R	B.C.		
34,58	0.0055	1.28	end rings	single rectangle, 120°, 0.3 L	Drop 7%
55	0.01	2	simple supports	2 rectangles, diamet. oppos.,90°, 0.3 L	" 56%
56	0.004	3.06	clamp free	2 circular diamet. oppos.,diameter = 0.5R	" 22%
57	0.027	2.5	end rings	single rectangle, 120° 0.143 L	" 11%

where h = thickness , L = length

R = radius , B.C.= boundary condition

Table 2.1

A survey on the effect of cutouts on vibrations of cylindrical shells

The first three models of table 2.1 were manufactured from aluminium, while the fourth one was made from steel. The general conclusion from table 2.1 is that the cutouts reduce the frequencies, but the question is how much? This seems to

depend, to a certain extent, on the boundary conditions and thickness to radius ratio for a given size of the cutouts. In the present work, the latter influences were examined for the fixed-free condition only; in the proposal for further work it is suggested that the influence of boundary conditions should also be examined.

2.3.6. Clamped-supporting heavy mass shell

To the author's knowledge, the vibration problem of clamped-supporting heavy mass cylinder has not been investigated so far in the literature. Only Holmes (36) presented a simple method to study the axisymmetric vibrations of a conical shell supporting a mass. The problem is covered in a more general fashion in the present work.

2.4 Closing Remarks

The general complications associated with vibrations of the cylindrical shell have been pointed out and different relevant theories have been discussed. The problem has been widened to include stiffened as well as unstiffened shells and yet some important points are still uncovered and need more investigation or sometimes require a new modelling, particularly the cutouts effects and shells supporting heavy masses. In regard to the theories of thin shell, since the discrepancies between various theories are quite small, the Love-Timoshenko theory has been chosen as the basis for the work reported in this thesis.

CHAPTER THREE

ESSENTIAL THEORY

3.1. General:

The analysis of this study is based on the well known energy method, employing the Rayleigh-Ritz procedure. The technique can be summarized as follows:

First, the general expressions for both the kinetic and potential energy are written for the whole structure comprising the cylindrical wall shell, rings and ribs as well as the kinetic energy of the rigid supported mass, if required, in the case of the free vibration analysis, or the total potential energy of the whole system, i.e. the structure and the applied load, in the static case analysis. The mode shapes are, then, assumed as a function of the spatial coordinates, with undetermined coefficients, to satisfy the appropriate (prescribed) end conditions; i.e. to satisfy the kinematic boundary conditions, but not necessarily the kinetic one, as Meirovitch illustrated in reference (11). From the assumed displacement functions, the strain can then be re-expressed in terms of the undetermined coefficients which are the generalized coordinates for the substitute finite degree of freedom system which has thus been created.

At this stage, the energies are re-expressed as functions of the generalized coordinates, a process which

requires a significant amount of integration. Finally, applying the principle of minimum potential energy, in the static case, one may obtain the equations of equilibrium, or in the free vibration analysis, applying the Hamilton's principle on a limited time integral of the difference between the strain and kinetic energies the equations of motion of the system can be formulated. The solution in the static case gives the values of the generalized coordinates, while in the free vibration case the natural frequencies and the associated mode shapes can be found as a solution of the formulated eigen value problem.

3.2. Analysis:

The structure under investigation is modelled as a thin wall cylindrical shell fixed at one end and free or supporting a heavy rigid mass at the other, stiffened with rings (flanges) and longitudinal ribs (stringers) and with machined rectangular cutouts. A typical bell housing mount is shown in Figure 3.1.

The middle surface of the shell is taken as the reference surface. The coordinate lines x and θ are the parametric lines of the reference surface and coincide with the orthogonal lines of principal curvature - where the lines x = constant and θ = constant intersect orthogonally. The coordinate z is the outward normal to the reference surface at the point (x, θ). The location and the size of

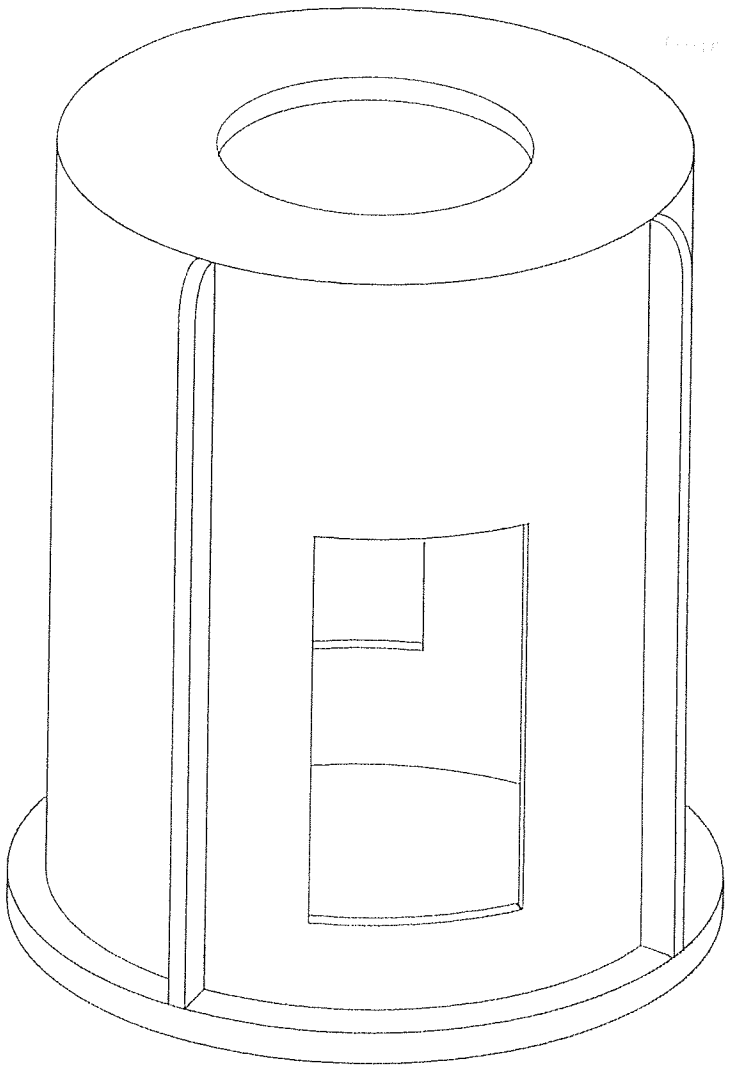

Fig. 3.1 A Typical Bell-housing

Pump Mounting

cutout are specified by the coordinates of its four corners, (x_{1i}, θ_{1i}), (x_{2i}, θ_{1i}), (x_{2i}, θ_{2i}) and (x_{1i}, θ_{2i}). The coordinate system used is illustrated in Figure 3.2. The geometries of a typical stringer and ring (both of rectangular section) as well as their local coordinate systems are shown in Figure 3.3. Although the stringers are located externally, rings may be external or internal to the shell.

3.2.1. Stiffener-shell compatibility relations:

The term "compatibility" here means the relations that signify the mode of attachment of the stiffeners to the shell in order to express the displacements of any point in the stiffener interior in terms of those of the middle surface of the shell. These relations were derived under the following assumptions:

1. The stiffeners are attached to the shell along a single line of attachment.
2. A stiffener cross section normal to the line of attachment before deformation remains normal to the line of attachment after deformation.
3. The components of rotation transferred from the shell middle surface to the stiffeners at any point of attachment are small.

In addition to that, it is also assumed that the stiffeners have a uniform shape along their length, with rectangular cross-section. The derivation of the stiffeners-shell compatibility relations are presented in Appendix A, which

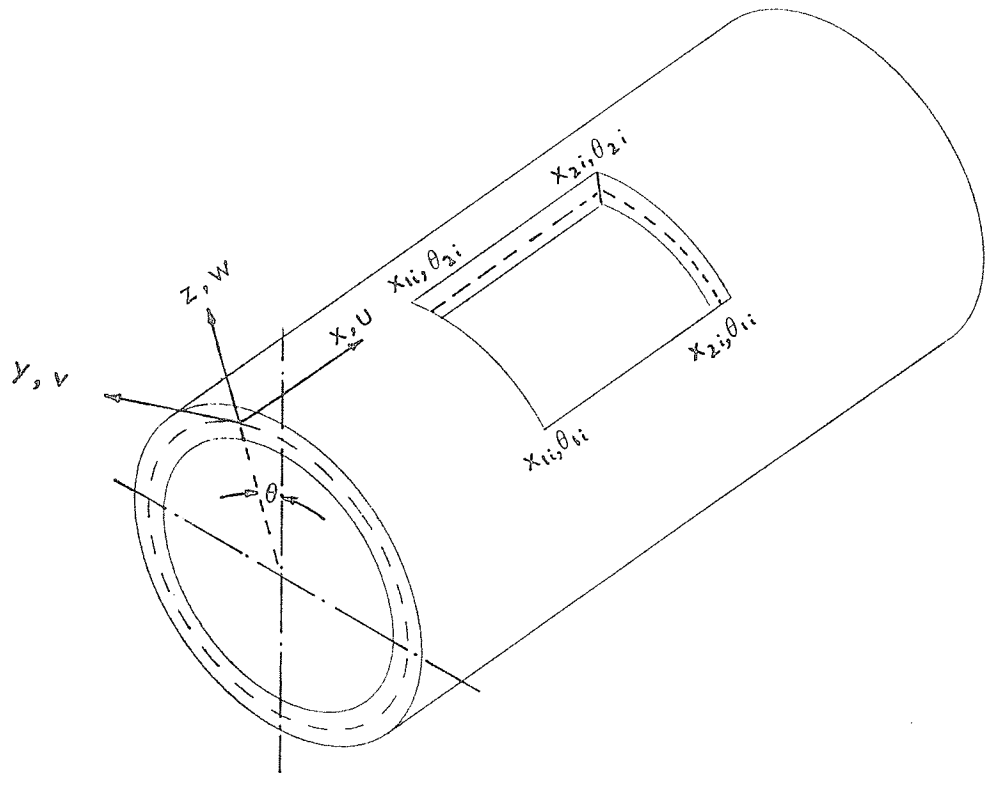

Fig. 3.2 Geometry of a Circular Cylindrical Shell

with Cutout

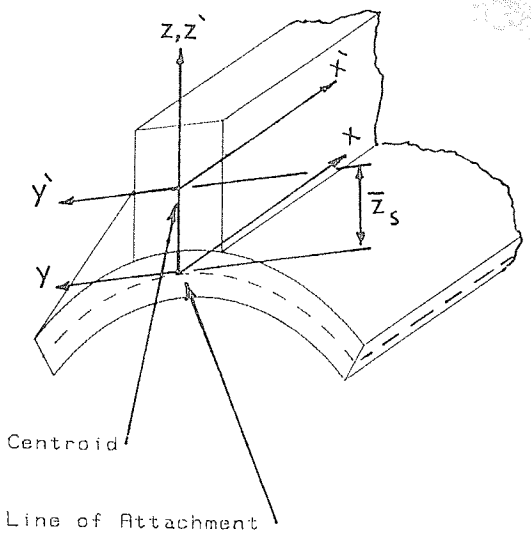

a) Stringer Coordinate System

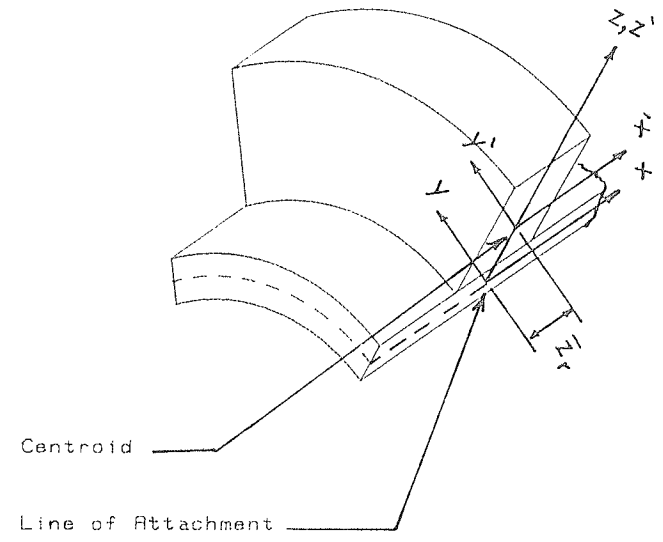

b) Ring Coordinate System

Fig. 3.3 Geometry of Typical Stringer and Ring

gives the following expressions:

3.2.1.1 Stringer-shell compatibility relations:

$$u_s = u - y'_s\, v_{,x} - (\bar{z}_s + z'_s)\, w_{,x} \qquad 3.1.a$$

$$v_s = \left(1 + \frac{\bar{z}_s + z'_s}{R}\right) v - \frac{\bar{z}_s + z'_s}{R}\, w_{,\theta} \qquad 3.1.b$$

$$w_s = -\frac{y'_s}{R}\, v + w + \frac{y'_s}{R}\, w_{,\theta} \qquad 3.1.c$$

where u, v and w refer to the displacement components of the shell middle surface, and u_s, v_s, w_s are those of the point (y'_s, z'_s) in the stringer interior.

3.2.1.2 Ring-shell compatibility relations:

$$u_r = u - (\bar{z}_r + z'_r)\, w_{,x} \qquad 3.2.a$$

$$v_r = -\frac{x'_r}{R_c}\, u_{,\theta} + \left(1 + \frac{\bar{z}_r + z'_r}{R}\right) v - \frac{(\bar{z}_r + z'_r)}{R}\, w_{,\theta} + \frac{x'_r}{R_c}\, \bar{z}_r\, w_{,x\theta} \qquad 3.2.b$$

$$w_r = w + x'_r\, w_{,x} \qquad 3.2.c$$

where u_r, v_r, and w_r are the displacement components of the point (x'_r, z'_r) in the ring interior.

3.3 Strain-displacement relations:

3.3.1 Shell strain-displacement relations:

The strain displacement relations used here are based on the assumption in Love's first approximation theory,

previously discussed in Chapter two, section 2.3. Based on those assumptions, Timoshenko (12) derived the following strain-displacement relations:

$$e_{xx} = u_{,x} - zw_{,xx} \qquad 3.3.a$$

$$e_{\theta\theta} = \frac{1}{R}(v_{,\theta} + w) + \frac{z}{R^2}(v_{,\theta} - w_{,\theta\theta}) \qquad 3.3.b$$

$$e_{x\theta} = \frac{1}{R}u_{,\theta} + v_{,x} + \frac{z}{R}(v_{,x} - 2w_{,x\theta}) \qquad 3.3.c$$

Equations 3.3 may be given the following mechanical interpretation by recasting them into another form. The terms free from the z coordinate represent the strains of the middle surface element arising from the "membrane" theory:

$$\bar{e}_{xx} = u_{,x} \qquad 3.4.a$$

$$\bar{e}_{\theta\theta} = \frac{1}{R}(v_{,\theta} + w) \qquad 3.4.b$$

$$\bar{e}_{x\theta} = \frac{1}{R}u_{,\theta} + v_{,x} \qquad 3.4.c$$

The terms multiplied by z give the change of curvatures and twist:

$$\chi_x = -w_{,xx} \qquad 3.5.a$$

$$\chi_\theta = \frac{1}{R^2}(v_{,\theta} - w_{,\theta\theta}) \qquad 3.5.b$$

$$\tau = \frac{1}{R}(v_{,x} - 2w_{,x\theta}) \qquad 3.5.c$$

3.3.2. Stiffener strain-displacement relations:

The strain-displacement relationship for the stiffeners takes into account the effect of both bending and twist deformation of the stiffeners.

3.3.2.1. Stringer strain-displacement relations:

The stringer is assumed to be subjected to normal strains and shearing strains. The extension strain for a string is given by:

$$e_{xx_s} = u_{s,x} \qquad 3.6.a$$

while the angle of twist per unit length is:

$$\tau_s = \frac{1}{R}(w_{,x\theta} - v_{,x}) \qquad 3.6.b$$

Substituting for u_s in equation 3.6.a from the stringer shell compatibility relation 3.1.a, e_{xx_s} has the forms

$$e_{xx_s} = u_{,x} - (\bar{z}_s + z'_s)\, w_{,xx} - y'_s\, v_{,xx}$$

$$= u_{,x} - \bar{z}_s\, w_{,xx} - z'_s\, w_{,xx} - y'_s\, v_{,xx} \qquad 3.7$$

Equation 3.7 shows the direct strain at the centroid of the stringer cross section,

$$\bar{e}_{xx_s} = u_{,x} - \bar{z}_s\, w_{,xx} \qquad 3.8.a$$

In addition, there are the strains due to both changes in curvature; namely, sagging curvature change:

$$\chi_{xz_s} = -w_{,xx} \qquad 3.8.b$$

and yawing curvature change

$$\chi_{xy_s} = -v_{,xx} \qquad 3.8.c$$

In the above expressions, e_{xx_s} is the normal strain of the stringer in x direction, and τ_s is the angle of twist per unit length about the x axis.

3.3.2.2. Ring strain displacement relations:

Only the normal strain in the θ direction and shearing strain due to twist of the cross-section about the θ axis are considered significant. The normal strain in this case is given by:

$$e_{\theta\theta_r} = \frac{1}{Rc}\,(v_{r,\theta} + w_r) \qquad 3.9.a$$

and the angle of twist per unit length is:

$$\tau_r = \frac{1}{Rc}\left[-\frac{u_{,\theta}}{Rc} + \left(-1 + \frac{\bar{z}_r}{Rc}\right) w_{,x\theta}\right] \qquad 3.9.b$$

where Rc is the radius of the centroidal line of the ring. Substituting for v_r and w_r in equation 3.9.a from 3.2.a, the normal strain of the ring may then be written as a function of the shell middle surface displacements as:

$$e_{\theta\theta_r} = \frac{1}{Rc}\left[\left(1 + \frac{\bar{z}_r + z'_r}{R}\right) v_{,\theta} - \left(\frac{\bar{z}_r + z'_r}{R}\right) w_{,\theta\theta} + w + x'_r\, w_{,x} - \frac{x'}{Rc}\, u_{,\theta\theta} + \frac{x'_r}{Rc}\,\bar{z}_r\, w_{,x\theta\theta}\right] \qquad 3.10.a$$

, which, again, can be split into the strain due to extension in the centroidal line, $\bar{e}_{\theta\theta_r}$, and the two changes in curvature χ_{yz_r} , χ_{yx_r}

$$\bar{e}_{\theta\theta_r} = \frac{1}{Rc}\left[\left(1 + \frac{\bar{z}_r}{R}\right) v_{,\theta} - \frac{\bar{z}_r}{R}\, w_{,\theta\theta} + w\right] \qquad 3.10.b$$

$$\chi_{yz_r} = -\frac{1}{RcR}\,(v_{,\theta} - w_{,\theta\theta}) \qquad 3.10.c$$

$$\chi_{yx_r} = -\frac{1}{Rc}\left(\frac{1}{Rc}u_{,\theta\theta} - w_{,x} - \frac{\bar{z}_r}{Rc}w_{,x_{\theta\theta}}\right) \qquad 3.10.d$$

3.4 Stress - Strain Relations:

The next step is to express the state of stress developed in the structure. The stress- strain relations are empirical ones and depend on the material of the structure. Here the linearized form, Hooke's law, is employed with the material of the structure considered to be isotropic.

3.4.1 Shell stress-strain relations:

Since the shell is considered to be thin, it is assumed that the small element is in a state of plane stress. The last assumption leads to neglect of the direct stress in z direction, σ_{zz} as well as the shearing stresses parallel to it, σ_{x_z} and σ_{θ_z} . Thus, Hooke's law in this case has the form:

$$\sigma_{xx} = \frac{E}{(1-\nu^2)}(e_{xx} + \nu\, e_{\theta\theta}) \qquad 3.11.a$$

$$\sigma_{\theta\theta} = \frac{E}{(1-\nu^2)}(e_{\theta\theta} + \nu\, e_{xx}) \qquad 3.11.b$$

$$\sigma_{x\theta} = Ge_{x\theta} = \frac{E}{2(1+\nu)}e_{x\theta} \qquad 3.11.c$$

The above relations may be expressed in terms of the displacement components and their derivatives by substituting

equations 3.3 into 3.11. Having done that and integrating through the shell thickness h, the following stress resultants can be obtained - i.e. the force or moment per unit length:

$$N_x = \frac{Eh}{(1-\nu^2)} \left[\bar{e}_{xx} + \nu \bar{e}_{\theta\theta} \right]$$

$$= \frac{Eh}{(1-\nu^2)} \left[u_{,x} + \frac{\nu}{R} (v_{,\theta} + w) \right] \qquad 3.12.a$$

$$N_\theta = \frac{Eh}{(1-\nu^2)} \left[\bar{e}_{\theta\theta} + \nu \bar{e}_{xx} \right]$$

$$= \frac{Eh}{(1-\nu^2)} \left[\frac{1}{R} (v_{,\theta} + w) + \nu u_{,x} \right] \qquad 3.12.b$$

$$N_{x\theta} = Gh \bar{e}_{x\theta}$$

$$= \frac{Eh}{2(1+\nu)} \left[\frac{1}{R} u_{,\theta} + v_{,x} \right] \qquad 3.12.c$$

$$M_x = \frac{Eh^3}{12(1-\nu^2)} \left[\chi_x + \nu \chi_\theta \right]$$

$$= \frac{Eh^3}{12(1-\nu^2)} \left[-w_{,xx} + \frac{\nu}{R^2} (v_{,\theta} - w_{,\theta\theta}) \right] \qquad 3.12.d$$

$$M_\theta = \frac{Eh^3}{12(1-\nu^2)} \left[\chi_\theta + \nu \chi_x \right]$$

$$= \frac{Eh^3}{12(1-\nu^2)} \left[\frac{1}{R^2} (v_{,\theta} - w_{,\theta\theta}) - \nu w_{,xx} \right] \qquad 3.12.e$$

$$M_{x\theta} = \frac{Gh^3}{12}\,\tau$$

$$= \frac{Eh^3}{24(1+\nu)R}\left[\, v_{,x} - 2\, w_{,x\theta}\right] \qquad 3.12.f$$

3.4.2. Stringer Stress-strain relations:

The stringer is assumed to be subjected to both extension and twisting, and this gives a normal force N_{x_s}, sagging bending moment M_{y_s}, yawing bending moment M_{z_s} and torque M_{x_s}. The expressions for these forces are:

$$N_{x_s} = E\, A_s\, \bar{e}_{xx_s} \qquad 3.13.a$$

$$M_{y_s} = E\, I_{yy_s}\, \chi_{xz_s} \qquad 3.13.b$$

$$M_{z_s} = E\, I_{zz_s}\, \chi_{xy_s} \qquad 3.13.c$$

$$M_{x_s} = (GJ)_s\, \tau_s \qquad 3.13.d$$

J_s is the torsion constant of the cross-sectional area of the stringer, given by

$$J_s = k_1\, b_s\, a_s^3 \qquad 3.14$$

where b_s and a_s are stringer depth and thickness respectively, and $b > a$. The dimensionless constant k_1 depends on the ratio b/a as given in (13).

3.4.3. Ring Stress - strain relations:

The ring is assumed to be subjected to both normal strain in θ direction, and shearing strain due to twisting. As in the case of stringer, the resultant normal force N_{y_r}, two bending moments M_{x_r}, M_{z_r} and the torque M_{y_r} on a cross-section of coordinate θ may be written as:

$$N_{y_r} = E A_r \bar{e}_{\theta\theta_r} \qquad 3.15.a$$

$$M_{x_r} = E I_{xx_r} \chi_{yz_r} \qquad 3.15.b$$

$$M_{z_r} = E I_{zz_r} \chi_{yx_r} \qquad 3.15.c$$

$$M_{y_r} = (GJ)_r \tau_r \qquad 3.15.d$$

The sign conventions of the expressions 3.12, 3.13, 3.15 are given in Figure 3.4.

3.5 Strain Energies:

3.5.1. Shell strain energy:

Provided the shell is considered to be in a state of plane stress, the strain energy per unit volume, U_e, (strain energy density) takes the form

$$U_e = \frac{1}{2} (\sigma_{xx} e_{xx} + \sigma_{\theta\theta} e_{\theta\theta} + \sigma_{x\theta} e_{x\theta}) \qquad 3.16$$

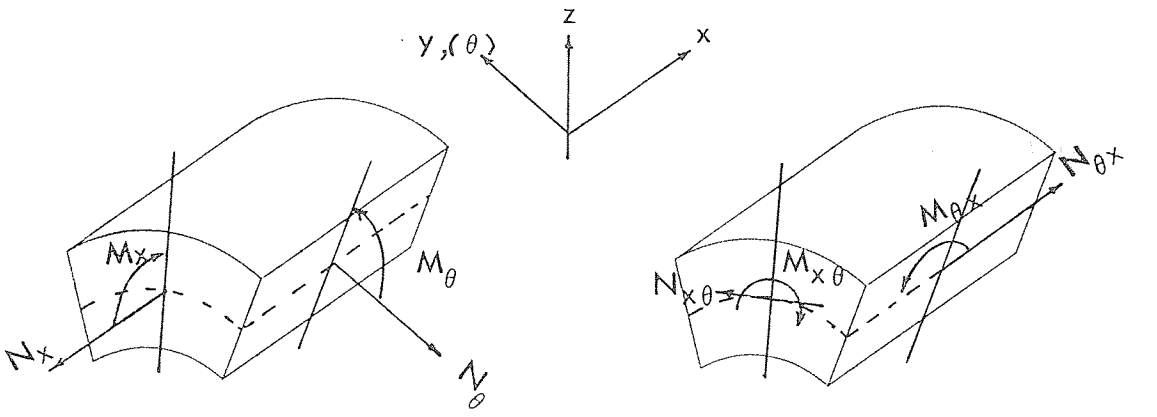

a) Shell Element

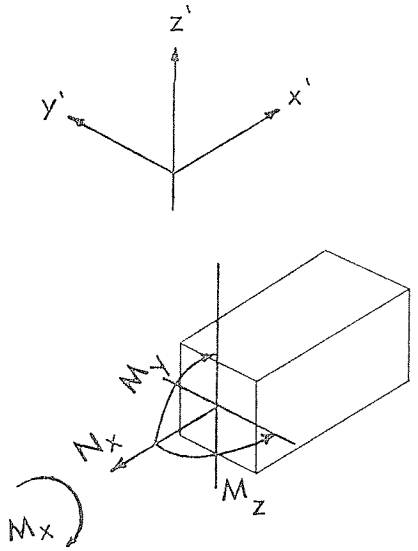

b) Stringer Element

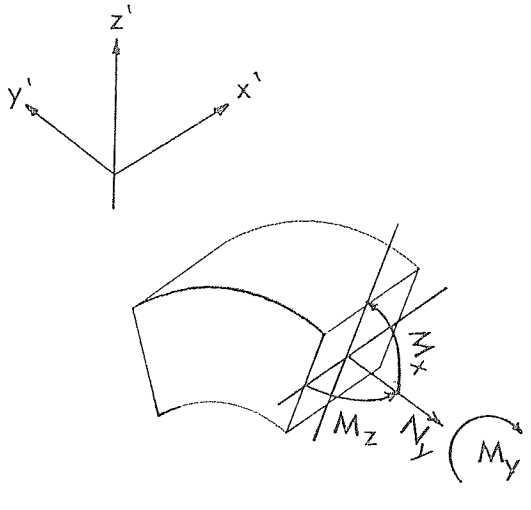

c) Ring Element

Fig. 3.4 Sign Convension of Forces and Moments

Substituting for stresses σ_{xx}, $\sigma_{\theta\theta}$, $\sigma_{x\theta}$ from equation 3.11 into 3.16 yields:

$$U_e = \frac{E}{2(1-\nu^2)}\left[e_{xx}^2 + e_{\theta\theta}^2 + 2\nu e_{xx}\, e_{\theta\theta} + \frac{(1-\nu)}{2}\, e_{x\theta}^2 \right] \qquad 3.17$$

The strain-displacement relations of the shell, 3.3 are then used to give the strain energy density in terms of the displacements u, v, w of the middle surface and their derivatives.

The total strain energy of the whole shell is found by integrating the resultant expression over the entire volume of the shell. Having done that, the total strain energy of the shell, U_o is, then, expressed as:

$$U_o = \frac{EhR}{2(1-\nu^2)} \int_0^{2\pi} \int_0^{L} \Big\{ u_{,x}^2 + \frac{1}{R^2}(v_{,\theta} + w)^2 + \frac{2\nu}{R} u_{,x}(v_{,\theta} + w)$$

$$+ \frac{(1-\nu)}{2}\left(\frac{1}{R} u_{,\theta} + v_{,x}\right)^2 + \frac{h^2}{12}\Big[w_{,xx}^2 + \frac{1}{R^4}(v_{,\theta} - w_{,\theta\theta})^2$$

$$+ \frac{2\nu}{R^2} w_{,xx}(w_{,\theta\theta} - v_{,\theta}) + \frac{2(1-\nu)}{R^2}(v_{,x} - 2w_{,x\theta})^2 \Big] \Big\} dx d\theta \qquad 3.18$$

The expression 3.18 presents the strain energy due to the extensional - membrane - deformation, (the terms including h), and that due to inextensional, or bending, deformation, the terms including h^3.

3.5.2 Stringer strain energy:

The strain energy stored in a stringer is due to extension and twisting deformation; it can be expressed as:

$$U_s = \frac{1}{2}\int_0^L (N_{x_s}\,\bar{e}_{xx_s} + M_{y_s}\,\chi_{xz_s} + M_{z_s}\,\chi_{xy_s} + M_{x_s}\,\tau_s)\Big|_{\theta=\theta_s} dx \qquad 3.19$$

Substituting for N_{x_s}, M_{y_s}, M_{z_s} and M_{x_s} from 3.13 into 3.19 and then for $\bar{e}_{xx_s}$, χ_{xz_s}, χ_{xy_s} and τ_s from 3.6, 3.8 into the resultant equation, the strain energy contribution of a stringer has the form:

$$U_s = \frac{1}{2}\int_0^L (EA_s(u_{,x} - \bar{z}_s w_{,xx})^2 + EI_{yy_s} w_{,xx}^2 + EI_{zz_s} v_{,xx}^2 + \frac{GJ_s}{R^2}(w_{,x\theta} - v_{,x})^2)\Big|_{\theta=\theta_s} dx \qquad 3.20$$

where θ_s is the circumferential location of sth stringer.

3.5.3. Ring Strain energy:

The strain energy of a ring can be expressed as:

$$U_r = \frac{1}{2}\int_0^{2\pi} (N_{y_r}\,\bar{e}_{\theta\theta_r} + M_{x_r}\,\chi_{yz_r} + M_{z_r}\,\chi_{yx_r} + M_{y_r}\,\tau_r)\Big|_{x=x_r} Rc\, d\theta \qquad 3.21$$

Substituting for N_{y_r}, M_{x_r}, M_{z_r} and M_{y_r} from 3.15 into 3.21

and then for $\bar{e}_{\theta\theta_r}$, χ_{yz_r}, χ_{yx_r} and τ_r from 3.9,3.10 into the resulting equation the strain energy expressed as a function of u, v, w and their derivatives becomes:

$$U_r = \frac{1}{2} \int_0^{2\pi} \left\{ \frac{EA_r}{Rc^2} \left[\left(1 + \frac{\bar{z}_r}{R}\right) v_{,\theta} - \frac{\bar{z}_r}{R} w_{,\theta\theta} + w \right]^2 + \right.$$

$$\frac{EI_{xx_r}}{R^2Rc^2} \left[v_{,\theta} - w_{,\theta\theta} \right]^2 + \frac{EI_{zz_r}}{Rc^2} \left[\frac{u_{,\theta\theta}}{Rc} - w_{,x} - \frac{z_r}{Rc} w_{,x\theta\theta} \right]^2$$

$$\left. + \frac{GJ_r}{R_c^2} \left[\frac{-u_{,\theta}}{R_c} + \left(-1 + \frac{z_r}{R_c}\right) w_{,x\theta} \right]^2 \right\} R_c \Big|_{x=x_r} d\theta \qquad 3.22$$

where x_r is the axial location of r^{th} ring.

For subsequent manipulation in formulating stiffness matricies, it is convenient to expand equations 3.20 and 3.22. Details of this are given in Appendix B.

3.6 Kinetic Energies:

In the following expressions for the system kinetic energy, the rotary inertia contribution of the thin wall shell is neglected, while the same effects for stringers and rings are taken into account.

3.6.1. Shell kinetic energy:

Neglecting the contribution of rotary inertia, the shell kinetic energy may be written as:

$$T_o = \frac{1}{2}\rho Rh \int_0^L \int_0^{2\pi} (\dot{u}^2 + \dot{v}^2 + \dot{w}^2)\, d\theta\, dx \qquad 3.23$$

where ρ is the mass density of the shell material, and the dot refers to the derivative with respect to time.

3.6.2. Stringer kinetic energy:

The kinetic energy of a stringer is:

$$T_s = \frac{1}{2}\rho \int_0^L \int_{area} (\dot{u}_s^2 + \dot{v}_s^2 + \dot{w}_s^2)\, d(area).\, dx \qquad 3.24$$

Substituting for u_s, v_s and w_s from 3.1 into 3.24, the stringer kinetic energy takes the form:

$$T_s = \frac{1}{2}\rho \int_0^L \Big\{ A_s (\dot{u}^2 + \dot{v}^2 + \dot{w}^2) - 2\bar{z}_s A_s \Big[\dot{u}\, \dot{w}_{,x} + \dot{v}\, \frac{(\dot{w}_{,\theta} - \dot{v})}{R} \Big] + I_{zz_s} \Big[\dot{v}_{,x}^2 + \frac{(\dot{w}_{,\theta} - \dot{v})^2}{R} \Big] + (\bar{z}_s^2 A_s + I_{yy_s}) \Big[\dot{w}_{,x}^2 + \frac{(\dot{w}_{,\theta} - \dot{v})^2}{R} \Big] \Big\}_{\theta=\theta_s} dx \qquad 3.25$$

Note that equation 3.25 includes both the translation and rotary inertia effects.

3.6.3. Ring kinetic energy:

The kinetic energy of a ring is:

$$T_r = \frac{1}{2}\rho \int_0^{2\pi} \int_{area} (\dot{u}_r^2 + \dot{v}_r^2 + \dot{w}_r^2)\, d(area)\, Rc\, d\theta \qquad 3.26$$

Substituting for u_r, v_r and w_r from equation 3.2 into 3.26, and integrating over the ring area cross section, the kinetic energy of a ring has the form:

$$T_r = \frac{1}{2}\int_0^{2\pi} \Big\{ A_r (\dot{u}^2 + \dot{v}^2 + \dot{w}^2) - 2\bar{z}_r A_r \left(\dot{u}\,\dot{w}_{,x} - \frac{\dot{v}^2}{R} + \frac{\dot{v}\,\dot{w}_{,\theta}}{R}\right)$$

$$+ (\bar{z}_r^2 A_r + I_{xx_r}) \left(\dot{w}_{,x}^2 + \frac{\dot{v}^2}{R^2} - \frac{2\dot{v}\dot{w}_{,\theta}}{R^2} + \frac{\dot{w}_{,\theta}^2}{R^2}\right)$$

$$+ I_{zz_r}\left[\frac{\dot{u}_{,\theta}^2}{R^2} + \frac{\bar{z}_r^2}{R^2}\dot{w}_{,x\theta}^2 - \frac{2\bar{z}_r}{R^2}\dot{u}_{,\theta}\,\dot{w}_{,x\theta} + \dot{w}_{,x}^2\right]\Big\} \Big|_{x = x_r} Rc\, d\theta \qquad 3.27$$

Again, one might note that expression 3.27 includes both the translation and rotation kinetic energies of the ring.

3.6.4. Pump kinetic energy:

It is assumed that the pump is a rigid body with a relatively heavy mass, attached rigidly to the "free" end of the cylindrical shell. As a rigid body, the pump has 6 degrees of freedom, three translations of the centre of gravity (C.G.) of the pump in the X, Y and Z directions, and three rotations about the X, Y and Z axes. The three C.G. translations denoted by U_{CG}, V_{CG} and W_{CG} respectively, while the three rotations denoted by Φ_X, Φ_Y and Φ_Z.

The relations governing these displacements and rotations to the displacements of the "free" end of the mounting may be written as:

$$U_{CG} = u^{As} \qquad 3.28.a$$

$$V_{CG} = v^{a} + \frac{lu^{a}}{R} \qquad 3.28.b$$

$$W_{CG} = w^{s} + \frac{lu^{Rs}}{R} \qquad 3.28.c$$

$$\Phi_{X} = \frac{v^{Ta}}{R} \qquad 3.28.d$$

$$\Phi_{Y} = \frac{u^{Rs}}{R} \qquad 3.28.e$$

$$\Phi_{Z} = \frac{u^{a}}{R} \qquad 3.28.f$$

where the superscripts s and a refer to the symmetric and antisymmetric displacements with respect to the plane "θ=0". The superscripts A, T and R refer to axial, torsion and rotation in the X direction, about the X axis and about the Y axis respectively. Also, l is the distance of the pump C.G. from the"free" end of the shell. Here u, v and w should be interpreted as the displacements of the middle surface of the shell at the "free" end; i.e. where x = L. The equations 3.28 are based on the assumption that the plane circular "free" end of the cylindrical shell remains plane and circular after deformation. The deformed shape of the shell as well as the C.G. set of axes are shown in Figure 3.5.

The vibrations of a cylindrical shell supporting a heavy mass at the "free" end, may be represented as a superposition of terms symmetric and antisymmetric with respect to θ=0 plane, as discussed later.

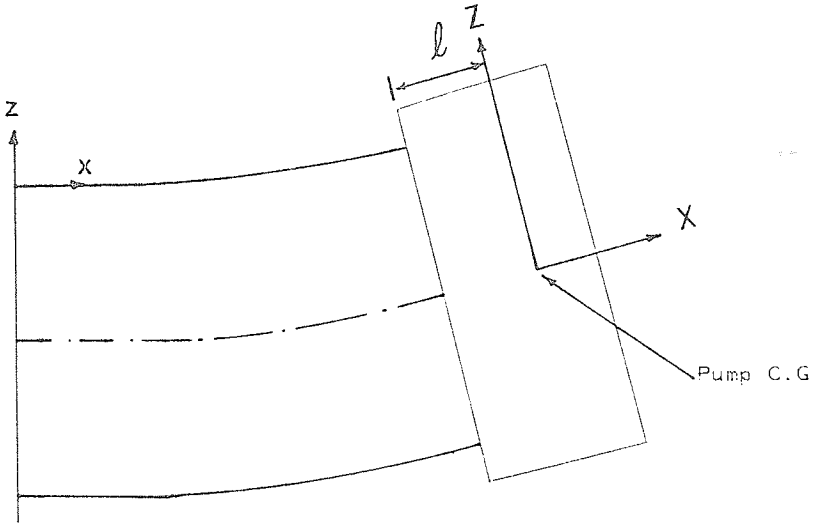

a) Symmetric Mode

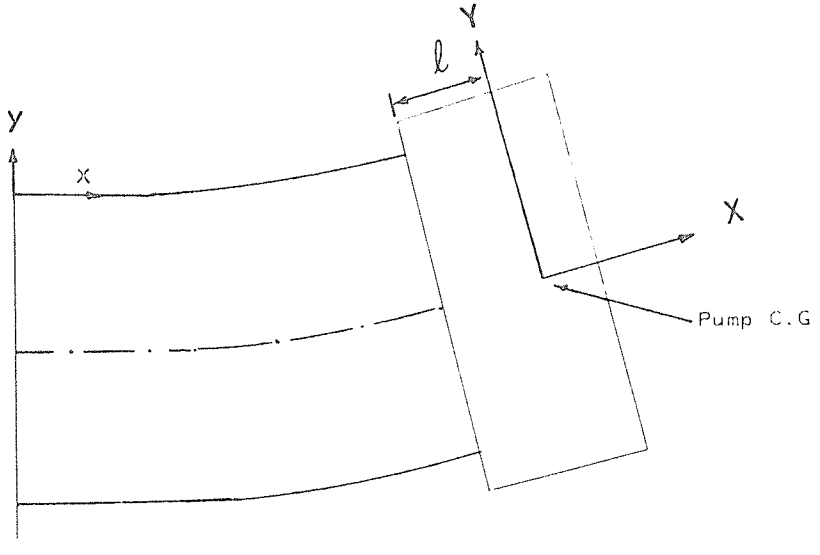

b) Antisymmetric Mode

Fig. 3.5 Deflected Shape of Pump-Mount and Pump C.G.

Coordinate System

To this end, the relations 3.28 may, then, be divided into two groups, concerned with the symmetric and the anti-symmetric modes. Relations 3.28.a, 3.28.c and 3.28.e are related to the former group, while relations 3.28.b, 3.28.d and 3.28.f are those of the second group.

Having clarified these points, the kinetic energy of the pump associated with the symmetric modes may be written as:

$$T_{p_s} = \frac{1}{2} M_p \left\{ (\dot{w}^s + \frac{l\dot{u}^{Rs}}{R})^2 + \dot{u}^{As^2} \right\} + \frac{1}{2} \frac{I_{yy_p}}{R^2} \dot{u}^{Rs^2} \qquad 3.29$$

For the anti-symmetric modes we have:

$$T_{p_a} = \frac{1}{2} M_p (\dot{v}^a + \frac{l\dot{u}^a}{R})^2 + \frac{1}{2} \frac{I_{zz_p} \dot{u}^{a^2}}{R^2} + \frac{1}{2} \frac{I_{xx_p} \dot{v}^{T^2}}{R^2} \qquad 3.30$$

In equations 3.29 and 3.30, M_p is the mass of the pump, I_{XX_p}, I_{YY_p} and I_{ZZ_p} are the three moments of inertia of the pump mass about the three axes X, Y, Z respectively, having their origin coinciding with the C.G. of the pump. Also, it is assumed that these axes are the principal axes of inertia, otherwise there will be coupling terms between symmetric and anti-symmetric modes as indicated by Meriam (60). Since the mounting is short and movements are small, gyroscopic effects are considered negligible.

3.7 External work of the pump weight:

Considering the mounting to be held horizontally in

the gravitational field, at the "free" end of the shell we have the pump weight ($M_p g$) and a couple ($\ell M_p g$) arises from transferring the pump weight to the "free" end of the shell. In the static case, the external work done by these forces may be written as:

$$W_e = - M_p g \; w^s(L,0) + \ell M_p g \; \Phi_Y \qquad 3.31$$

where $w^s(L,0)$ is the outward radial displacement of the "free" end at x=L, θ=0, and the rotation angle Φ_Y is given by equation 3.28.e.

3.8 Total potential and kinetic energies:

Since the displacement field is assumed to apply to the entire cylindrical shell, it is necessary to subtract the terms corresponding to the cutout regions. So if there are cutouts of total number N_c, then, the following terms should be subtracted from the corresponding potential and kinetic energy expressions of the whole shell, 3.19 and 3.23 respectively:

$$U_c = \frac{1}{2} \sum_{i=1}^{N_c} \int_{-\frac{h}{2}}^{h/2} \int_{x_{1i}}^{x_{2i}} \int_{\theta_{1i}}^{\theta_{2i}} U_e \; R d\theta \; dx \; dz \qquad 3.32$$

$$T_c = \frac{1}{2} \sum_{i=1}^{N_c} \rho R h \int_{x_{1i}}^{x_{2i}} \int_{\theta_{1i}}^{\theta_{2i}} (\dot{u}^2 + \dot{v}^2 + \dot{w}^2) \; d\theta dx \qquad 3.33$$

The total strain energy of the system is, then, given by:

$$U_T = U_o + U_s + U_r - U_c \qquad 3.34$$

where U_o and U_c are those related to the shell and cutouts, while U_s and U_r should be interpreted as the strain energies of all stringers and rings respectively. U_o and U_c have the expressions 3.18 and 3.32, U_s and U_r are the summation of individual stringer and ring strain energies, given in 3.20 and 3.22 respectively.

Similarly, the total kinetic energy of the system is given by:

$$T_T = T_o + T_s + T_r + T_p - T_c \qquad 3.35$$

where T_o, T_p and T_c are given by expressions 3.23, 3.29 (for symmetric modes) or 3.30 (for anti symmetric modes) and 3.33 respectively. Also, here T_s and T_r are the total kinetic energies of all stringers and rings, given individually by 3.25 and 3.27.

3.9 Modal functions:

The modal or displacement functions should be chosen in such a way as to satisfy the prescribed end conditions. Here, the displacements u, v and w of the middle surface of the shell are assumed to be double finite series. Each term of the series is a product of a circumferential and axial modal function, weighted by time dependent generalized coordinates - unknown amplitude factors. Each term in the chosen functions satisfied the boundary conditions and so, consequently, will the whole series.

3.9.1 Shell with fixed-free end condition:

The displacements u, v and w defining the deflected middle surface of the shell are chosen in the form:

$$u(x,\theta,t) = \sum_m \sum_n \left[q^{us}_{mn}(t) \cos n\theta + q^{ua}_{mn}(t) \sin n\theta \right] \Phi'_m(x) \qquad 3.36.a$$

$$v(x,\theta,t) = \sum_m \sum_n \left[q^{vs}_{mn}(t) \sin n\theta - q^{va}_{mn}(t) \cos n\theta \right] \Phi_m(x) \qquad 3.36.b$$

$$w(x,\theta,t) = \sum_m \sum_n \left[q^{ws}_{mn}(t) \cos n\theta + q^{wa}_{mn}(t) \sin n\theta \right] \Phi_m(x) \qquad 3.36.c$$

The periodic functions - cos $n\theta$ and sin $n\theta$ - are used for the circumferential direction, θ, since the shell is closed in that direction. The functions q^{us}_{mn}, q^{vs}_{mn} and q^{ws}_{mn} are the time dependent generalized coordinates associated with the θ-symmetric modes for the displacement u,v and w respectively. Similarly, the functions q^{ua}_{mn}, q^{va}_{mn} and q^{wa}_{mn} are those associated with the θ-anti-symmetric modes. The functions q^{us}_{mn} ----q^{wa}_{mn} are assumed to be harmonic functions of time. Functions $\Phi_m(x)$ are the axial mode functions, and $\Phi'_m(x)$ their first derivatives with respect to the spatial coordinate x. These functions were chosen to be the characteristic functions representing the normal (lateral) modes of vibration of a uniform beam, fixed at the end x=0, and free at the other end, x=L. These functions are the

solution of the well known partial differential equation of motion for the uniform beam:

$$EIy_{,xx} + \rho y_{,tt} = 0 \qquad 3.37$$

where I is the second moment of area of the beam cross-section, y is lateral deflection, and ρ is the mass per unit length of the beam. Functions $\Phi_m(x)$, then, satisfy the equation:

$$\frac{d^4 \Phi_m}{dx^4} = \beta^4_m \Phi_m \qquad 3.38$$

and may be written in the form:

$$\Phi_m(x) = \cosh\beta_m x - \cos\beta_m x - \alpha_m(\sinh\beta_m x - \sin\beta_m x) \qquad 3.39.a$$

Then

$$\Phi'_m(x) = \beta_m \{\sinh\beta_m x + \sin\beta_m x - \alpha_m(\cosh\beta_m x - \cos\beta_m x)\} \qquad 3.39.b$$

where $\beta^2_m = \omega_m \sqrt{\frac{\rho}{EI}}$ is given by the roots of the transcendental equation:

$$\cosh\beta_m L \cos\beta_m L + 1 = 0 \qquad 3.39.c$$

and

$$\alpha_m = \frac{\sinh\beta_m L - \sin\beta_m L}{\cosh\beta_m L + \cos\beta_m L} \qquad 3.39.d$$

with the following boundary conditions

$$\Phi_m(0) = \Phi'_m(0) = 0 \qquad 3.39.e$$

$$\Phi''_m(L) = \Phi'''_m(L) = 0 \qquad 3.39.f$$

The choice of the beam mode functions for $\Phi_m(x)$ allows some simplification in the analysis, through the orthogonal properties:

$$\int_0^L \Phi_r(x)\ \Phi_s(x)\ dx = \int_0^L \Phi_r''(x)\ \Phi_s''(x)\ dx = 0 \qquad (r \neq s) \qquad 3.40$$

Further properties and numerical values of the beam characteristic functions are given in (37), (38).

3.9.2. Shell clamped at one end, supporting a heavy mass at the other

The problem here is quite difficult due to the end condition imposed on the shell by the supported heavy mass. It is assumed that the pump is integrated rigidly into the shell at the "free" end. Since the pump is considered as a rigid body, this leads to the following considerations when the displacement functions are chosen:

1. The pump should be allowed to move with six degrees of freedom, namely, three translations in X, Y and Z directions, and three rotations about these axes.
2. The end face of the shell (x=L), which is circular and plane before deformation, should preserve these conditions during deformation. In other words, the end face suffers no warping.

These requirements can be achieved if the following functions are incorporated as displacement functions:

$$u(x,\theta,t) = u^{s}(x,\theta,t) + u^{a}(x,\theta,t) \qquad 3.41.a$$

$$v(x,\theta,t) = v^{s}(x,\theta,t) + v^{a}(x,\theta,t) \qquad 3.41.b$$

$$w(x,\theta,t) = w^{s}(x,\theta,t) + w^{a}(x,\theta,t) \qquad 3.41.c$$

where, as before, the superscripts s and a refer to the symmetric and anti-symmetric modes, respectively. The functions $u^{s}(x,\theta,t)$ through $w^{a}(x,\theta,t)$ have the form:

$$u^{s}(x,\theta,t) = \sum_{m}\left(\sum_{n} q^{usR}_{mn}(t)\left[(1-x/L)\cos n\theta + \cos\theta\right] + q^{usA}_{m}(t)\right)\Phi'_{m}(x)$$

$$= u^{sR} + u^{sA} \qquad 3.42.a$$

$$u^{a}(x,\theta,t) = \sum_{m}\sum_{n} q^{ua}_{mn}(t)\left[(1-x/L)\sin n\theta + \sin\theta\right]\Phi'_{m}(x)$$

$$= u^{a} \qquad 3.42.b$$

$$v^{s}(x,\theta,t) = \sum_{m}\sum_{n} q^{vs}_{mn}(t)\left[(1-x/L)\sin n\theta + \sin\theta\right]\Phi_{m}(x)$$

$$= v^{s} \qquad 3.42.c$$

$$v^{a}(x,\theta,t) = \sum_{m}\left(\sum_{n} q^{va}_{mn}(t)\left[(1-x/L)\cos\theta + \cos\theta\right] + q^{vT}_{m}(t)\right)\Phi_{m}(x)$$

$$= v^{ac} + v^{aT} \qquad 3.42.d$$

$$w^{s}(x,\theta,t) = \sum_{m}\sum_{n} - q^{ws}_{mn}(t)\left[(1-x/L)\cos n\theta + \cos\theta\right]\Phi_{m}(x)$$

$$= w^{s} \qquad 3.42.e$$

$$w^{a}(x,\theta,t) = \sum_{m}\sum_{n} q^{wa}_{mn}(t)\left[(1-x/L)\sin n\theta + \sin n\theta\right]\Phi_{m}(x)$$

$$= w^{a} \qquad 3.42.f$$

In the expressions 3.42, the superscripts R, A and T refer to rotation about Y axis, purely axial displacement, and pure torsion respectively. It is quite clear that the requirements set in 1 and 2 mentioned earlier can be achieved if x = L is substituted in 3.42, with the following constraint conditions:

a) for the symmetric modes:

$$v^{s}(L,\theta,t) \sin\theta + w^{s}(L,\theta,t) \cos\theta = \text{const.} \qquad 3.43.a$$

b) for the anti-symmetric modes:

$$v^{ac}(L,\theta,t)\cos\theta + w^{a}(L,\theta,t) \sin\theta = \text{const.} \qquad 3.43.b$$

$v^{a}(x,\theta,t)$, as shown in equation 3.42.d, may be divided into two parts, the pure torsion modes associated with the generalized coordinates $q_{m}^{vT}(t)$, and the radial-circumferential coupled modes, associated with q_{mn}^{va}, which given the symbol v^{ac}, appears in 3.43.b.

It should be noticed that the two constraints 3.43.a and 3.43.b must be fulfilled over all modes. These conditions may be achieved if the relations between the corresponding generalized coordinates can be cast in the forms:

$$q_{mn}^{vs}(t) = q_{mn}^{ws}(t) = q_{mn}^{sc}(t) \qquad 3.44.a$$

and

$$q_{mn}^{va}(t) = q_{mn}^{wa}(t) = q_{mn}^{ac}(t) \qquad 3.44.b$$

3.10 The Frequency Equation:

Having expressed the displacements as functions of the system of generalized coordinates, now the total strain energy, U_T, and the total kinetic energy, T_T, can be re-expressed as a function of those coordinates. Hence,

$$U_T = U_T \left(q_{mn}^{us}, \text{----}, q_{mn}^{wa}\right) \qquad 3.45.a$$

$$T_T = T_T \left(\dot{q}_{mn}^{us}, \text{----}, \dot{q}_{mn}^{wa}\right) \qquad 3.45.b$$

Hamilton's principle may be, mathematically, stated as:

$$\delta A = \delta \int_{t1}^{t2} (T_T - U_T)\, dt = \int_{t1}^{t2} (\delta T_T - \delta U_T)\, dt = 0 \qquad 3.46$$

where A is the action integral, t_1 and t_2 are two arbitrary points in the time domain, δ is the variational operator which is assumed to be commutative with the integral operator.

Using the expressions 3.45 and 3.46 leads to the familiar algebraic eigen value problem, which may be expressed in different forms, for different set of mode shapes, for different kinds of boundary conditions, as explained in the following sub-sections, 3.10.1 and 3.10.2.

3.10.1 Equations of motion for fixed-free case:

The total strain energy of the structure may be written in this case as:

$$U_T = \frac{1}{2} \sum_m \sum_n \sum_{\bar{m}} \sum_{\bar{n}} K_{mn,\,\bar{m}\bar{n}}\; q_{mn}\; q_{\bar{m}\bar{n}} \qquad 3.47.a$$

where

$$K_{mn,\,\bar{m}\bar{n}} = K_{\bar{m}\bar{n},\,mn} = \frac{\partial^2 U_T}{\partial q_{mn}\,\partial q_{\bar{m}\bar{n}}} = \frac{\partial^2 U_T}{\partial q_{\bar{m}\bar{n}}\,\partial q_{mn}} \qquad 3.47.b$$

are known as elements of the stiffness matrix.

Likewise, the total kinetic energy may be written as:

$$T_T = \frac{1}{2} \sum_m \sum_n \sum_{\bar{m}} \sum_{\bar{n}} M_{mn,\,\bar{m}\bar{n}}\; \dot{q}_{mn}\; \dot{q}_{\bar{m}\bar{n}} \qquad 3.47.c$$

where

$$M_{mn,\,\bar{m}\bar{n}} = M_{\bar{m}\bar{n},\,mn} = \frac{\partial^2 T_T}{\partial \dot{q}_{mn}\,\partial \dot{q}_{\bar{m}\bar{n}}} = \frac{\partial^2 T_T}{\partial \dot{q}_{\bar{m}\bar{n}}\,\partial \dot{q}_{mn}} \qquad 3.47.d$$

are known as elements of the mass matrix.

The mass and stiffness matrices obtained by the above operation (3.47) together with application of Hamilton's principle (3.46), were used to formulate the regular equation of motion for free vibration, in the form:

$$[M]\,\{\ddot{q}\} + [K]\,\{q\} = \{0\} \qquad 3.48$$

where $[M]$ and $[K]$ are the generalized mass and stiffness matrices, and the q's are the generalized coordinates, associated with θ symmetric modes and θ - anti-symmetric modes. $[M]$ and $[K]$ are square matrices of size $6M(N+1)$,

where M present the highest integer index associated with the longitudinal mode shape function, and N the corresponding integer for the circumferential direction.

Equation 3.48 can be re-arranged in the following partitioned form:

$$\begin{bmatrix} M^{ss} & M^{sa} \\ M^{sa^T} & M^{aa} \end{bmatrix} \begin{Bmatrix} \ddot{q}^s \\ \ddot{q}^a \end{Bmatrix} + \begin{bmatrix} K^{ss} & K^{sa} \\ K^{sa^T} & K^{aa} \end{bmatrix} \begin{Bmatrix} q^s \\ q^a \end{Bmatrix} = \{0\} \qquad 3.49$$

where superscript T denotes the transposed matrix.

In equation 3.49, the off-diagonal submatrices M^{sa} and K^{sa} as well as their transposes, vanish if the cross-section of the structure is symmetric with respect to the plane $\theta = 0$. Thus in this case, the above equation is uncoupled into two independent matrix equations, one for the symmetric and the other for the anti-symmetric modes. Moreover, assuming the motion to be simple harmonic, of frequency ω, the equation of motion for the symmetric modes may be written as:

$$\left[\begin{bmatrix} K11 & K12 & K13 \\ K12^T & K22 & K23 \\ K13^T & K23^T & K33 \end{bmatrix} - \omega^2 \begin{bmatrix} M11 & M12 & M13 \\ M12^T & M22 & M23 \\ M13^T & M23^T & M33 \end{bmatrix} \right] \{q^s\} = \{0\}$$

3.50

In equation 3.50, each of the 18 submatrices is a square of order M(N+1).

Similar equations can be written for the anti-symmetric modes. The elements of the mass and stiffness matrices in equation 3.50 are presented in Appendix C.

3.10.2 Equations of motion for fixed-supporting heavy mass cases:

a) Symmetric modes:

Following the same procedures as in article 3.10.1, the symmetric modes equation of motion has the form 3.50, but the generalized coordinates $\{q^s\}$ are:

$$\{q^s\} = \begin{Bmatrix} \{q^{usR}\} \\ \{q^{usA}\} \\ \{q^{sc}\} \end{Bmatrix} \qquad 3.51$$

The submatrices K11, K13, K22 and K33 are - in this case - square, of order M N, M N, M and M N respectively, while K12 and K23 are rectangular, of size M(M N) and (M N)M respectively.

The elements of these submatrices may be formed, using the following expressions:

$$K11_{mn,\,\overline{\overline{mn}}} = \frac{\partial^2 U_T}{q^{usR}_{mn}\, q^{usR}_{\overline{\overline{mn}}}} \qquad 3.52.a$$

$$K12_{mn,\,\bar{m}} = \frac{\partial^2 U_T}{\partial q^{usR}_{mn}\,\partial q^{usA}_{\bar{m}}} \qquad 3.52.b$$

$$K13_{mn,\,\bar{\bar{m}}\bar{n}} = \frac{\partial^2 U_T}{\partial q^{usR}_{mn}\,\partial q^{sc}_{\bar{\bar{m}}\bar{n}}} \qquad 3.52.c$$

$$K22_{m,\,\bar{m}} = \frac{\partial^2 U_T}{\partial q^{usA}_{m}\,\partial q^{usA}_{\bar{m}}} \qquad 3.52.d$$

$$K23_{m,\,\bar{\bar{m}}\bar{n}} = \frac{\partial^2 U_T}{\partial q^{usA}_{m}\,\partial q^{sc}_{\bar{\bar{m}}\bar{n}}} \qquad 3.52.e$$

$$K33_{mn,\,\bar{\bar{m}}\bar{n}} = \frac{\partial^2 U_T}{\partial q^{sc}_{mn}\,\partial q^{sc}_{\bar{\bar{m}}\bar{n}}} \qquad 3.52.f$$

The mass matrix can be obtained, using similar expressions to those in 3.52, by replacing U_T, q's and K's by T_T, $\dot{q}$'s and M's respectively. The resulting overall stiffness matrix $[K]$ and mass matrix $[M]$ are square of order $M(2N+1)$. The expanded form of the stiffness and mass matrices are presented in Appendix D.

b) Antisymmetric modes:

Here, the generalized coordinate vector $\{q^a\}$ has the form:

$$\{q^a\} = \begin{Bmatrix} \{q^{ua}\} \\ \{q^{vT}\} \\ \{q^{ac}\} \end{Bmatrix} \qquad 3.53$$

The stiffness and mass matrices for this case can be obtained using similar expressions for the symmetric modes, replacing q_{mn}^{usR}, q_{m}^{usA}, q_{mn}^{sc} and their time derivatives, by q_{mn}^{ua}, q_{m}^{vT}, q_{mn}^{ac} and their time derivatives, respectively.

3.11 Equations of Equilibrium for the clamped-supporting heavy mass case:

In this section, the equations of equilibrium for the static solution of the clamped-supporting heavy mass case is developed.

The starting point is the principle of minimum total potential energy. The total potential energy, Π, may be written as:

$$\Pi = U_o - W_e \qquad 3.54$$

where U_o is the strain energy of the shell, given by equation 3.18, and W_e is the external work done by the applied load, given by equation 3.31. Since the mounting is considered to be held horizontally and the applied load acts in the plane of symmetry $\theta = 0$ at the "free" end of the shell, only the symmetric solution exists.

The principle of minimum total potential energy may be, mathematically, expressed as:

$$\delta\Pi = \delta(U_o - W_e) = \delta U_o - \delta W_e = 0 \qquad 3.55$$

using equations 3.54 and 3.55 leads to the familiar

equations of equilibrium in the form:

$$[K]\{q^s\} = \{Q\} \qquad 3.56$$

where the elements of the generalized coordinate vector $\{q^s\}$ and the stiffness matrix $[K]$ are those expressed in equations 3.51 and 3.52 respectively.

The force vector $\{Q\}$ may be written as

$$\{Q\} = \begin{Bmatrix} \{Q^{us}\} \\ \{Q^{uA}\} \\ \{Q^{sc}\} \end{Bmatrix} \qquad 3.57$$

The expanded form of $\{Q\}$ is given in Appendix E

3.12 Closing Remarks:

In this chapter, numerical models have been established for the statics and dynamics of the pump mounting. It has been noticed that, though orthogonal functions were used to describe the displacements of the shell middle surface, there are coupling terms in the off-diagonal elements in both mass and stiffness matrices, which, in result, gives sometime a strong dynamic and static coupling between different modes due to the presence of the stiffening elements and cutouts. But, in general, the solution shows

a dominant element in the eigen vector, which in turn, taken to identify the different mode shapes. The phenomenon of coupled modes is discussed in detail in chapter six.

In view of the present problem complexity, it will only be practically useful if implemented on a computer. This is the subject of the next chapter.

CHAPTER FOUR

COMPUTER IMPLEMENTATION

4.1 General:

A computer program "PUMOME", an acronym for "Pump Mounting Mechanics", was developed to determine the static and dynamic response (free vibration) of the bell-housing type pump mounting, modelled as discussed in chapter three.

The structure is assumed to be at least singly symmetric with respect to the meridional plane $\theta = 0$; vibration modes symmetric and antisymmetric with respect to $\theta = 0$ thus uncoupled for both types of boundary conditions modelled and this was exploited in the design of the program.

The program was required for implementation on the Hewlett Packard HP9845B desk top graphics computer. The machine has an available Read/Write memory (RAM) of 187060 bytes, with mass storage provided by two tape cartridge drives and a single flexible disk unit; graphics may be output to screen or Benson 1301 incremental plotter. Virtually all desk top (micro) computers are hard-wired to interpret the BASIC language only, so that the program was, naturally, written in this language. All calculations are performed with 12 digit precision.

The stringers and rings are treated as discrete elements. It is assumed that all stringers have the same geometric properties and equally distributed in the circumferential direction, but the rings may have arbitrarily dimensions and locations in the longitudinal

direction. Both stringers and rings are assumed to be uniform along their axes, with rectangular cross-sections. As previously explained in chapter three, the analysis here considers the extension and flexure of the shell, neglecting its shear deformation and rotary inertia. For stringers and rings, extension, torsion and flexure about both cross-sectional axes have been considered. Moreover, the rotary inertia of stringers and rings was taken into account.

Note: The effect of shear deformation and rotary inertia was studied in the case of thin shell by Tang (40) and his results indicated that such effect was negligible in that case. Reismann and Medige (41) came to the same conclusion by comparing frequency parameters with and without inclusion of shear deformation and rotary inertia effects. On the other hand, Huffington et al (39) have demonstrated that the rotary inertia of the stiffeners can substantially affect the natural frequencies of stiffened plates.

It is worthwhile to mention that the effect of the shear deformation and rotary inertia become increasingly significant - in the case of unstiffened shells - as the thickness ratios R/h and L/h decrease; i.e. for thick and short cylinders, as Mirsky et al indicated (59).

4.2. Computer Program Limitations:

The following limitations in the computer implementation of the model should be observed:-

A. Shell

1. Circular cross-section
2. Constant small thickness
3. Homogeneous and isotropic material properties (Constant Young's modulus, constant Poisson's ratio)

B. Stringers

1. Maximum number is arbitrary
2. Uniform along length
3. Same material as shell
4. Every stringer has the same rectangular cross-section area
5. Externally located, equally spaced in the circumferential sense.

C Rings

1. Maximum number is Four
2. Uniform rectangular cross-section around circumference
3. Same material as shell
4. Arbitrary dimensions
5. Externally or internally located

D Cutouts

1. Maximum number is two and diametrally opposed
2. Rectangular in shape
3. Same longitudinal spatial coordinates.

E. Pump

1. Centre of gravity on central line

2. Arbitrary mass, inertia

4.3. Input Data:

The input data to the program falls into seven categories:

1. General data:

The general data includes the title of the program, number of terms used in the assumed displacement series M, N, the total number of stringers, rings and cutouts.

2. Shell data

This includes the shell material constants (Young's modulus, Poisson's ratio, density), shell radius, length and thickness.

3. Stringer data

This includes numbers and dimensions of stringers (thickness and width), location of the first stringer (circumferential angle).

Note: Location of the first stringer should maintain the geometric symmetry of the structure.

4. Ring data

This includes the state of each ring (external or internal), longitudinal location, and dimensions (width and thickness) of each individual ring.

5. Cutout data

This includes the longitudinal and circumferential coordinates of all corners of each cutout. All cutouts have the same longitudinal coordinates, and the circumferential coordinates should be symmetric with respect to the plane "$\theta = 0$".

6. Pump data

This includes the mass of the pump, the three moments of inertia about the three principal axes passing through the C.G. of the pump, distance of the C.G. from the shell "free" face.

7. Required solution data

This includes the boundary conditions involved, symmetric or anti-symmetric mode solution- In the fixed-supporting heavy mass boundary conditions, for the symmetric modes, there is either the free vibration or the static solution.

The user should provide these input data from the key board as they appear, in a question form, on the computer screen.

4.4. Calculating the elements of the mass and stiffness matrices:

Having input the data described in section 4.3, the program calculates and locates the elements of the mass and

stiffness matrices, in the appropriate position within the overall mass and stiffness matrices preserved area in the computer memory. The calculations involved in the program, in general, can be classified as the following integrals and function values:-

1. Shell longitudinal integrals over the whole length
2. Shell longitudinal integrals over the span of cutouts
3. Shell circumferential integrals over the arcs of cutouts.
4. Discrete evaluations of certain functions relating to the circumferential position of the stringer - see Appendix C.
5. Similar to 4 but relating to rings and their various longitudinal positions - see Appendix C.
6. Pump displacement function values (longitudinal function values).

Since the shell and rings are circular in shape, their circumferential integrals have already been explicit ly determined and incorporated in the general expressions for the mass and stiffness elements. The exact evaluation of all integrals is possible and included in the program to avoid any inaccuracy if numerical integrations are employed.

The general expressions for the elements of the mass and stiffness matrices are presented in Appendices C and D

The program computes the torsion constants for the stiffeners rectangular sections in accordance with Timoshenko, (13), page 312. The values of α_m and β_m involved in the longitudinal integrals are those given in (37).

In the case of the symmetric modes, for example, of the fixed-free end conditions, for a certain set of the subscripts (m, n, $\bar{m}$, $\bar{n}$), the program calculates six elements of the stiffness matrix, and six elements of the mass matrix, i.e. one element from each of the twelve submatrices k11,...,M33 in equation 3.50, chapter three.

If these calculated elements of the stiffness matrix k(i1, j1), k(i1, j2), k(i2, j2), k(i2,j3) and k(i3,j3) are those expressed in Appendix C, where k(i1, j1) = $k11_{mn,\ \bar{m}\ \bar{n}}$ and so on, then the relationship between these new subscripts i1, j1,...,j3, and the old ones m, n, $\bar{m}$, $\bar{n}$ can be put in the following form to describe the essentially two dimensional nature of the array of stiffness coefficients

$$i1 = M\,n + m \qquad 4.1.a$$

$$j1 = M\,\bar{n} + \bar{m} \qquad 4.1.b$$

$$i2 = M(N+1) + M\,n + m = M(N+1) + i1 \qquad 4.1.c$$

$$j2 = M(N+1) + M\,\bar{n} + \bar{m} = M(N+1) + j1 \qquad 4.1.d$$

$$i3 = 2M(N+1) + M\,n + m = 2M(N+1) + i1 \qquad 4.1.e$$

$$j3 = 2M(N+1) + M\,\bar{n} + \bar{m} = 2M(N+1) + j1 \qquad 4.1.f$$

where $0 \leq n \leq N$, $0 \leq \bar{n} \leq N$

$1 \leq m \leq M$, $1 \leq \bar{m} \leq M$

M and N are the final longitudinal and circumferential terms in the displacement series.

For example if M = 3 and N = 4, then the element with subscripts 2, 3, 3, 0 in the sub matrix K33 will be located in the position (41,33) in the assembled stiffness matrix, $[K]$; i.e.:

$$K33_{23,30} = K(41,33) \qquad 4.1.g$$

Note that in this case, the $[K]$ matrix is of size(45, 45). The same process is applied to locating the mass elements. With the aid of the expressions 4.1, the program, then, can locate the calculated elements in the proper position in the overall assembled stiffness and mass matrices.

If the overall matrices $[K]$ or $[M]$ become singular due to the presence of zeros on the leading diagonals, the matrices are condensed by eliminating those corresponding rows and columns. The computer program has the ability of doing such checking and elimination process, automatically.

The same procedure holds for the anti-symmetric modes of the clamped-free shell.

In the case of the symmetric modes for the clamped-supporting a heavy mass end condition, the corresponding relations to those in equations 4.1 have the form:

$$i1 = M(n-1) + m \qquad 4.2.a$$

$$j1 = M(\bar{n}-1) + \bar{m} \qquad 4.2.b$$

$$i2 = MN + m \qquad 4.2.c$$

$$j2 = MN + \bar{m} \qquad 4.2.d$$

$$i3 = M(N+1) + M(n-1) + m \qquad 4.2.e$$

$$j3 = M(N+1) + M(\bar{n}-1) + \bar{m} \qquad 4.2.f$$

where, $1 \leq n \leq N$, $1 \leq \bar{n} \leq N$

$1 \leq m \leq M$, $1 \leq \bar{m} \leq M$

M and N as before.

Again, the same procedure holds for the anti-symmetric modes for the clamped-supporting heavy mass end condition.

4.5. Method of Solution:

In this section, the methods used for solving the equations of equilibrium in the static case and the eigen value problem in the free vibration case are discussed.

4.5.1. Static Solution

The equations of equilibrium for the clamped-supporting a heavy mass end condition are of the form

$$[K] \{q\} = \{Q\} \qquad 4.3$$

which represented non homogeneous linear system of algebraic equations.

The solution vector $\{q\}$ is obtained by the following method, which requires that $[K]$ be a symmetric positive-definite matrix.

A triangular decomposition is performed on the matrix $[K]$ by the square root method of Cholesky:

$[K] = [U]^T [U]$ where $[U]$ is an upper triangular matrix. Then equation 4.3 has the form

$$[U]^T [U] \{q\} = \{Q\} \qquad 4.4$$

This represents two triangular systems

$$[U]^T \{r\} = \{Q\} \qquad 4.5.a$$

$$[U] \{q\} = \{r\} \qquad 4.5.b$$

First, equations 4.5.a is solved for $\{r\}$ by forward elimination, and then, the second system, 4.5.b is solved for $\{q\}$ by back substitution.

A subroutine was developed in the program to perform the above steps.

4.5.2. Free Vibration Solution:

The eigen value problem (for free vibration) has the form:

$$[K] \{q\} = \lambda [M] \{q\} \qquad 4.6$$

where λ is the eigen value ($=\omega^2$) and $\{q\}$ is the eigen vector (= generalized coordinates vector).

The method adapted for solving equation 4.6 to get eigen values and eigen vectors of the system requires $[M]$ to be symmetric positive definite, and $[K]$ to be symmetric, Wilkinson (42).

A triangular decomposition is performed on the matrix $[M]$ by the square root method of Cholesky:

$[M] = [L]\ [L]^T$, where $[L]$ is a lower triangular matrix.

Therefore, from equation 4.6

$$[K]\ \{q\} = \lambda [L]\ [L]^T \{q\}$$

This can be expressed as

$$[L]^{-1}[K][L]^{T^{-1}}[L]^T\ \{q\} = \lambda[L]^T\ \{q\} \qquad 4.7$$

By defining $[S] = [L]^{-1}[K][L]^{T\ -1}$ 4.8

and $\{y\} = [L]^T\ \{q\}$ 4.9

equation 4.7 becomes

$$[S]\ \{y\} = \lambda\{y\} \qquad 4.10$$

which is an eigen value problem where $[S]$ is a symmetric matrix with eigen values λ which are the same as the original problem, 4.6. The eigen vectors of the original system, $\{q\}$ are found from the eigen vectors of equation 4.10, $\{y\}$, by substitution in equation 4.9.

The advantage of this method is that no matrix inversions are required (in particular, $[L]^{-1}$ is not explicitely determined), since the transformation of equation 4.8 involves triangular matrices. The sequence of operations is as follows :

1. Decompose $[M]$: $[M] = [L]\ [L]^T$
2. Perform a forward substitution through

   $[L]\ ([L]^{-1}[K]) = [K]$

   to solve for each column of $[L]^{-1}[K]$

3. Perform a forward substitution through

$$[L]\left([L]^{-1}[K][L^T]^{-1}\right) = ([L]^{-1}[K])^T$$

to solve for each column of $[L]^{-1}[K][L^T]^{-1} = [S]$

4. Find the eigen values, λ and eigen vectors $\{y\}$ of $[S]$ Householder's method was used in this analysis.

5. Determine the eigen vectors $\{q\}$ from $\{y\}$ by backward substitution through $[L^T]\{q\} = \{y\}$

The programs "Trans" and "Evlvec" of reference (43) were used to perform the above procedures, where the Sturm sequence technique was employed to determine the eigen values.

4.6. Program Output Format

The program outputs may be classified into 7 items:

1. General information; that includes the solved problem boundary conditions, solution type (symmetric or anti-symmetric), number of terms employed in the assumed displacement functions, number of zeros which occurred in the leading diagonals of the mass and/or stiffness matrices (prior to condensation).

2. Number and dimensions of stringers.

3. Number, dimensions and kinds (internal or external) of rings.

4. Number and coordinates of cutouts.

5. Pump parameters

6. Calculated natural frequencies, in Hz

7. Indices of the largest element in the eigen vector, which are taken to identify the dominant mode shape associated with each of the natural frequencies, in 6 - explained later.

8. In the static solution, the output data are the generalized coordinates, displacements, strains and stresses.

The items 1 through 5 are for checking purposes.

Now, in the vibration of shells, there are, basically, three sets, or type,of motion; axial, circumferential and radial. These three sets are not always separated, in other words, they are, normally, coupled except for the axisymmetric motion where they are completely uncoupled. This fact was noticed in the result eigen vectors which are, generally, populated with elements. Since the eigen vector presents the displacement generalized coordinates, it is useful if we imagine that it could be partitioned into three subvectors parts, associated with the axial, circumferential and radial displacements, respectively. Each of these subvectors, in turn, presents many modes relating to that specified set of motion. Once more, there is a coupling inside each of these subvectors. But the largest element in the whole eigen vector is taken to identify the motion associated with the corresponding natural frequency. This identification is presented by the category of motion

in which the largest element falls, as well as the indices of that element; i.e. number of nodal lines and nodal circles associated with it.

To illustrate the process, consider the symmetric vibration of the clamped-free case. First, locate the largest element of the partitioned eigen vector, and if it is within the first part, then the motion is, dominantly, axial one, and number 1 is given to this type of motion. If the largest element falls in the second part of the eigen vector, then the motion is dominantly circumferential and number 2 is given to it. If that element falls in the last part of the eigen vector, then the motion is radial and number 3 is given to it. Now, if the largest element has a position Z in the first part, then the associated number of nodal circles ml and nodal lines nl are given by the formula:

$$ml = Z1 - M\left[(Z1-1)/M\right]_T \qquad 4.11.a$$

$$nl = \left[(Z1-1)/M\right]_T \qquad 4.11.b$$

where Z1 = Z

The subscript T represents the operation of truncation after the decimal point (only integer value retained), and this mode shape is identified by (1, ml nl) S, where S refers to a symmetric mode.

If Z lies in the second part of the eigen vector, then Z1 should be replaced by Z - M(N+1) in equation 4.11, and

this mode is identified by (2, ml nl)S. Finally if Z lies in the last part of the eigen vector, then Zl is replaced by Z-2M(N+1), in equation 4.11, and the mode shape has the form (3, ml nl)S.

For example if M=3, N=4 and Z=33, then the mode shape is radial one with:

ml = 3 , nl = 0

Note that the whole eigen vector, in this case, has 45 elements, partitioned into 3 subvectors, each contains 15 elements presenting the resultant 3 types of motion.

A similar discussion holds for the anti-symmetric modes, except that the letter A is used instead of S. One can identify the following special cases:

a)	Bar axial modes	N(1, ml 0)S
b)	Beam flexural modes	N(3, ml 1)S - (and A)
c)	Pure torsion modes	N(2, ml 0)A
d)	Ring modes	N(3, ml 0)S
e)	"Ovalling" modes	N(3, ml 2)S - (and A)

where N refers to natural frequency.
Some of these shapes are presented in figure 4.1.

The same approach is used to identify the modes in the case of the clamped-supporting heavy mass end condition, but the symbols have a slightly different interpretation as follows:

1. For modes symmetric in θ

   l, implies rotation about $\theta=90^{o}$ for the end cross-section

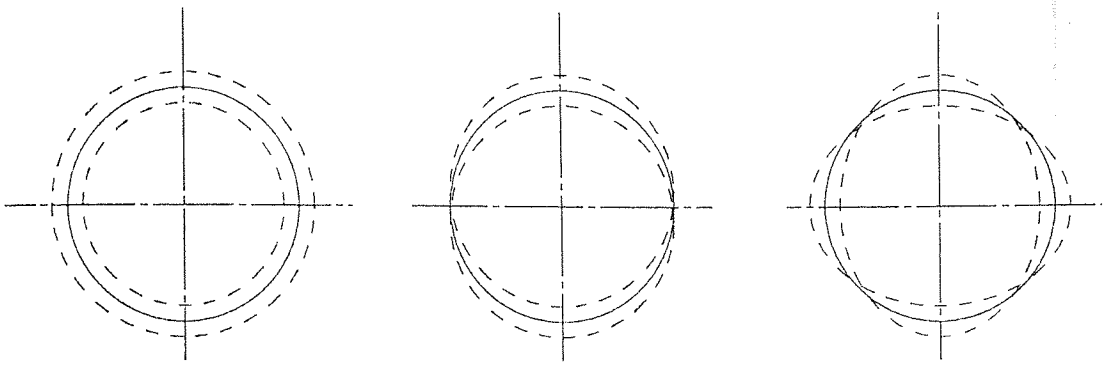

a) Circumferential Nodal Patterns

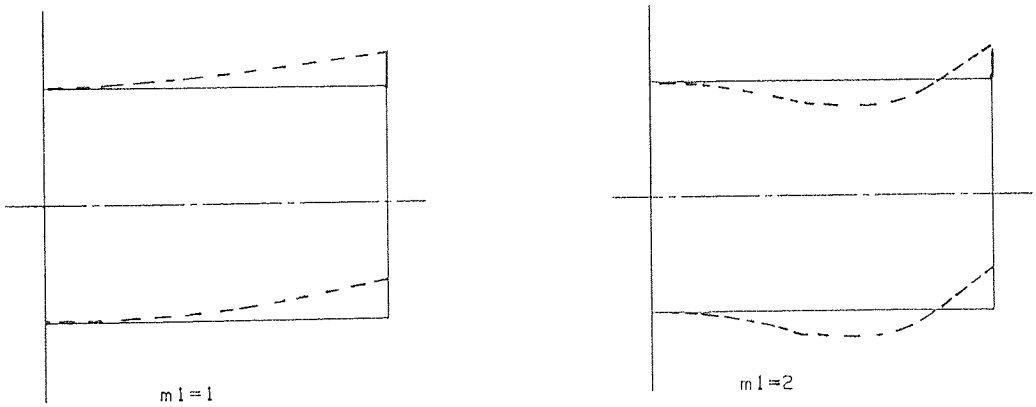

b) Axial Nodal Patterns

Fig.4.1 Nodal Patterns for Clamped-Free Circular

Cylindrical Shells

2, purely axial motion

3, indicates the constraining condition, or the coupling between v^s and w^s - (the coordinate q^{sc})

2. For modes anti-symmetric in θ

1, implies rotation about $\theta = 0^o$ for the end cross-section.

2, pure torsion

3, indicates the constraining condition, or the coupling between v^{ac} and w^a - (the coordinate q^{ac})

The program has been written so that modes may be output in a graphical form, at user's option; some examples are given in chapter six.

4.7. Closing Remarks:

In this chapter, the computer program "PUMOME", developed to solve the problem under consideration, has been discussed.

In summary, the main program consists of the following programs:

1. "PUMOSD"; pump mounting symmetric dynamics:- to formulate the mass and stiffness matrices of the model for symmetric free vibration analysis in the clamped-free end condition case.
2. "PUMOAD"; pump mounting anti-symmetric dynamics:- as 1, but for the anti-symmetric analysis.

3. "P&MOSD"; pump and mounting symmetric dynamic;
   as 1, but for the clamped-supporting heavy mass end condition.
4. "P&MOAD": pump and mounting anti-symmetric dynamic:
   as 3, but for the anti-symmetric analysis.
5. "P&MOSS": pump and mounting symmetric static:
   to formulate the stiffness matrix and force vector, for the static solution of the clamped-supporting heavy mass end condition.
6. "TRANS": reference (43).
   to decompose the mass matrix, in the dynamic case, and formulate the eigen value problem.
7. "EVLVEC": reference (43)
   to solve the eigen value problem and give the natural frequencies and associated eigen vectors.
8. "CHOLSK":
   to decompose the stiffness matrix, in the static case, and give the generalized coordinates, displacements, strains and stresses.
9. "Graph 1":
   to give the mode shapes in a graphic form for the clamped-free end condition - symmetric or anti-symmetric modes.
10. "Graph 2":
    to give the mode shapes in a graphic form for the clamped-supporting heavy mass end condition - symmetric or anti-symmetric modes.

11. "Graph 3":

to give the displacements, strains and stresses in a graphic form, for the static solution.

Some of the program results were tested experimentally and against some known solutions. These are the subject of the following chapters five and six.

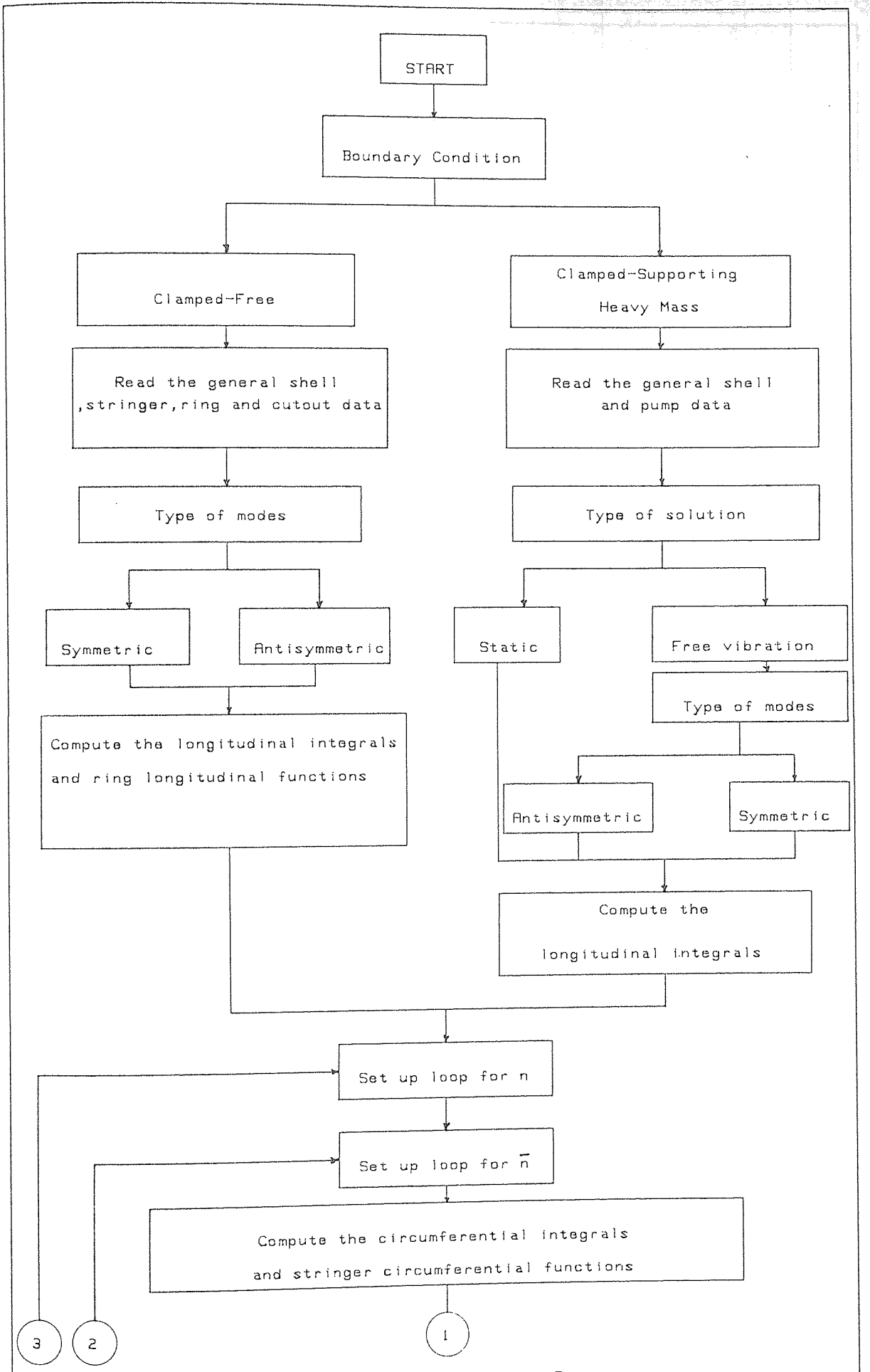

Fig.4.2 Flow Chart of the Main Program

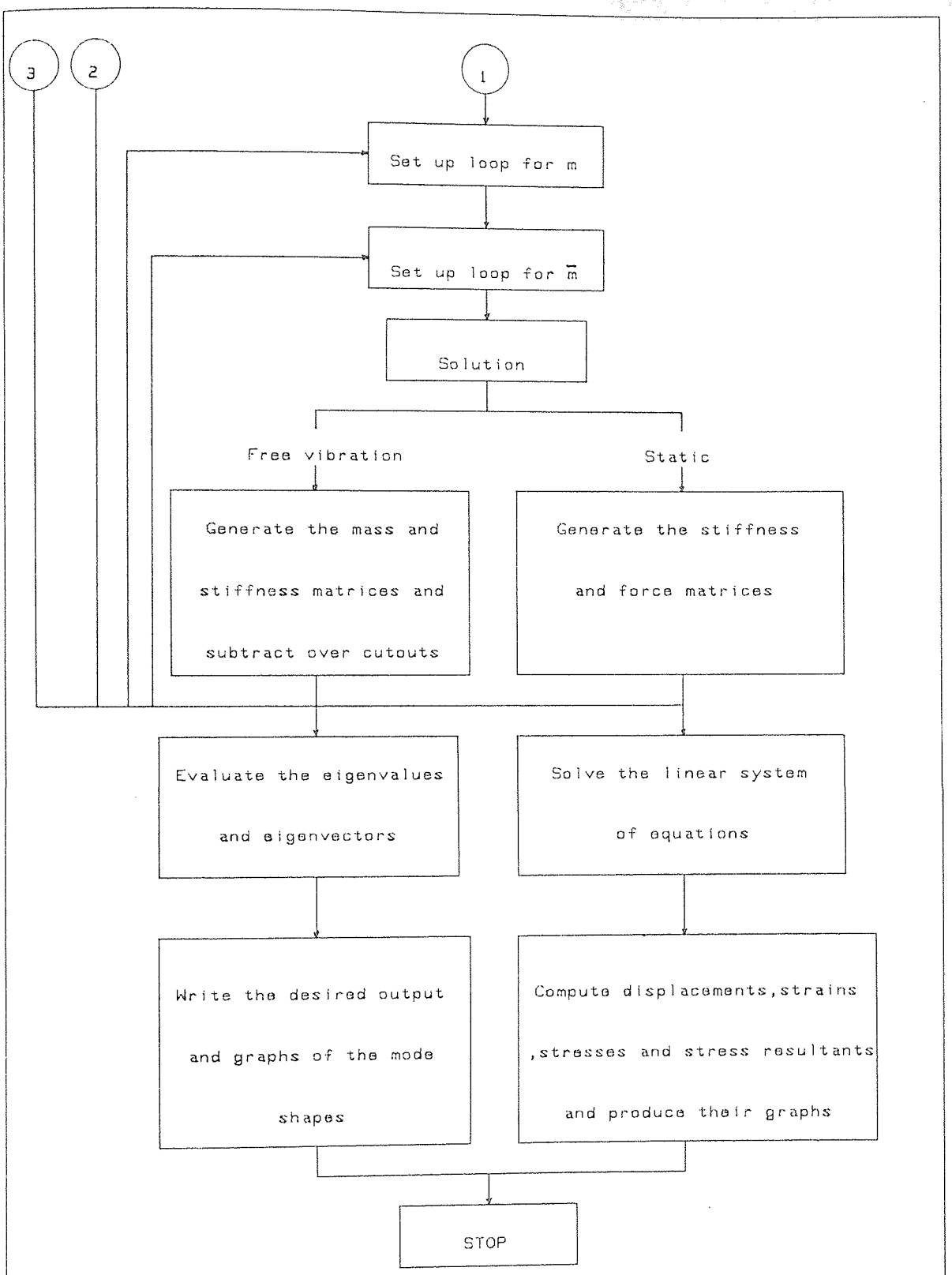

Fig.4.2 Flow Chart of the Main Program (cont.)

CHAPTER FIVE

EXPERIMENTAL INVESTIGATION

5.1. Introduction:

The experimental work was performed on a commercially available steel bell housing mounting, constructed from a steel cylindrical shell with two cutouts diametrically opposite; stiffening was provided by four longitudinal equally spaced stringers and two end circular flanges. The dimensions (in m) of the model are given in Figure 5.1. The work falls into 2 phases:

1. Sweep test, to pick up the natural frequencies.
2. Identification of mode shapes associated with those frequencies.

Previously, analog systems have been used to monitor and control experimental work in the vibrations field. Such techniques have limitations in flexibility, accuracy and ease data processing. A major step has been taken in recent years by introducing digital computers into the field as a laboratory controller of experimental rigs. One problem involved with the introduction of digital systems is how to communicate with the tested structure. Signals picked up by transducers are in analog form - i.e. continuous functions of time - whether they represent structure response or vibrator driving forces. That is to control the vibrator and then to

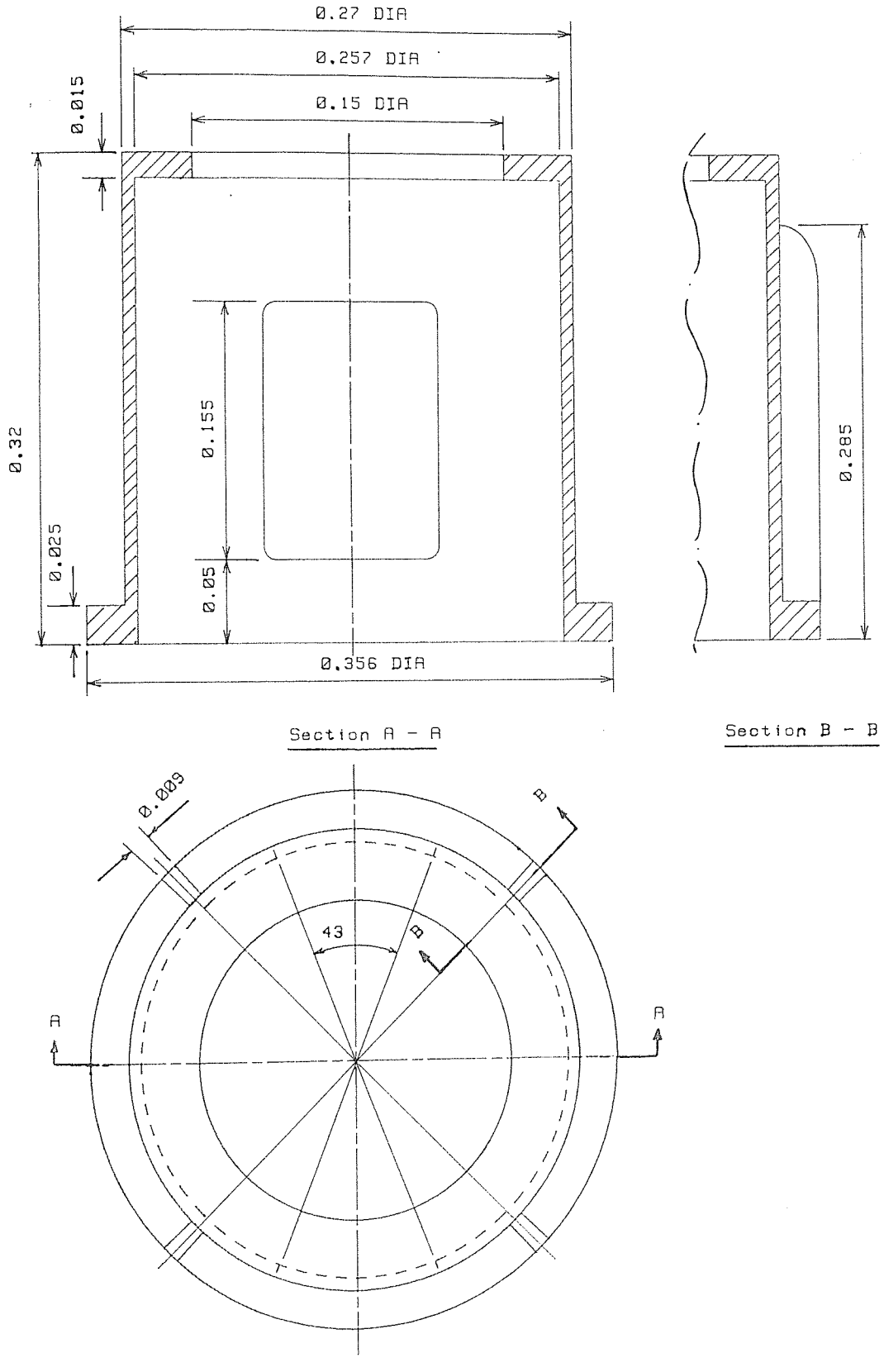

Fig. 5.1 Dimensions of Experimentally Tested Bell-housing (in m)

analyse transducers signals, a digital to analog (D to A) and analog to digital (A to D) converters are required to fulfil the task. The Frequency Response Analyser (FRA) does both functions, as explained later.

5.2. Instrumentation:

5.2.1. Vibrator and Amplifiers:

A Goodmans, type 390A electrodynamic vibrator was used to provide the exciting force on the structure. The maximum Frequency can be obtained from the vibrator is of order 4.5 kHz. The signal to drive the vibrator was magnified by means of a Radford MA25, series 3 power amplifier, with maximum input 500m Volt, rms. Transducers output signals were fed into a two channel CVA2 charge amplifier, manufactured by Environmental Equipment Ltd. Each channel had a variable sensitivity between 0 and 30 mv/pc, and whilst performing the experiments, both channels were set to the maximum sensitivity.

5.2.2. Transducers:

To measure the input force function which excites the bell housing, a Bruel and Kjaer piezo electric force transducer, type 8200 was used. It had a mass of 21 gm, a force range of 1 kN tensile to 5 kN compression and a charge sensitivity of 4pc/N. The response of the structure was measured by a Bruel and Kjaer piezo electric accelerometer,type 4367 of 13 gm in

mass. The charge sensitivity was approximately 20 pc/g with a resonance frequency of 32 kHz. A magnetic mount was used to attach the accelerometerto the structure.

Although cables are considered passive elements, under certain condition of use and environment, spurious signals may be induced in, or generated by them. That, in turn, implies that the signals at the receiving end of the line contain components that were not initially present in the transducer output. Such undesirable signals are described as "noise", and low noise cables made by Bruel and Kjaer were used, to reduce such interference effects.

5.2.3. Frequency Response Analyser (FRA):

The Solatron-Schlumberger Frequency Response Analyser (FRA), type 1172 was used to drive the vibrator by means of an analog output signal, and to convert the transducers signal from analog form into digital one, and analyse them, display the results, in a digital form. The magnitude ratio and phase difference of the transducers signals could, then, be obtained, or sent to the computer, in a digital form, through the General Purpose Interface Bus (GPIB) - known as IEEE488 Standard Interface Bus.

The FRA's generator has a range from 0.1mHz to 9.999kHz, with sine, square or triangular wave shape, output volt range 10mV to 9.99 V. Other specifications can be obtained from relevant manuals.

5.2.4. IEEE488 Standard Interface Bus:

The function of the IEEE488 Standard Interface Bus is to transmit the digital data back and forth between the computer and the FRA. It is commonly used and implemented on all Hewlett Packard desk top computers and Solatron Frequency Response Analysers. It allows data to be transmitted bi-directionally between the computer and other peripheral devices via 8 data lines, as 8 Boolean parallel signals (forming one byte), while bytes are transmitted in serial fashion. All peripheral devices, as well as the computer, may transmit or receive data.

5.2.5. Hewlett Packard HP9825A Desk-Top Computer (HP9825A)

The HP9825A computer has a work space of 22k bytes of random access read and write memory (RAM). The programming language is HPL, which is quite similar to BASIC and so is interpretive; the interpreter is stored in a read only memory (ROM). The computer has an accuracy of 12 significant digits. The language allows matrix operations and was found to be adequate for all necessary processing of the experimental data. The program can be executed and controlled interactively from the keyboard.

The HP9825A was used to control the FRA, and to accept the digital signals that came from it. There were

some other peripheral devices connected to the computer including an X-Y plotter, integral thermal printer and a flexible disk unit for mass storage of information. Also, for mass storage, there is a tape cartridge drive seldom used because of its slow and limited capacity compared with the flexible disk unit.

5.3. Test Rig:

The bell housing was mounted on a massive cast iron machine tool base provided with T slots. The test bed had a low natural frequency to keep the transmissibility ratio very low. The outer ring flange was used to bolt the pump mounting on the test bed. To prevent the bell housing from rocking and to achieve the "clamped end condition", 8 clamping dogs were used. The vibrator was connected to the structure through a small steel rod, carrying the force transducer at the end nearer the mount under test. The vibrator input was connected to the power amplifier, which in turn, was connected to the FRA output. Transducer signals were fed to the charge amplifier whose outputs were fed back to the FRA inputs. Finally the FRA was connected to the HP9825A computer through the IEEE488 interface bus.. The block diagram of the circuit is illustrated in Figure 5.2.

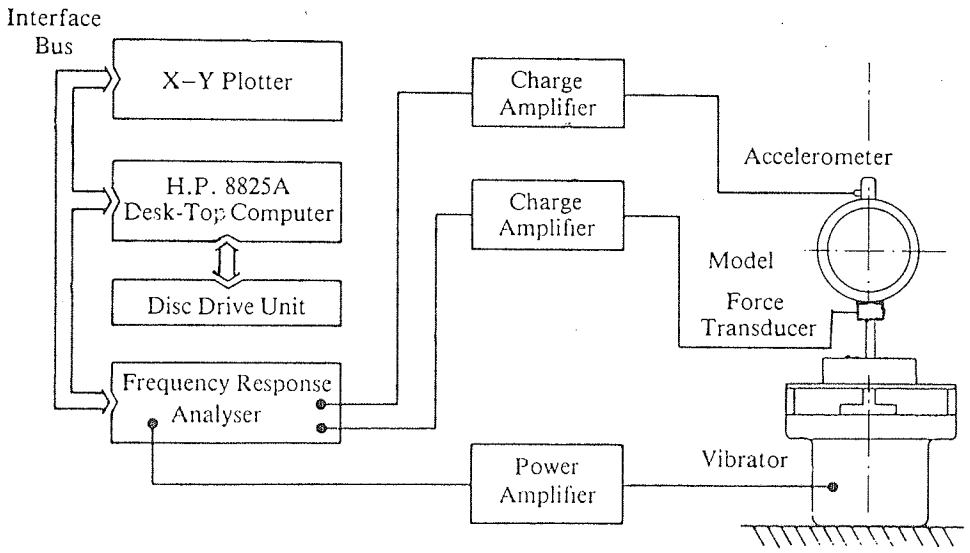

Fig. 5.2 Block Diagram of the Experimental Rig

5.4. Test Procedure:

5.4.1. Sweep test:

The rig was connected as described in section 5.3, and the sweep test was conducted using the computer as a remote controller for the FRA. The computer program "TFASET" was written,(62) to perform the task in hand, with the following instructions to be fed from the key board.

1. Frequency range of the test between 1Hz and 3kHz (This is the range of frequencies relevant for noise production).
2. Input volts to the power amplifier not to exceed 500mV rms. Although a sine wave shape was used, other forms like square or triangular wave shape were allowed in the program.
3. Direction of the sweep test, up or down.
4. Frequency incremental step, arbitrary but 0.5 Hz or 1 Hz were used.
5. Measurement mode of input signals to the FRA; the ratio mode Y/X, where $\vec{X}$ and $\vec{Y}$ refer to the force and acceleration signals respectively. Here, Y/X means the amplitude ratio and the phase difference of the two signals.
6. Measurement delay time between two successive frequency incremental steps; arbitrary within the FRA specifica-

tion but is recommended to be longer for a slow responding system i.e. system with large time constant which is characterized by low natural frequency.

7. Integration time: arbitrary within the FRA specification.

After input of these instructions from the computer key board, the FRA output the analog signal to drive the vibrator and the sweep test was started over the specified frequency range. The measured values Y/X (both the magnitude ratios, and phase differences) were then transmitted to the computer memory . . whence they could be output, either in a tabulated or graphical form, showing the structure response as a function of the frequency. A typical graphical output is given in Figure 5.3.

Since the technique described above was suitable to control one experiment at a time - with a single accelerometer - the test was repeated with different appropriate accelerometer positions, along the axial and circumferential directions, to pick up the radial, axial and circumferential modes. On conclusion, the term "sweep' means two things:

1. Sweeping the applied force frequency over the test sweep range, while the accelerometer is at a certain point on the structure.
2. Sweeping (scanning) the accelerometer around the structure and repeating the test.

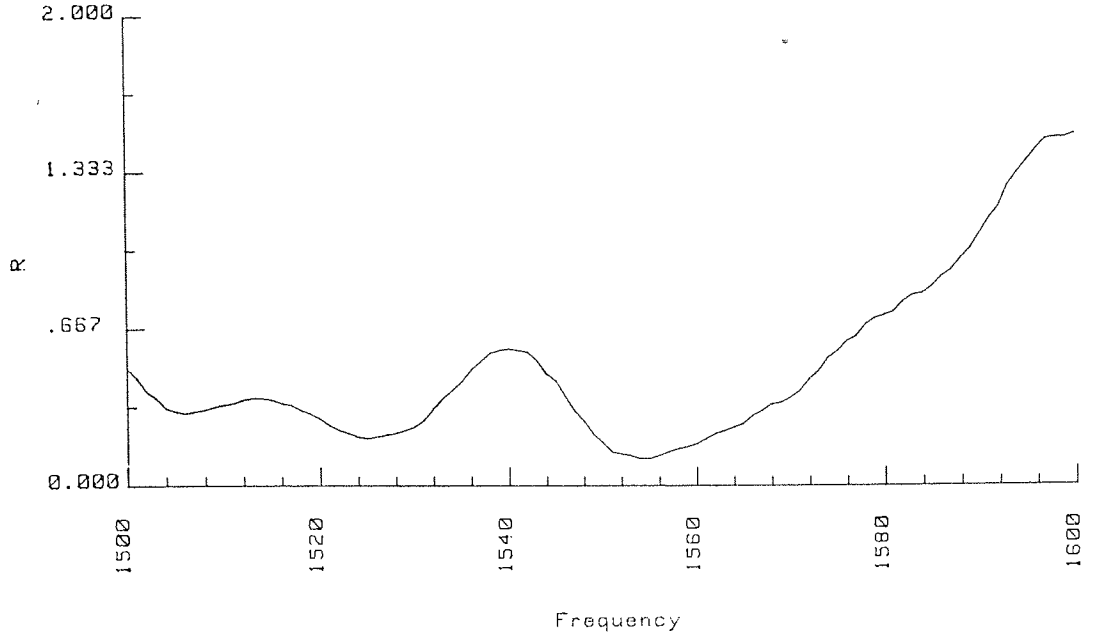

R v Frequency

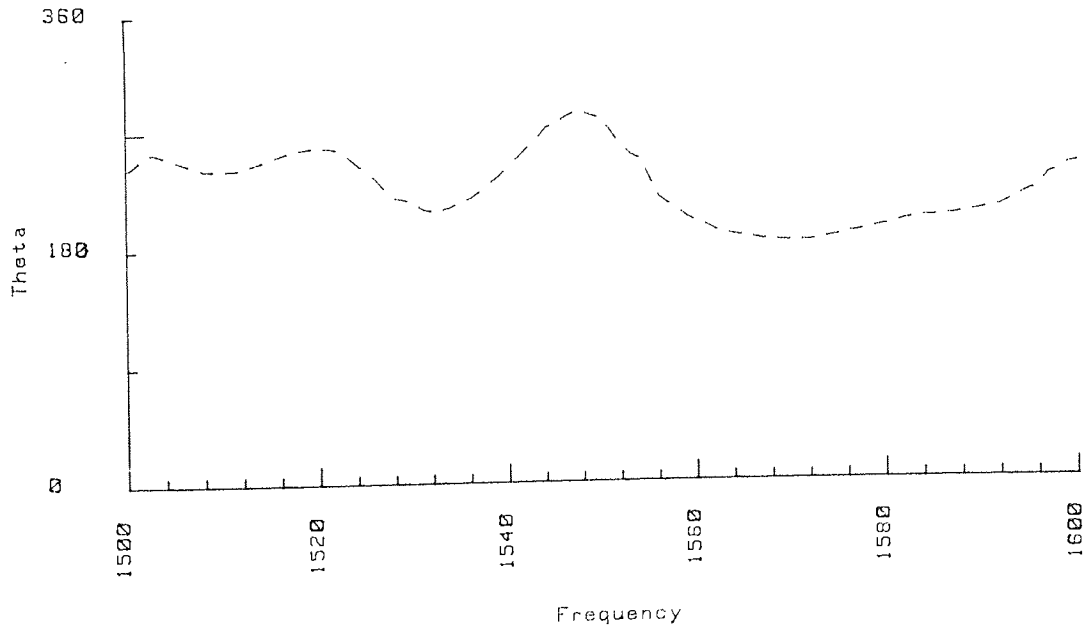

Theta v Frequency

Fig. 5.3 A Typical Sweep Test Diagram

5.4.2. Mode shapes:

Investigating the graphs produced in the sweep test, one may locate the natural frequencies of the structure as they correspond to peaks in the magnitude ratio and sudden changes in the phase angle, in the response curves.

The next step was to identify the mode shape associated with each of these natural frequencies. To do that, the vibrator was driven at a specified natural frequency, and the response of the structure was recorded at many points around its surface. The same circuit as in Figure 5.2 was used, except that the computer was disconnected and the FRA was controlled locally from its own key board. With different locations of the accelerometer on the structure, the displacement pattern of the model was produced, and hence, the corresponding mode shape may be identified. Comparisons of the experimental and theoretical results are presented in chapter six.

5.5. Closing Remarks:

The employed technique in the experimental part of the present work allowed the experiments to be performed quickly and accurately hence, a more comprehensive test program can be undertaken. However, the FRA is limited to two channel analysis, i.e. to measure the force input and one response for each test. Therefore tests

requiring more than two channels analysis would need a more complex arrangement of instrumentation. Also this type of test procedure requires mechanical contact between the vibration generator and the structure, which by necessity requires the addition of small masses and slight modification to the boundary condition, since the connector has stiffness properties. These effects were reduced to a minimum by designing the connector to have long and slender proportions which give high transverse flexibility, and by connecting the force transducer directly to the structure in order to keep the added mass to a minimum.

CHAPTER SIX

RESULTS AND DISCUSSION

6.1. Introduction:

Results and discussion of the previously described analysis, both theoretical and experimental, are presented here. First, the reliability of the theoretical work and the computer program output is studied by making comparisons of the present analysis results with some known experimental and theoretical solutions, which correspond to special or limiting cases of the problem under consideration.

Next to this comparison study, several results are presented to display the effect of varying certain parameters associated with this particular problem, such as cutout size, location and the supported heavy mass, on the mechanical characteristics of the mount.

In summary, the range of parameters that can be studied is :

1. Complete cylindrical shell:
   a. thickness to radius ratio
   b. length to radius ratio
   c. Poisson's ratio
2. Stringers:
   a. Stringer length to shell length ratio
   b. number and locations of stringers
   c. stringer cross-sectional area properties

3. Rings:

   a. ring eccentricity location

   b. number and locations of rings

   c. ring cross-sectional area properties

4. Cutouts:

   a. Cutout span to shell length ratio

   b. cutout arc

   c. cutout location and number

5. Pump:

   a. pump mass

   b. pump mass moments of inertia

   c. pump centre of gravity location

The computer program can give a result for each of those cases individually as a special case, or the result for any combination of them as a general case. Some of these results are presented here.

Finally a comparison of the experimental results with the theoretical predicted ones of the free vibration test, performed on a specific commercial bell housing, is given.

6.2. Comparison with some known theoretical and experimental results:

This section presents the comparison study of natural frequencies and corresponding mode shapes for:

1. unstiffened circular cylindrical shell

2. ring stiffened circular cylindrical shell

3. stringer stiffened circular cylindrical shell

4. ring and stringer stiffened circular cylindrical shell

6.2.1. Comparison of results for the unstiffened circular cylindrical shell :

Table 6.1 shows a comparison between the analytical and experimental work of Sewall et al, ref (44) and those of the present analysis for clamped-free unstiffened shell. Parameters of the shell used in this example are:

$L = 23.422$ in $(59.49 \times 10^{-2}$ m) , $R = 12$ in $(30.48 \times 10^{-2}$ m)

$h = 0.032$ in $(8.128 \times 10^{-4}$ m) , $E = 10^7$ lb/in^2 $(6.895 \times 10^{10}$ N/m^2)

$\rho = 2.588 \times 10^{-4}$ lb sec^2/in^4 $(2.766 \times 10^3$ kg/m^3), $\nu = 0.3$

It is clear that the comparisons are good, in general. The slight differences in the analytical results may be due to the different shell theories employed. Sewall et al (44) used Novozhilov theory, while Love-Timoshenko theory is used in the present analysis.

A comparison was also made with the experimental results of Park et al, (45), the analytical results of Boyd and Rao, (46) and the present analysis results. The comparison is presented in Table 6.2.

nl	ml=1			ml=2		
	Present Analy.	Ref.(44) Analy.	Ref.(44) Exp.	Present Analy.	Ref.(44) Analy.	Ref.(44) Exp.
2	444	395.9	-	1592.2	1314	-
3	237	219.3	201&206	1065.1	876.8	-
4	146.2	138.2	131.7	726.3	613.6	-
5	106.9	103.3	100.8	516.1	449.7	429.1
6	98.9	97.9	96.9	385.3	346.3	326.3 & 334.4
7	111.9	112.1	113	305.9	283.8	273.5
8	137.2	138.1	140.4	263.4	252.6	247.4
9	170.3	171.3	174.3	249.9	246.8	244.2
10	209	210.1	214.6	259.1	260.9	261.5
11	252.5	253.7	258.4	284.9	289.6	292.1
12	300.6	301.7	307.6	322.5	328.8	335.2
13	353	354.1	361.2	368.7	375.8	381.1 & 393.2

Table 6.1

Comparison of Analytical and Experimental Frequencies of a Clamped-Free Unstiffened Circular Cylinder (Hz.)

nl	ml=1			ml=2		
	Present Analy.	Ref.(45) Exp.	Ref.(46) Analy.	Present Analy.	Ref.(45) Exp.	Ref.(46) Analy.
2	106.2	87.2 & 95.1	104.4	538.2	-	508.2
3	56.4	51.5	55.6	291.4	-	281.3
4	52.3	50.4	52.0	181.9	168.5 & 170.2	177.9
5	71.6	70.9	71.6	137.1	132.8	135.4
6	101.9	101.4	101.8	132.8	128.8 & 130.1	132.0
7	139.1	138.8	139.1	154.5	153.6	154.2
8	182.6	182.2	182.6	191.4	191.3	191.2
9	232	-	-	237.9	-	-

Table 6.2

Comparison of Analytical and Experimental Frequencies of a Clamped-Free Unstiffened Circular Cylinder (Hz.)

The parameters of the shell used for this comparison are:

$L = 48$ in $(1.2192$ m$)$, $R = 10$ in $(0.254$ m$)$

$h = 0.03$ in $(7.62 \times 10^{-4}$ m$)$, $E = 3 \times 10^{7}$ lb/in^2 $(2.068 \times 10^{11}$ N/m$^2)$

$\rho = 0.7332 \times 10^{-3}$ lb sec^2/in^4 $(7.836 \times 10^{3}$ kg/m$^3)$, $\nu = 0.29$

In their analytical solution, Boyd et al (46) used the Flügge theory of thin shells, so the discrepancy between their results and the present study results might be attributed to the differences in the shell theories, although most of the frequencies are identical in both analyses. The discrepancy between the analytical and experimental results increases as the number of circumferential waves (n) decreases. Egle et al, (45) suggested that the shell clamped end may not have been absolutely fixed in the experiments. This assumption seems to be true since the experimental results are lower than the theoretical ones, which physically means "less stiff" end condition in the experiment.

The last comparison relating to the vibration of clamped-free unstiffened circular cylindrical shell was made between the present analysis results and those of Ref.(47), where the finite element technique was employed. Table 6.3 shows this comparison as well as the experimental results due to Gill (48).

nl	ml=1			ml=2		
	Present Analy.	Ref.(47) Analy.	Ref.(48) Exp.	Present Analy.	Ref.(47) Analy.	Ref.(48) Exp.
1	481	468	364	-	2055	-
2	289.2	316	293	936.3	941	827
3	769.5	779	760	923.2	932	886
4	1465.5	1527	1451	1524.1	1597	1503
5	2366	-	2236	2409	-	2384
6	3469	-	3429	3509	-	3476
7	4773	-	-	4812	-	-

Table 6.3

Comparison of Frequencies of a Clamped-Free Unstiffened Circular Cylinder Obtained by Rayleigh-Ritz and Finite Element Methods (Hz.)

The parameters of the shell used for this example are:

$L = 19.764$ in$(0.502m)$, $R = 2.5$ in $(0.0635m)$

$h = 0.06417$ in$(1.63 \times 10^{-3} m)$, $E = 3.046 \times 10^{7} lb/in^{2} (2.1 \times 10^{11} N/m^{2})$

$\rho = 7.3 \times 10^{-4} lb/sec^{2}/in^{4} (7.8 \times 10^{3} kg/m^{3})$, $\nu = 0.28$

It is evident from Table 6.3 that the results of the present analysis are lower than those of the finite element solution, over the range of comparison. Also the present analysis results are closer to the experimental values of Ref.(42) than those of Ref.(47). The over estimation of the frequencies in the finite element solution indicates that the used element, Ref.(47), was over stiff. In general, the agreement between the results of the present analysis and those of the finite element and experimental ones, is good.

6.2.2. Comparison of results for ring stiffened circular cylindrical shell:

Sewall et al (50) reported experimental results for a ring stiffened cylindrical shell with various support conditions. The results given in table 3 of Ref.(50) are compared with the present ones, in Table 6.4. Sewall et al used a cylinder stiffened with 6 similar outer rings, nearly equally spaced along the cylinder, the first ring at the free end. Rings were manufactured from wide flange, I cross section beam. So the present program was ocasionally

nl	ml=1		ml=2	
	Present Analy.	Ref.(50) Exp.	Present Analy.	Ref.(50) Exp.
2	205.9	169 and 196	792.5	752
3	339.3	321	600.25	574
4	566.2	504 and 545	705.7	607,644 and 686
5	890.2	-	850.36	803

Table 6.4

Comparison of Analytical and Experimental Frequencies of a Clamped-Ring Stiffened Circular Cylinder (Hz.)

modified to meet such configurations.

Parameters for the shell and rings are:

For the shell:

$L = 29.014$ in $(7.369 \times 10^{-1}$ m) , $R = 14.1245$ in $(3.587 \times 10^{-1}$ m)

$h = .049$ in $(1.245 \times 10^{-3}$ m) , $E = 3 \times 10^{7}$ lb/in^2 $(2.0685 \times 10^{11}$ N/m^2)

$\rho = 7.332 \times 10^{-4}$ lb sec^2/in^4 $(7.8357 \times 10^{3}$ kg/m^3) $\nu = 0.3$

For the rings:

$A_r = 0.19545$ in^2 $(1.261 \times 10^{-4}$ m^2) $I_{xx_r} = 2.5278 \times 10^{-2}$ in^4 $(1.05215 \times 10^{-8}$ m^4)

$J_r = 4.961 \times 10^{-4}$ in^4 $(2.065 \times 10^{-10}$ m^4) $I_{zz_r} = 8.3136 \times 10^{-3}$ in $(3.46 \times 10^{-9}$ m^4)

$\bar{z}_r = 0.4645$ in $(1.1798 \times 10^{-2}$ m)

Since ring-stiffened circular cylindrical shell is an axisymmetric structure, there is no coupling in the circumferential mode functions, but due to the presence of the rings, there is a strong coupling between the axial mode functions. So to obtain reasonable results, the structure should be analysed with many axial modes sufficient to achieve a converged solution. The results presented in Table 6.4 were obtained with a single circumferential mode function and 15 axial mode functions at a time. During solution of this example, the author noted that this number of terms in the modal functions is sufficient to get a good agreement with the results given in Ref.(50).

From Table 6.4, the discrepancies between the theoretical and experimental results are of order 5% which is acceptable in engineering applications.

One more study was made to compare the present analysis results with those due to Forsberg (51) and Sharma et al (52), for clamped-ring stiffened cylindrical shells. Table 6.5 shows such a comparison for a single ring at the "free" end. Frequencies are presented in terms of a frequency parameter, Δ defined to be:

$$\Delta = \frac{\rho R(1-\nu^2)}{E} \omega^2$$

Parameters used in this study were:

$R/h = 250$ $\quad$ $L/R = 9$ $\quad$ $\nu = 0.3$

For the ring (outer, rectangular cross-section):

(ring breadth)/R = 0.1

(ring depth)/R = 0.3

To obtain Δ from the present program, ρ, R and E were set to be equal to unity.

An overall agreement between the present analysis results and those of Ref.(51), (52) is quite good. The discrepancies in results may be attributed to the differences in the thin shell theories employed in the analysis. In both Ref.(51) and (52), the Flügge thin shells theory was used. Also the discrepancies between these three types of results may be due to the errors in computation and the different ring-shell compatibility relations employed in the three solutions.

n1	m1=1		
	Present Analy.	Ref.(51) Analy.	Ref.(52) Analy.
1	1.3452	1.3080	1.3707
2	4.082	3.6980	3.3519
3	1.8802	2.2390	1.8573
4	2.4752	2.1640	1.9440
5	2.9945	-	2.8031
6	4.0872	-	4.0259
7	5.54	-	5.5109
8	7.244	-	7.2355
9	9.20	-	9.1938

Table 6.5

Comparison of Analytical Frequency Parameters of a Clamped-Ring Stiffened Circular Cylinder

$(\Delta^{1/2} \times 10^{2})$

6.2.3. Comparison of results for stringer-stiffened circular cylindrical shells:

Sewall et al, (53) carried out extensive series of experiments on the vibration of longitudinally stiffened cylindrical shells, with arbitrary boundary conditions. The corresponding results for the problem under consideration, namely fixed-free longitudinally stiffened cylinder, were compared with the present ones in Table 6.6. There were 60 similar external stringers, of rectangular cross-section area. The following parameters were used for this study:

For the shell:

$L = 24.625$ in $(0.625m)$, $R = 9.537$ in $(0.2422\ m)$

$h = 0.0256$ in $(6.5\times10^{-4}m)$, $E = 10^7 lb/in^2 (6.895\times10^{10} N/m^2)$

$\rho = 2.54\times10^{-4} lb\ sec^2/in^4 (2.7145\times10^3 kg/m^3)$, $\nu = 0.315$

For the stringers (same material as the shell):

stringer height $= 0.2764$ in $(7.021\times10^{-3}m)$

stringer width $= 0.1$ in $(2.54\times10^{-3}m)$

$A_s = 0.029319\ in^2\ (1.892\times10^{-5}m^2)$

$\bar{z}_s = 0.1439$ in $(3.655\times10^{-3}m)$

Table 6.6 shows a good correlation between the experimental results of Ref.(53) and those of the present analysis for this type of configuration. As might be expected, the results based on Rayleigh-Ritz method are

n1	m1=1		m1=2	
	Present Analy.	Ref.(53) Exp.	Present Analy.	Ref.(53) Exp.
1	518	-	-	-
2	250	277	-	-
3	148.6	161 & 166	-	-
4	109.1	110 & 114	527.1	473
5	98.7	94 & 97	424.8	377
6	105.6	100	363.7	340
7	123.2	121	331.3	308 & 310
8	147.6	147	319.8	298 & 301
9	177.3	181	324.0	-
10	211.4	217 & 222	340.3	328 & 330
11	249.3	259	365.9	365

Table 6.6

Comparison of Analytical and Experimental Frequencies of a Clamped-Free Stringer Stiffened Circular Cylinder (Hz)

higher than the experimental or the "exact" results. This fact is true here except for few modes, particularly for lower circumferential wave number (n). This underestimation of the frequencies may be due to the higher contribution to the kinetic energy of the system due to the presence of the stringers in the analysis than occurs in practice.

6.2.4. Comparison for Ring-Stringer stiffened shells:

Table 6.7 shows the theoretical results due to Egle et al (54) and the experimental ones of Park et al (45) compared with the present analysis results. The model used for this comparison was a clamped-free cylindrical shell, stiffened with 3 similar rings and 16 similar stringers, internally located and equally spaced, i.e. rings were located at $x/L = \frac{1}{3}, \frac{2}{3}, 1$ and stringers were equally spaced around the circumferential direction. Properties of the shell, rings and stringers were as follows:

For the shell:

$L = 48$ in $(1.22m)$, $R = 10$ in $(0.254m)$

$h = 0.03$ in $(7.62 \times 10^{-4} m)$, $E = 3 \times 10^{7} lb/in^{2} (2.069 \times 10^{11} N/m^{2})$

$\rho = 7.332 \times 10^{-4} lb\ sec^{2}/in^{4} (7.834 \times 10^{3} kg/m^{3})$, $\nu = 0.29$

For stringers (same material as shell):

$A_s = 0.311 \times 10^{-1} in^{2} (2.006 \times 10^{-5} m^{2})$

$\bar{z}_s = -0.1376$ in $(-3.5 \times 10^{-3} m)$

$I_{yy_s} = 0.3895 \times 10^{-3} in^4 (1.621 \times 10^{-10} m^4)$

$I_{zz_s} = 0.1652 \times 10^{-3} in^4 (6.876 \times 10^{-11} m^4)$

$(GJ)_s = 0.306 \times 10^3 lb\ in^2 (0.87816\ N.m^2)$

For rings (same material as shell):

$A_r = 0.6251 \times 10^{-1} in^2 (4.033 \times 10^{-5} m^2)$

$\bar{z}_r = -0.1219\ in\ (-3.1 \times 10^{-3} m)$

$I_{zz_r} = 0.4945 \times 10^{-3} in^4 (2.06 \times 10^{-10} m^4)$

$I_{xx_r} = 0.3253 \times 10^{-3} in^4 (1.354 \times 10^{-10} m^4)$

$(GJ)_r = 0.5146 \times 10^4 lb\ in^2 (14.768\ N.m^2)$

It is interesting to notice in Table 6.7 that the results of the present analysis are consistently lower and closer to the experimental results, than those of Egle et al, Ref.(54). This high improvement in the quality of the frequency predictions may be attributed to the improved stiffener theories of the present analysis, particularly the stiffener-shell compatibility relations.

Due to the double symmetry of the stiffened shell cross-section with respect to both vertical and horizontal axes ($\theta=0$, $\theta=\frac{\pi}{2}$ respectively), the frequencies of even and

nl	ml	Present Analy.	Ref.(54) Analy.	Ref.(45) Exp.
2	1	100.3	105.8	80.2 & 88.2
	2	433.7	433.9	-
	3	914	-	-
4	1	206.5	216.9	184.6
	2	276.8	285.9	251.5
	3	439.7	447.1	397.0 & 430.4
6	1	314.5	315.0	-
	2	350.9	353.8	-
	3	412.2	414.0	-

Table 6.7

Comparison of Analytical and Experimental Frequencies of a Clamped-Free Ring - and Stringer - Stiffened Circular Cylinder (Hz.)

odd circumferential modes, (n) could be evaluated separately. In other words, there is no coupling between the modes with even and those with odd circumferential wave numbers. This interesting result is proven below.

The circumferential functions, for jth stringer, appearing in the mass and stiffness elements take either one of the following forms- see Appendix C:

$$SCF1 = \cos n \theta_j \cos \bar{n} \theta_j \qquad 6.1$$

$$SCF2 = \sin n \theta_j \sin \bar{n} \theta_j \qquad 6.2$$

And for the total number of stringers, S, equally distributed in circumferential direction, equations 6.1, 6.2 take the form:

$$SCF1 = \sum_{j=1}^{S} \cos n \frac{2\pi j}{S} \cos \bar{n} \frac{2\pi j}{S} \qquad 6.3$$

$$SCF2 = \sum_{j=1}^{S} \sin n \frac{2\pi j}{S} \sin \bar{n} \frac{2\pi j}{S} \qquad 6.4$$

Equation 6.3 may be written:

$$SCF1 = \frac{1}{2} \sum_{j=1}^{S} \left(\cos \frac{2\pi j}{S} (n+\bar{n}) + \cos \frac{2\pi j}{S} (n-\bar{n})\right) \qquad 6.5$$

Re-calling that the finite sum of cosine functions is:

$$\sum_{r=1}^{n} \cos r\theta = \frac{\sin \frac{n\theta}{2} \cos \frac{(n+1)\theta}{2}}{\sin \theta/2} \qquad 6.6$$

the sums in equation 6.5 take the form:

$$SCF1 = \frac{1}{2}\left(\frac{\sin \pi(n+\bar{n}) \cos \pi\frac{(S+1)}{S}(n+\bar{n})}{\sin \frac{\pi}{S}(n+\bar{n})}\right.$$

$$\left. + \frac{\sin \pi(n-\bar{n}) \cos \pi \frac{(S+1)}{S}(n-\bar{n})}{\sin \frac{\pi}{S}(n-\bar{n})}\right) \qquad 6.7$$

The numerators in equation 6.7 are zeros for all integer values of n, $\bar{n}$. But if $(n+\bar{n})$ and $(n-\bar{n})$ are multiples of S, the denominators are also zeros and SCF1 has an indefinite value. To obtain SCF1 in this case, differentiation of the first and second part, right hand side of equation 6.7 with respect to $(n+\bar{n})$, $(n-\bar{n})$, respectively, gives

$$SCF1 = \frac{S}{2}\left(\frac{\cos \pi (n+\bar{n}) \cos \pi (n+\bar{n}) \frac{(S+1)}{S}}{\cos \frac{\pi}{S}(n+\bar{n})}\right.$$

$$\left. + \frac{\cos \pi (n-\bar{n}) \cos \pi (n-\bar{n}) \frac{(S+1)}{S}}{\cos \frac{\pi}{S}(n-\bar{n})}\right)$$

$$= S \qquad 6.8$$

Equation 6.8 is true if $n+\bar{n} = qS$ and $n-\bar{n} = pS$ where q and p are integer numbers.

If only $n+\bar{n}$ or $n-\bar{n}$ are multiple of S then:

$$SCF1 = \frac{S}{2} \qquad 6.9$$

Relations 6.8 and 6.9 imply that SCF1 has a value if $(n+\bar{n})$ and/or $(n-\bar{n})$ are multiples of S. But S is an even number from the symmetry assumption, so n and $\bar{n}$ are both odd or even numbers.

Similar argument can be applied to SCF2 in equation 6.2.

The conclusion of this proof is that there are no coupling terms in the mass or stiffness matrices between odd and even terms in the circumferential displacement functions.

From the comparison studies, of some of known results and those of the present solution for stiffened and unstiffened circular cylindrical shells, described in this section, a satisfactory confidence in the present analysis and the computer program established, has been obtained. The remainder of this Chapter will be concerned with some parameters, affecting the vibration of cylindrical shells, having relevance to the bell type hydraulic pump mounting.

6.3 Effect of rectangular cutout:

As it is already seen, the free vibration problem of ring and/or stringer stiffened cylindrical shells as well as the unstiffened ones has been studied theoretically and experimentally and reported in the literature. However, the effect of cutouts in the shell wall has had little

attention for both stiffened and unstiffened shells which are the structures of interest in the present work.

In this section, the free vibration of clamped-free circular cylindrical shells with rectangular cutouts is investigated in conjunction with the analysis given in Chapter three and the computer program described in Chapter four.

As pointed out in Chapter two, there is no clear idea about the effect of the cutout on the free vibration of the cylindrical shell. Moreover, none of the relevant references report a result for the effect of rectangular cutout on the vibration of the clamped-free stiffened or unstiffened circular cylindrical shell.

In the present section, the influence of the size and location of the cutouts as well as their effect on circular shells with different thickness to radius ratios are investigated. But first a convergence study is performed.

6.3.1. Convergence Study:

In application of Rayleigh-Ritz method, the problem of estimating the accuracy of the results is usually encountered. The accuracy of the results depends crucially on the capability of the employed admissible functions to approximate the true shape of the deflected surface to the required degree. An increase in the number of terms tends to improve the accuracy of the results in general, but on

the other hand the resulting increase in the size of the matrices will increase the round off errors and the solution time. A convergence study was made to estimate the number of terms in the displacement functions in order to obtain an accurate result within a reasonable matrices size. Table 6.8 shows such convergence study for various combinations of used terms in both axial and circumferential direction, for the symmetric modes. The results in Table 6.8 were obtained for the following parameters:

For the shell:

$L = 11.3$ in (0.287m) , $R = 5.45$ in (0.138m)

$h = 0.245$ in (6.22×10^{-3}m) , $E = 3 \times 10^{7}$ lb/in^2 (2.068×10^{11} N/m^2)

$\rho = 7.254 \times 10^{-4}$ lb sec^2/in^4 (7.752×10^{3} kg/m^3) , $\nu = 0.3$

For the cutouts (two cutouts, diametrically opposite)

$x1 = 3.767$ in (9.57×10^{-2}m) , $x2 = 7.533$ in (0.1913m)

$L_c/L = 1/3$

$\theta_{11} = -22.5^{o}$ $\theta_{12} = 22.5^{o}$

where L_c is the cutout span

Two cutouts were used to preserve the double symmetry of the structure in the circumferential direction; i.e. about the planes $\theta = 0$ and $\theta = \pi/2$ - see Fig. 3.2. Then since even and odd circumferential modes uncoupled, in such case, even and odd circumferential modes could be evaluated separately. The dimensions of the shell are

nl	ml=1						
	No Cutout	M=3 N=4	3 5	7 4	4 6	5 6	6 5
0	6248	6260	5998	6121	5984	5927	5921
1	1714	1653	1651	1504	1554	1548	1502
2	876	865	862	856	859	850	846
3	816	808	807	789	797	792	788
4	1294	1145	1142	1088	1090	1087	1079
5	2024	2001	1999	1971	1982	1976	1967
6	2938	2905	2901	2886	2878	2869	2878
7	4024	4001	4031	3950	3962	3956	3924
8	5279	-	5290	-	5272	5265	5268
9	6702	-	6726	-	6691	6681	6682
10	8292				8377	8368	
11	10051				10143	10134	

M: Total number of terms used in longitudinal direction

N: Total odd or even number of terms used in circumferential direction

(ml,nl) associated with the dominant vibration mode

Table 6.8

Convergence Study: Frequencies for a Shell With Two Diametrically Opposite Cutouts (Hz.)

those of an actual bell housing mount model, Fig. 5.1. The number of terms were increased from M = 3 to 7 in the axial direction and n = 0 to 11 in the circumferential one, (n odd and even were calculated separately as stated above). The frequencies show a trend towards convergence over the whole range of used terms. The difference of frequencies values in the last two columns of Table 6.8 are indeed negligible. So, the subsequent calculation will be performed by limiting the number of degrees of freedom in any one run to a maximum of 90. This means that, in effect, the system modelled to have 360 degrees of freedom has been utilized, although it was not required to tackle a 360 x 360 order eigen value problem.

Reading Table 6.8 shows that the cutout tends to reduce the frequencies, in general, and for this particular configuration, the fundamental frequency was reduced by about 3.4%, while the ring mode (nl=0) was reduced by 5.2% and the beam type mode (nl=1) reduced by 12.3%.

6.3.2. Effect of the cutout size:

This section presents the natural frequencies and mode shapes of vibration of a clamped-free cylinder with two rectangular cutouts, symmetrically located with respect to shell diameter and centred half way along the cylinder. The following three cases were used to perform such a study:

Case 1, cutout coordinates;

$x1 = 3.767$ in $(9.57 \times 10^{-2} m)$, $x2 = 7.533$ in $(0.1913 m)$

$L_c/L = 1/3$

$\theta_{11} = -15^o$ $\theta_{12} = 15^o$

Case 2, cutout coordinates:

$x1 = 3.767$ in $(9.57 \times 10^{-2} m)$ $x2 = 7.533$ in $(0.1913 m)$

$L_c/L = 1/3$

$\theta_{11} = -22.5^o$ $\theta_{12} = 22.5^o$

Case 3, cutout coordinates:

$x1 = 2.825$ in $(7.17 \times 10^{-2} m)$ $x2 = 8.475$ in $(0.215 m)$

$L_c/L = 1/2$

$\theta_{11} = -22.5^o$ $\theta_{12} = 22.5^o$

In this study the parameters of the shell are those used in the convergence study, sub section 6.3.1.

Table 6.9 presents the results of this study, obtained for 6 axial terms and 5 odd and 5 even circumferential terms in the displacement functions. As a general observation, reduction in the frequencies increased as the cutout size increased. For example, the fundamental frequency (corresponding to the mode (1, 3)) was reduced by 1.5%, 3.4%, 4.5% in case 1, 2 and 3 respectively, while the reduction in the beam type mode (1,1) frequency was 6.4%, 12.4%, 15.6% respectively. However, there are few modes where the

Dominant wave form ml nl	No Cutout	Case 1	Case 2	Case 3
1 3	816	804	788	779
1 2	876	-	846	993
1 4	1294	1072	1079	1373
1 1	1714	1605	1502	1446
1 5	2024	1988	1967	1883
2 4	2097	1703	1599	-
2 3	2159	2186	2193	2258
2 5	2583	2585	2544	-
1 6	2938	2826	2878	2830
2 6	3405	3240	3295	3248
3 4	3733	3540	3325	3086
3 5	3889	3722	3492	3411

Table 6.9

Effect of Cutout Size on the

Frequencies of a Shell With

Two Cutouts (Hz.)

frequencies increased as the size of the cutout increased. For instance, the frequencies corresponding to modes (1,4), (2,3) in case 3 are higher than those in the case of complete shell. This observation was also reported experimentally in Ref. (58), (56) and analytically in Ref. (55); physically this means that although the overall reduction in the strain energy of the system is higher than that of the kinetic energy due to the presence of the cutout, this is not true for each individual mode.

6.3.3. Effect of cutout location:

This section presents a study of the influence of the axial location of the cutout on frequencies. Two cutouts, diametrically opposite, were used to preserve the double symmetry of the structure. Three cases were presented, all the cutouts have the same size and the circumferential coordinates with the following locations:

Case 1:

$x1 = 1.767$ in $(4.49 \times 10^{-2}$m) $\qquad x2 = 5.533$ in (0.141m)

$L_c/L = 1/3$

$\theta_{11} = -22.5^{o} \qquad \theta_{12} = 22.5^{o}$

Case 2:

$x1 = 3.767$ in $(9.57 \times 10^{-2}$m) $\qquad x2 = 7.533$ in (0.1913m)

Case 3:

$x1 = 5.765$ in (0.146m) $\qquad x2 = 9.533$ in (0.242m)

The shell properties are those used in sub section 6.3.1 and the results are shown in Table 6.10.

Taking case 2, where the cutouts were centred at the middle of the shell length, as a reference, some interesting observations may be made. When the cutouts were very near to the "clamped" end - case 1 - reductions in the fundamental frequency and many other frequencies are quite clear. This phenomenon may be interpreted as follows:

As the cutouts move towards the clamped end, the structure becomes less stiff and the boundary conditions "clamped-free" tend toward "hinged-free" conditions. The cylinder with "hinged-free" end conditions has a lower frequency than that with "clamped-free" one for the same dimensions and properties.

On the other hand, when the cutouts move towards the "free" end - case 3 - an increase in frequencies is gained. This means that the structure tends to behave as a "clamped-free shorter" cylinder.

This discussion demonstates the importance of the cutout location with regards to the natural frequencies of the clamped-free cylindrical shells.

6.3.4. Effect of cutout presence on different thickness to radius ratio of cylindrical shells:

This section presents the study made to investigate the effect of cutouts on frequencies and mode shapes of

Dominant wave form ml	nl	No Cutout	Case 1	Case 2	Case 3
1	3	816	756	788	819
1	2	876	-	846	-
1	4	1294	1444	1079	1102
1	1	1714	1483	1502	1610
1	5	2024	2002	1967	1937
2	4	2097	-	1599	1854
2	3	2159	2114	2193	-
2	5	2583	2502	2544	2511
1	6	2938	2909	2878	2830
2	6	3405	3237	3295	3349
3	4	3733	3394	3325	3272
3	5	3889	3609	3492	3481

Table 6.10

Effect of Cutout Location on

the Frequencies of a Shell

With Two Cutouts (Hz.)

shells with different thickness to radius ratios, clamped-free boundary conditions. Three cases were studied and presented in Table 6.11. Two cutouts were introduced in all cases to preserve double symmetry. All shells and cutouts have the same properties and dimensions given in subsection 6.3.1., except thicknesses, h's, which vary as follows:

Case 1: $h1 = h$

case 2: $h2 = h/10$

case 3: $h3 = h/100$

where h is given in 6.3.1.

In case 1, (h1=h), the reduction in the fundamental frequency - corresponding to mode (1,3) - is 3.4%, while the maximum reduction is about 23.7% in frequency of mode (2,4). For the second case, (h2=h/10), the fundamental frequency - corresponding to mode (1,5) - is reduced by 11.7%, i.e. more than 3 times the reduction in case 1, while the maximum reduction is about 21.6% in mode (1,3). In case 3, (h3=h/100), the fundamental frequency - corresponding to mode (1,9) - is reduced by 5.6%; i.e. 1.5 times the reduction in case 1, whilst the maximum reduction is observed in mode (2,10), of the order of 30.8%.

As far as the fundamental frequencies are concerned, for given dimensions of a shell and cutouts, the effect of such cutouts on these frequencies has a maximum value for certain thickness to radius ratio. For the present

Case 1 h				Case 2 h/10				Case 3 h/100			
ml	nl	No cutout	With cutout	ml	nl	No cutout	With cutout	ml	nl	No cutout	With cutout
1	3	816	788	1	5	273	241	1	9	89	84
1	2	876	846	1	4	304	400	1	8	92	86
1	4	1294	1079	1	6	322	315	1	10	96	99
1	1	1714	1502	1	7	414	413	1	7	105	95
1	5	2024	1967	1	3	458	359	1	11	108	107
2	4	2097	1599	1	8	534	533	1	6	134	148
2	3	2159	2193	1	9	673	689	1	5	185	156
2	5	2583	2544	2	7	699	658	2	11	261	256
1	6	2938	2878	2	8	713	713	1	4	277	---
2	6	3405	3295	2	6	776	---	2	10	298	206
3	4	3733	3325	2	9	793	798	2	9	353	347
3	5	3889	3492	1	2	834	687	1	3	453	375

Table 6.11

Effect of Cutout on Frequencies of Different Thickness to Radius Ratios of Shells (Hz.)

configuration, to obtain such a ratio, intermediate thickness to radius ratios should be investigated in some detail.

In this section, the effect of cutout on vibration of clamped-free cylindrical shell was studied. All the previous results were obtained for the symmetric modes, so the effect of cutouts on torsion modes was not observed. Such an effect as well as some other parameters will be investigated in section 6.5, but the next section will be concerned with the statics and dynamics of "clamped-supporting heavy mass" cylindrical shell.

6.4 Clamped-Supporting a Heavy Mass Cylindrical Shell:

In the practical situation, the function of the bell-housing type pump mounting is to support the pump, which in turn has a great effect on the mechanical behaviour of the mounting itself. In the present section such an effect on both the static and free vibration characteristics of the mounting is investigated. But first a convergence study was performed to determine the suitable number of terms in the displacement function series in order to obtain a reasonable estimate of the upper bound for the lowest frequency; in free vibration.

6.4.1. Convergence study:

Investigation of the assumed displacement functions for symmetric modes for the 'clamped-supporting heavy mass" boundary condition - equation 3.42, Chapter three - showed

that the symmetric pure axial modes, u^{sA}, are uncoupled from other symmetric modes which allows one to calculate the frequencies in 2 stages:

1. those associated with u^{sA}

2: those associated with u^{sR}, v^{s}, w^{s},

remembering that v^{s} and w^{s} have the same generalized coordinate, q^{sc} - see subsection 3.9.2.

Table 6.12 shows the results of a convergence study of the frequencies of vibration of a "clamped-supporting heavy mass" shell, symmetric modes.

These results were obtained for the following parameters:

a) For the shell

same parameters used in section 6.3

b) For the heavy mass (pump):

$l_p = 0.13$ m $\qquad M_p = 84$ kg

$I_{XX_p} = 2.15$ kg m^2 $\qquad I_{ZZ_p} = 2.6$ kg m^2

$I_{YY_p} = 2$ kg m^2

where l_p is the distance of centre of gravity of the pump from the "free" end of the shell.

The frequencies show a trend towards convergence as is clear from comparison of the results in the last two columns of Table 6.12. So the subsequent calculations will be performed by limiting the number of degrees of freedom to a maximum 90 for modes involving u^{sR}, q^{sc} and 10 for those

No pump	M=3 N=4	M=3 N=5	M=4 N=6	M=6 N=7	M=7 N=6
816(1,3)	320(1,2)	317(1,2)	312(1,1)	308(1,1)	308(1,1)
876(1,2)	1391(1,2)	1369(1,2)	1309(1,2)	1261(1,2)	1258(1,2)
1294(1,4)	4211(1,2)	4178(1,2)	4112(1,2)	4048(1,2)	4057(1,2)
1714(1,1)	4731(1,2)	4696(1,2)	4647(1,2)	4601(1,2)	4604(1,2)
2024(1,5)	5935(1,3)	5872(1,3)	5753(1,3)	5640(1,3)	5653(1,3)

Table 6.12

Convergence Study of Frequencies

for a Shell Supporting a Heavy

Mass (Hz.)

involving u^{sA}.

Investigation of Table 6.12 provides some observations which are of primary interest.

The presence of the heavy mass at the "free" end reduces the fundamental frequency by an order of 62%, compared with the "clamped-free" case. Physically this means that the contribution of the pump to the kinetic energy of the system is higher than the contribution to the strain energy through increased stiffness. But this process is reversed for higher modes where the frequencies are increased. Also there are some modes that have the same dominant generalized coordinate for certain combinations of terms used in the displacement functions. Actually such modes are not exactly the same. Investigation of the corresponding whole eigen vectors showed a different degree of coupling with other modes for certain pairs of results having the same dominant eigen vector element. This might indicate that one more parameter is required to describe each individual case. It is not very obvious how to choose this new parameter, but this might be taken to be the second dominant generalized coordinate beside the first one, to obtain such a distinction between different modes. A similar situation was facing Brogan et al (58), but they offered no suggestions to overcome such difficulties either. However, for the present purpose, it is not too important since the frequencies are of the prime interest,

even though a further examination might be useful.

6.4.2. Static Response:

In this subsection the static response of the bell housing pump mounting due to the weight of the pump is investigated. The parameters of the shell and the pump are those used in subsection 6.4.1. Figures 6.1 to 6.6 show such a response.

Investigation of Figure 6.1 shows the displacement pattern in which the negative radial movement is the dominant deflection - in the plane "θ=0". Actually the displacement in that plane is a resultant of the radial and axial movements. It is also clear that the rate of change of the radial movement increases as x increases, but near to the "free" edge such rate decreases. This upward "bend" at x=L indicates that the "free" edge is close to a vertically "guided" edge rather than being "free". In the plane "x=L" both axial and radial displacements are proportional to cosθ, while the tangential movement is proportional to sinθ. This displacement pattern at "x=L" is expected due to the restriction imposed on the "free" edge of the shell because of the presence of the pump.

Also in the plane "θ=0" the rate of change of u with respect to x has its maximum value at the fixed end; x=0, gradually decreases up to zero, and then has a negative value near the "free" edge. Such changes in

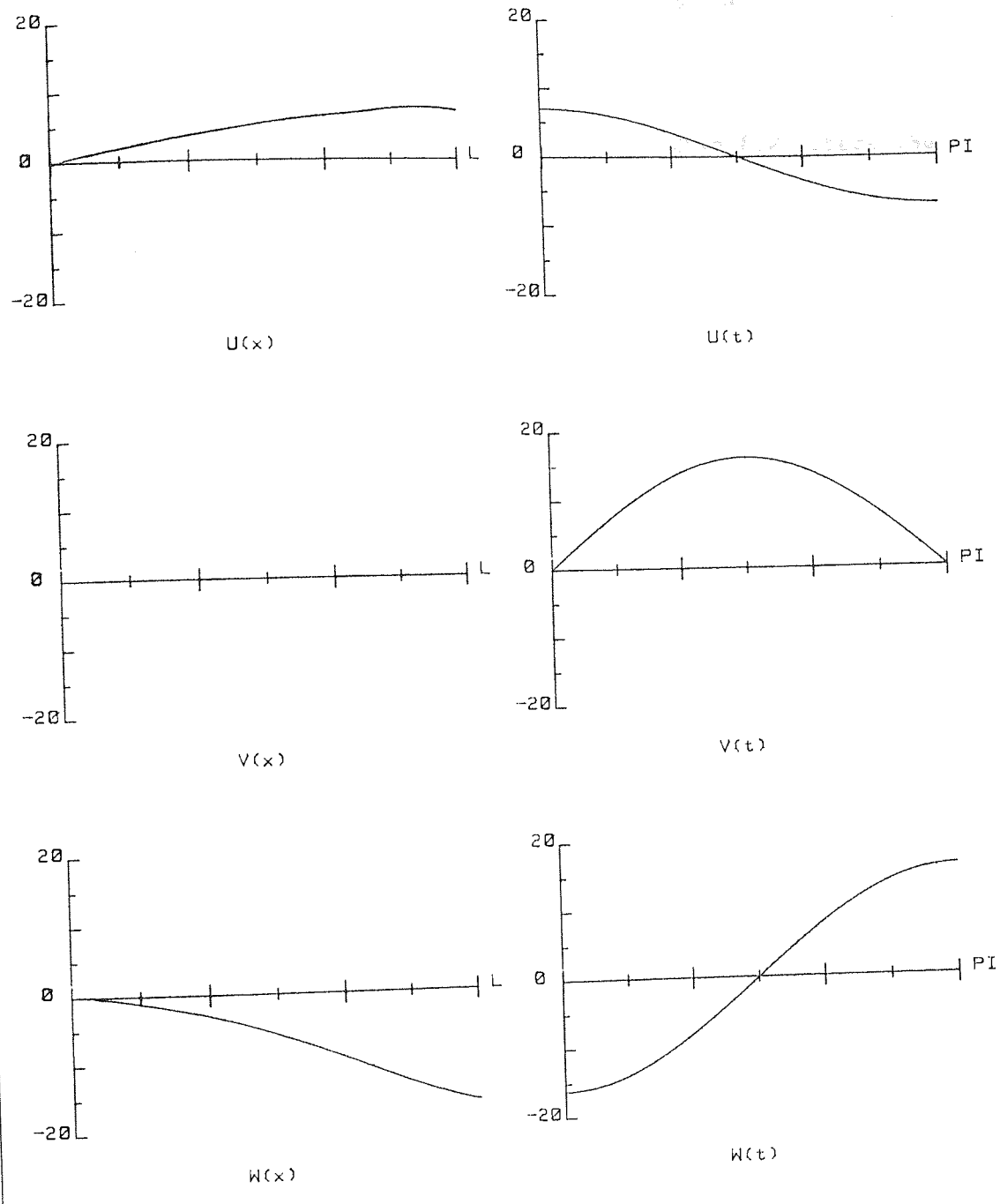

a) theta= 0^{o}

b) x/L= 1

Scale:

1mm= 1.0E-07 m

Fig. 6.1 Displacement Patterns of the Static Response of a Clamped-Supporting Heavy Mass Shell

$\frac{\partial u}{\partial x}$ ($= \bar{e}_{xx}$) can be seen clearly in Figure 6.2, where the strains were shown.

Figure 6.3 shows the membrane stress resultants. In the plane "θ=0" N_x has its maximum positive value (tension) at "x=0", gradually decreases to zero and then has a negative value (compression) near the "free" edge, x=L. This indicates, again, that the "free" edge is vertically guided. The inexact similarity between N_x (Figure 6.3) and $\bar{e}_{xx}$ (Figure 6.2) is due to the Poisson effect, since N_x is proportional to "$\bar{e}_{xx} + \nu\bar{e}_{\theta\theta}$" - see equation 3.12.a, Chapter three. But a complete similarity between N_x and $\bar{e}_{xx}$ is found in the plane "x=L", where $\bar{e}_{\theta\theta}=0$.

Note: "$\bar{e}_{\theta\theta}=0$" at x=L is a by-product of the constraint imposed on the shell at the "free" edge.

The Poisson effect can be traced through other membrane stress resultants as well; in particular for $N_{\theta\theta}$, $\bar{e}_{\theta\theta}$ and $\bar{e}_{xx}$. While $\bar{e}_{\theta\theta}=0$ in the plane "x=L", $N_{\theta\theta}$ has a value proportional to $\nu\bar{e}_{xx}$. The complete similarity between $N_{\theta\theta}$ and $\bar{e}_{xx}$ in the plane "x=L" is quite clear in Figures 6.2 and 6.3. In the plane "θ=0" both $\bar{e}_{x\theta}$ and $N_{x\theta}$ are zeros due to the symmetry of the structure and the applied load with respect to this plane.

Figure 6.5 shows the bending and twist stress resultants. In the plane "θ=0", M_x has its utmost negative value at x=0, gradually increases to zero and then

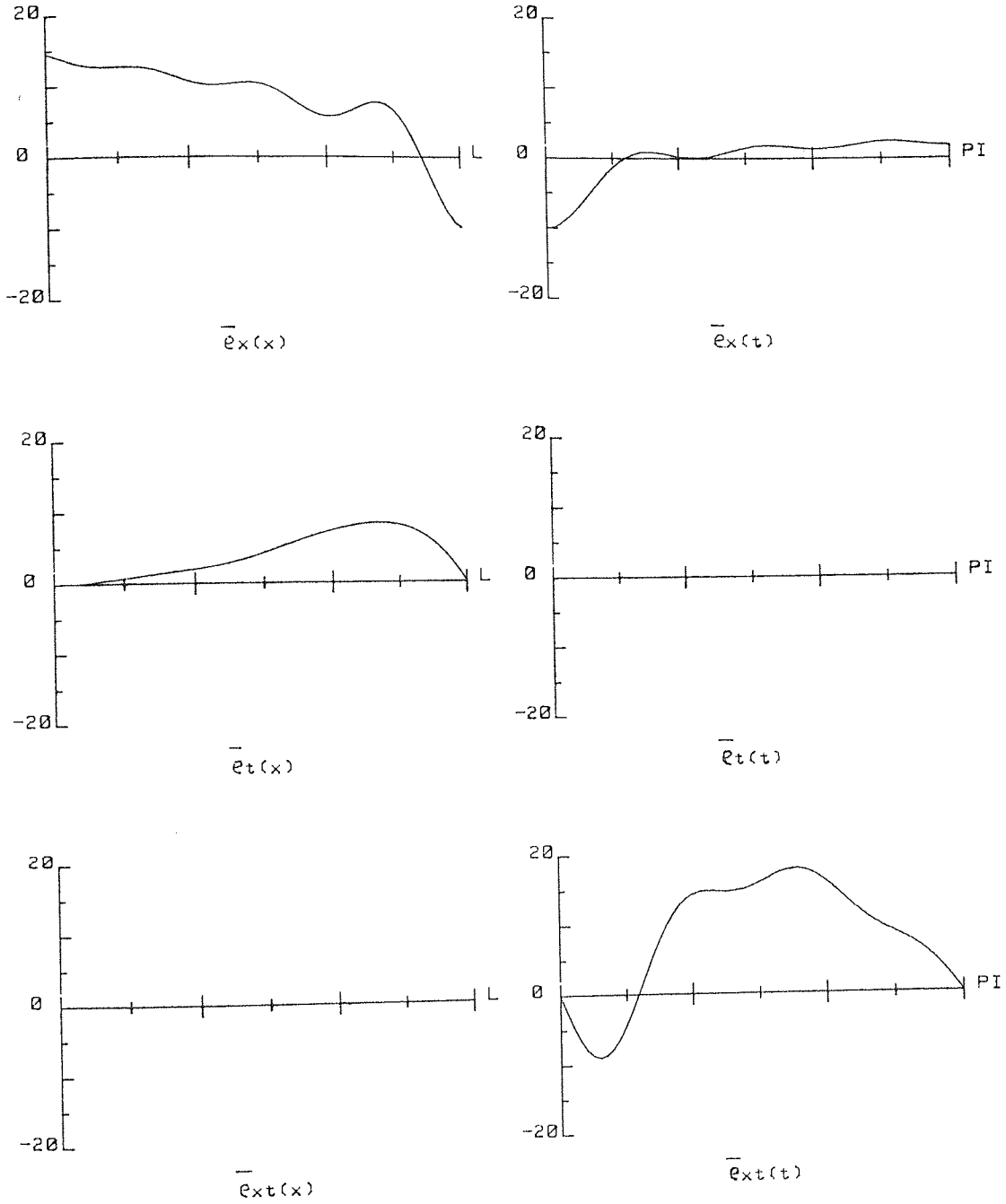

a) theta= 0^{o} b) x/L= 1

Scale:

1mm= 3.0E-07

Fig. 6.2 Membrane Strains of the Static Response of a Clamped-Supporting Heavy Mass Shell

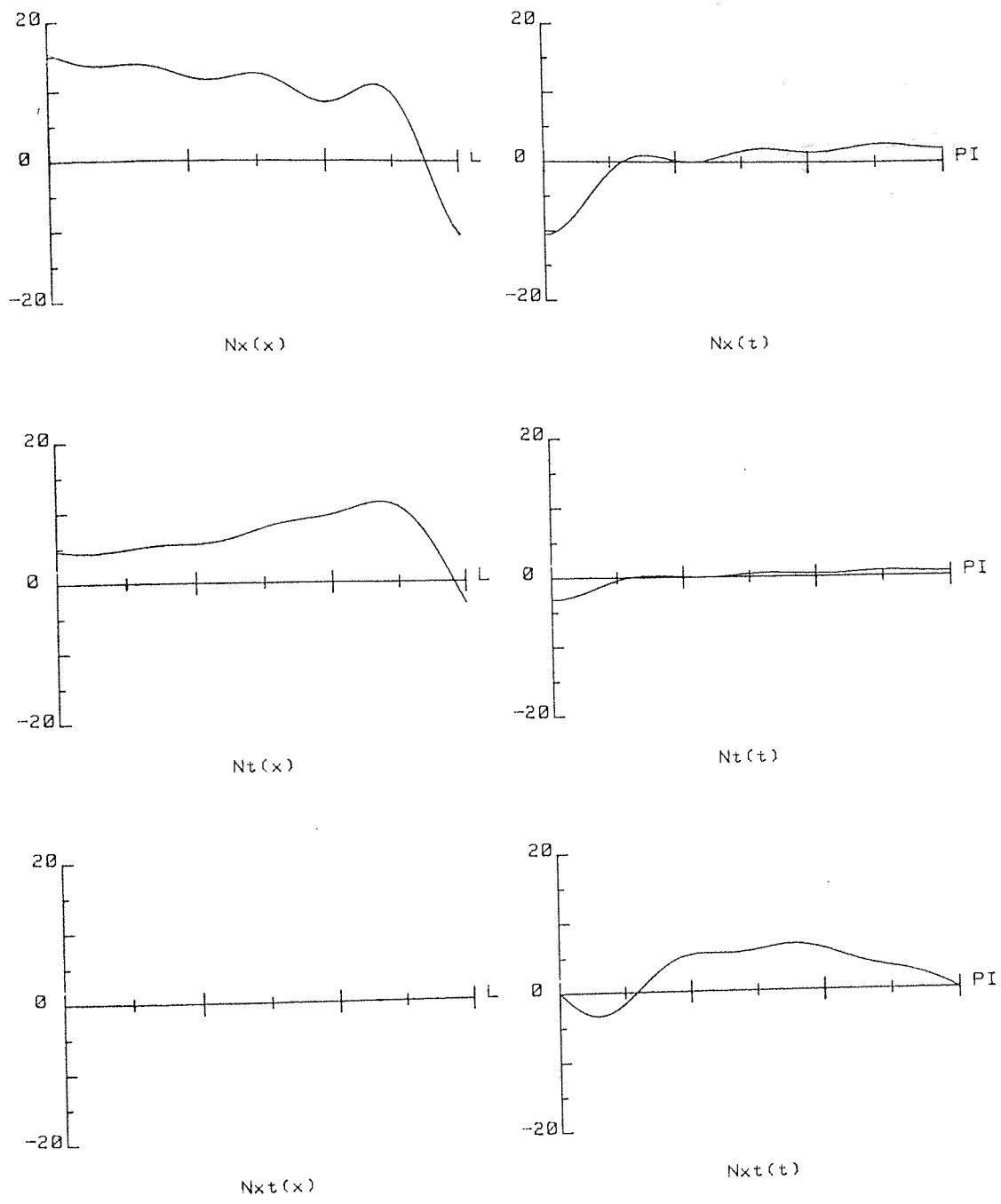

a) theta= 0°

b) x/L= 1

Scale:

1mm= 4.0E+02 N/m

Fig. 6.3 Membrane Stress Resultants of the Static Response of a Clamped-Supporting Heavy Mass Shell

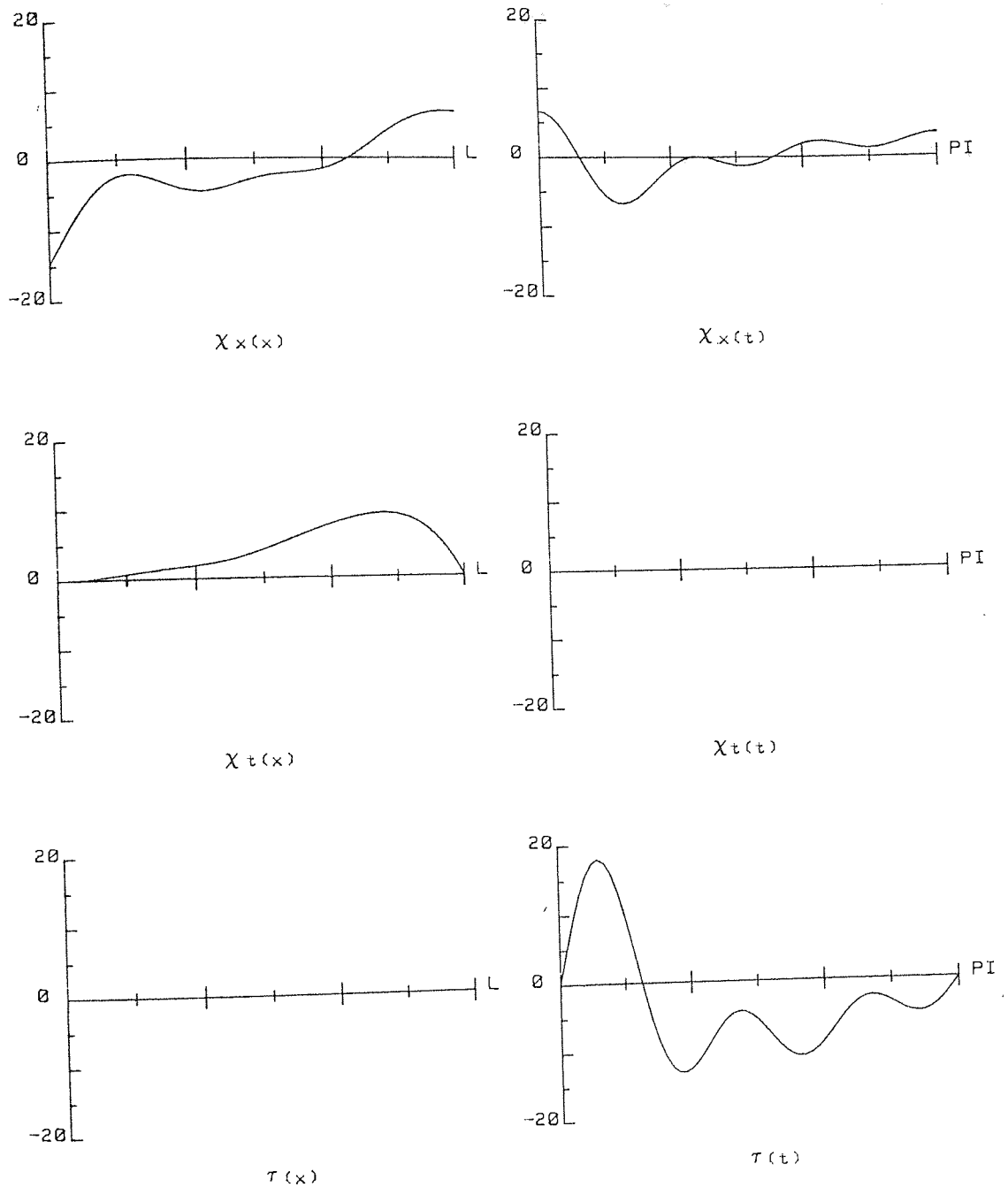

a) theta= 0^{0}

b) x/L= 1

Scale:

1mm= 1.0E-05 /m

Fig. 6.4 Changes of Curvature and Twist of the Static Response of a Clamped-Supporting Heavy Mass Shell

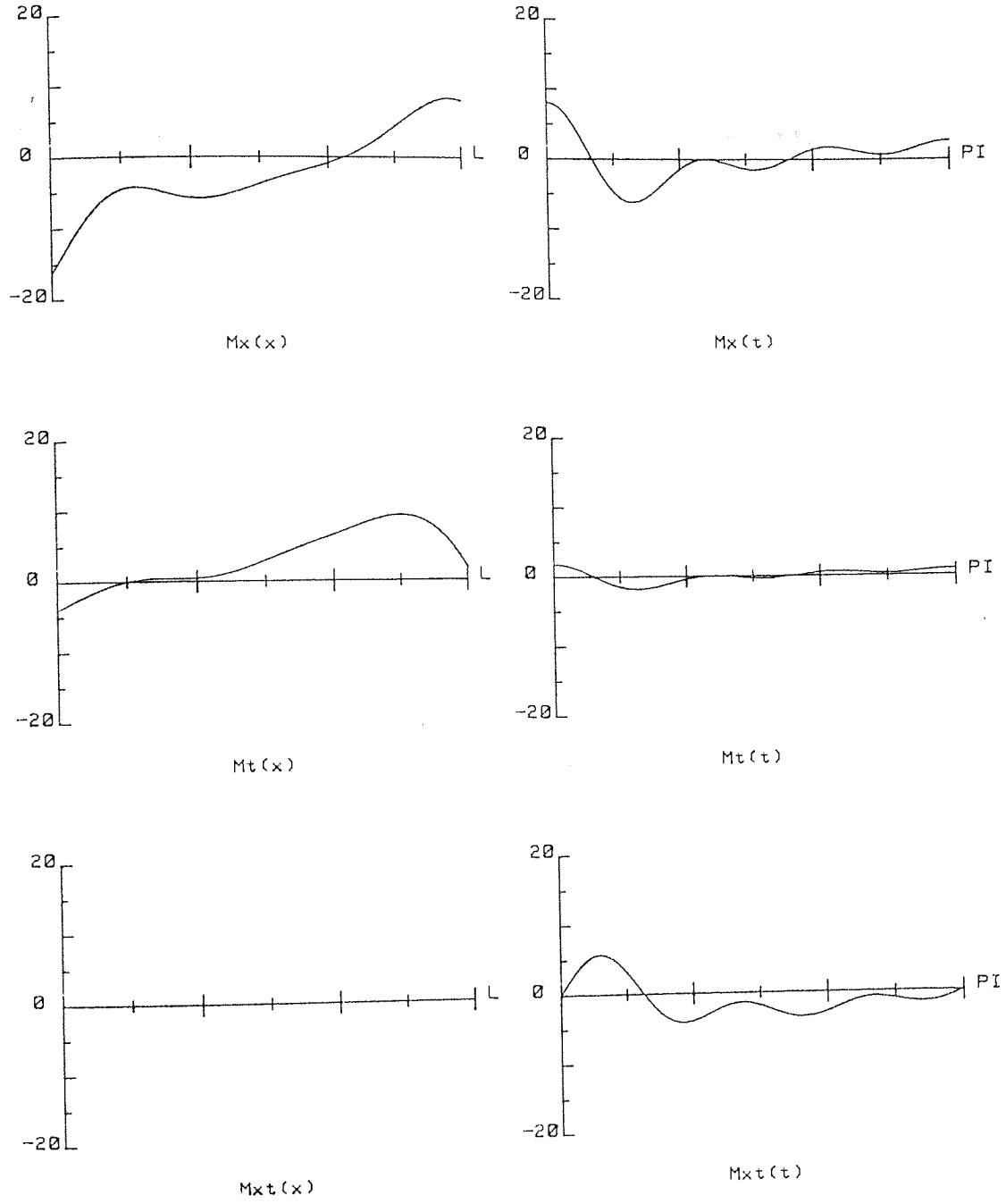

a) theta= 0^{0}

b) x/L= 1

Scale:

1mm= 5.0E-02 N.m/m

Fig. 6.5 Moment Stress Resultants of the Static Response of a Clamped-Supporting Heavy Mass Shell

has a positive value near the "free" edge, which indicates that the "free" edge is bent upward. Comparison of M_x (Figure 6.5) and χ_x (change of curvature in x direction, Figure 6.4) shows a similarity to a certain extent. The inexact similarity is due to the Poisson effect since M_x is proportional to "$\chi_x + \nu\chi_\theta$" - see equation 3.12.d, Chapter three. A similar discussion to that held for the direct stress resultants, N_x, N_θ can be done here to clarify the Poisson effect on the bending stress resultants M_x and M_θ. $M_{x\theta}=0$ in the plane "$\theta=0$" due to the symmetry of the structure and the applied load with respect to this plane.

Figure 6.6 shows the stress pattern for the shell at the outer fibre, $z=h/2$. It is interesting to notice the similarity between these graphs and those of Figure 6.3. The effect of the moments on the stresses is negligible compared with the effect of the direct stress resultants, and most of the applied load is carried by the membrane forces. This fact gives the shells a substantial advantage over the plates. In the case of plates the lateral load is carried by bending and twisting moments, accompanied by shearing forces, while a shell is able to transmit the surface load by membrane stresses, which makes shells much more rigid than plates, under the same condition of loading.

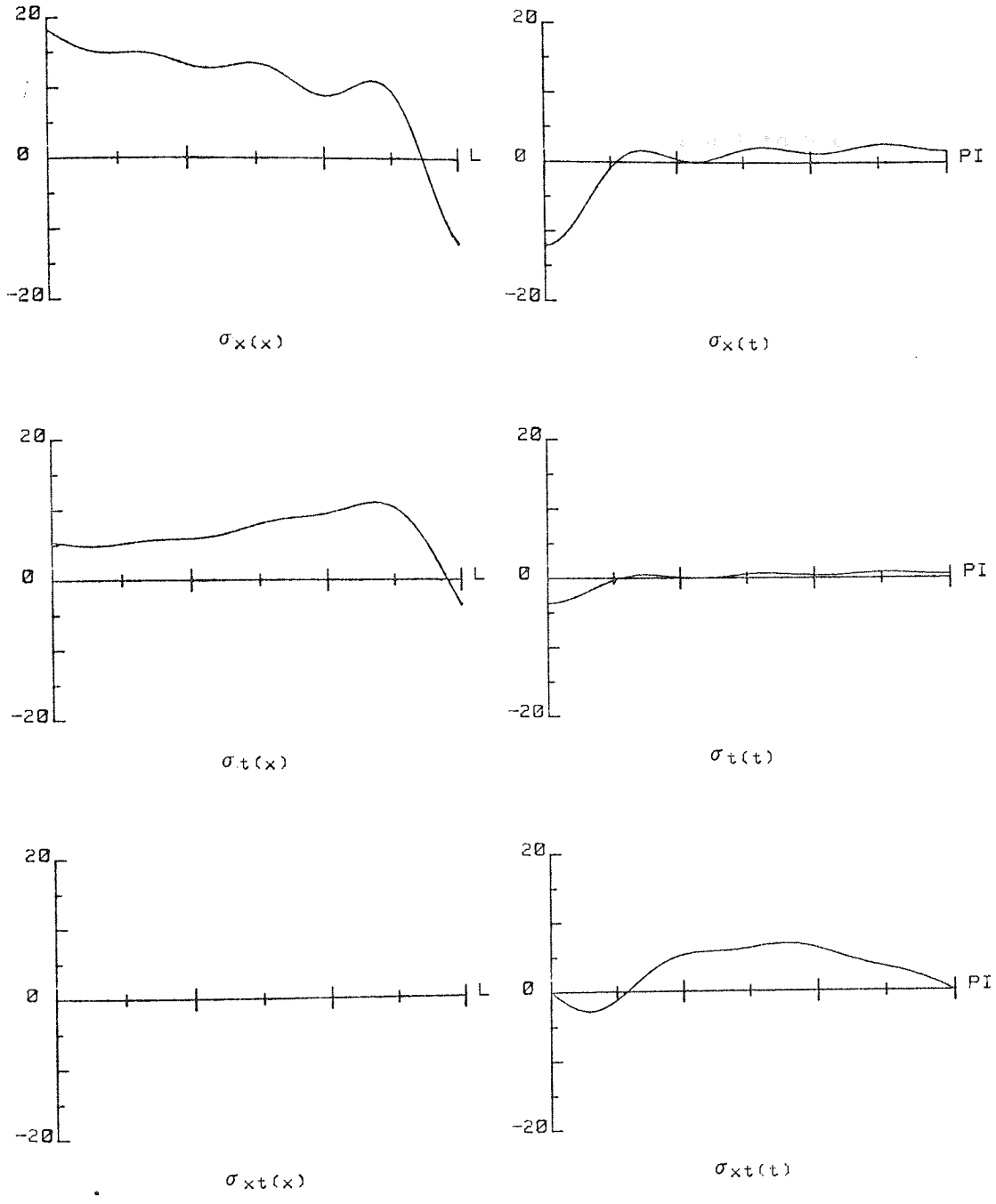

a) theta= 0°

b) x/L= 1

Scale:

1mm= 5.0E+04 N/m2

Fig. 6.6 Stress Patterns of the Static Response of a Clamped-Supporting Heavy Mass Shell

An inclusive look at the Figures 6.1 to 6.6 shows that although the displacement graphs are smooth, the subsequent graphs have more or less sort of fluctuations over some mean values. This is due to the fact that differentiation of a convergent finite series tends to worsen the rate of convergence. However, the accuracy of the present solution may be examined by the following check of the pump equilibrium.

The pump suffers the following loads and moment:

1. Its own weight, $- M_p g = -824.4$ N
2. Vertical component of the inplane shearing force of the shell at x=L, $\int_0^{2\pi} N_{x\theta} R \sin\theta \, d\theta$
3. Moment imposed on the pump due to the axial force of the shell at x=L, $\int_0^{2\pi} N_x R^2 \cos\theta \, d\theta$

For the pump to be in equilibrium, the following conditions must be fulfilled:

$$M_p g = \int_0^{2\pi} N_{x\theta} R \sin\theta \, d\theta \qquad 6.1$$

$$M_p g l_p = \int_0^{2\pi} N_x R^2 \cos\theta \, d\theta \qquad 6.2$$

Note: Sign conventions for forces and moments are given in Figure 3.4, Chapter three.

Numerical calculation of the right hand side of equation 6.1 gave a value of 902.5N which is slightly

higher than the pump weight. This discrepancy - of order 9.5% - is probably caused by differentiation of approximate functions which have been truncated and ignoring of the tilt of the originally vertical plane, x=L.

Numerical calculation of the right hand side of equation 6.2 gave a value of 95 N.m, which is slightly less than the left hand side, of value 107 N.m. The discrepancy is of order 11.2%.

It should be emphasized at this stage that these graphs give overall deflection and stress fields rather than a small local variation. But even with this fact in mind, local variation can be calculated within practical engineering accuracy as previously illustrated in the case of equilibrium of the pump.

6.4.3. Free vibration:

This section presents the study made for the free vibration of "clamped-supporting heavy mass" cylindrical shell. Both symmetric and antisymmetric modes - with respect to the plane $\theta=0$ - were investigated, and the results are presented in Table 6.13. Shell and pump parameters are those used in subsection 6.4.1.

These results were obtained in 4 steps:

Symmetric Modes		Antisymmetric Modes	
plain cylinder	cylinder & pump	plain cylinder	cylinder & pump
816(3, 1 3)	308(3, 1 1)	816(3, 1 3)	521(3, 1 2)
876(3, 1 2)	1131(2, 1 0)	876(3, 1 2)	576(2, 1 0)
1294(3, 1 4)	1258(3, 1 2)	1294(3, 1 4)	660(3, 1 1)
1714(3, 1 1)	4057(3, 1 2)	1714(3, 1 1)	4060(3, 1 2)
2024(3, 1 5)	4604(3, 1 2)	2024(3, 1 5)	4570(3, 1 2)
2097(3, 2 4)	5653(3, 1 3)	2097(3, 2 4)	5636(3, 1 3)
2159(3, 2 3)	6107(3, 1 3)	2159(3, 2 3)	5696(2, 2 0)
2583(3, 2 5)	6965(3, 2 3)	2583(3, 2 5)	6108(3, 1 3)
2938(3, 1 6)	7209(3, 1 4)	2938(3, 1 6)	6964(3, 2 3)
		2954(2, 1 0)	7212(3, 1 4)
3405(3, 2 6)	7983(3, 1 4)	3405(3, 2 6)	7999(3, 1 4)
3733(3, 3 4)	8733(3, 1 3)	3733(3, 3 4)	8708(3, 1 3)
4391(1, 1 0)	8947(3, 1 5)		

Table 6.13

Free Vibration Frequencies of a Clamped-

Supporting Heavy Mass Cylindrical Shell (Hz.)

1. Calculation of frequencies and associated mode shapes for symmetric solution, involves the generalized coordinates of U^{sR} and q^{sc}.

2. As step 1, but for purely axial modes, involves the generalized coordinates of U^{sA}.

3. As step 1, but for antisymmetric solution, involves the generalized coordinates of U^{a} and q^{ac}.

4. As step 3, but for purely torsion modes, involves the generalized coordinates of V^{T}.

Figures in brackets associated with frequencies in Table 6.13 to identify the mode shapes. These figures should be interpreted as follows:

For plain cylinder (both symmetric and antisymmetric modes), first figure gives the type of motion:

1, axial

2, circumferential

3, radial

second and third figures give the ml and nl indices of the dominant element in the eigen vector.

For cylinder supporting heavy mass; symmetric modes:

first figure gives the type of dominant motion:

1, associated with U^{sR}

2, associated with U^{sA} (pure axial)

3, associated with q^{sc}

second and third figures as before.

For cylinder supporting heavy mass; antisymmetric modes:

first figure gives the type of the dominant motion:

1, associated with u^a

2, associated with V^T (pure torsion)

3, associated with q^{ac}

second and third figures as before.

Investigation of Table 6.13 can provide an interesting observation. In the case of symmetric modes, presence of the pump reduces both the fundamental frequency by 62% and the first purely axial frequency by 74%. This reduction physically means that the pump contribution to the kinetic energy for these modes is higher than the contribution to the strain energy due to the constraint imposed on the shell at the "free" end. But for other modes, this process is reversed, and a substantial increase in other frequencies is quite clear. Also it might be noticed that the first beam type mode - indicated by (3, 1 1) - became the fundamental mode.

For the antisymmetric modes, a reduction of order 36% and 80% is noticed in the fundamental and the first torsion frequencies respectively. Also there is a reduction of order 61% in the frequency of the first beam type mode - (3, 1 1). Second torsion mode frequency is reduced from 8805 Hz (not shown in Table 6.13) to 5696 Hz, i.e. reduced by about 35%. For other modes, a substantial increase in frequencies may be observed.

One point should be clarified at once. It is noticed that there are some modes having the same identified parameters. For example the third, fourth and fifth modes in the symmetric solution of cylinder supporting heavy mass. Actually they are not the same, but each of themhas a different degree of coupling with other modes. Figures 6.8 to 6.10 present these modes. It is clear that none of these three modes looks similar to the other, but their eigen vectors have the same maximum elements in corresponding location. Investigation of their eigen vectors showed that these modes may be expressed, mathematically as follows:

a) mode 1258(3, 1 2) has the form:

$$u(x,\theta)=\Phi_1'(x)\{-.111\left[(1-x/L)\cos\theta+\cos\theta\right]+.024\left[(1-x/L)\cos2\theta+\cos\theta\right] + \text{---} \}$$

$$v(x,\theta)=\Phi_1(x)\{\left[(1-x/L)\sin2\theta+\sin\theta\right]-.786\left[(1-x/L)\sin\theta+\sin\theta\right]+ .718\left[(1-x/L)\sin3\theta+\sin\theta\right]+.503\left[(1-x/L)\sin4\theta+\sin\theta\right]\text{---} \}$$

$$w(x,\theta)=-\Phi_1(x)\{\left[(1-x/L)\cos2\theta+\cos\theta\right]-.786\left[(1-x/L)\cos\theta+\cos\theta\right]+ .718\left[(1-x/L)\cos3\theta+\cos\theta\right]+.503\left[(1-x/L)\cos4\theta+\cos\theta\right]+ \text{---} \}$$

b) Mode 4057(3, 1 2) has the form:

$$u(x,\theta)=\Phi_1'(x)\{.092\left[(1-x/L)\cos\theta+\cos\theta\right]-.089\left[(1-x/L)\cos2\theta+\cos\theta\right] + \text{---} \}$$

$$v(x,\theta)=\Phi_1(x)\{-[(1-x/L)\sin 2\theta+\sin\theta]+.82[(1-x/L)\sin\theta+\sin\theta]+---\}$$

$$+\Phi_2(x)\{.256[(1-x/L)\sin 2\theta+\sin\theta]-.173[(1-x/L)\sin\theta+\sin\theta]+--\}$$

$$w(x,\theta)=\Phi_1(x)\{[(1-x/L)\cos 2\theta+\cos\theta]-.82[(1-x/L)\cos\theta+\cos\theta]+---\}$$

$$-\Phi_2(x)\{.256[(1-x/L)\cos 2\theta+\cos\theta]-.173[(1-x/L)\cos\theta+\cos\theta]+---\}$$

c) Mode 4604(3, 1 2) has the form:

$$u(x,\theta)=\Phi_1'(x)\{-.058[(1-x/L)\cos 2\theta+\cos\theta]+.016[(1-x/L)\cos 3\theta+\cos\theta]$$

$$+\ ---\ \}$$

$$v(x,\theta)=-\Phi_1(x)\{[(1-x/L)\sin 2\theta+\sin\theta]+.186[(1-x/L)\sin\theta+\sin\theta]+---\}$$

$$-\Phi_2(x)\{0.302[(1-x/L)\sin 3\theta+\sin\theta]+.193[(1-x/L)\sin 4\theta+\sin\theta]$$

$$+\ ---\ \}$$

$$w(x,\theta)=\Phi_1(x)\{[(1-x/L)\cos 2\theta+\cos\theta]+.186[(1-x/L)\cos\theta+\cos\theta]+---\}$$

$$+\Phi_2(x)\ \{.302[(1-x/L)\cos 3\theta+\cos\theta]+.193[(1-x/L)\cos 4\theta+\cos\theta]$$

$$+\ ---\ \}$$

In the above expressions, all eigen vectors were normalized such that the largest element = 1.

These expressions for different modes demonstrate the point mentioned before about various degrees of coupling between the dominant and remaining modes.

Figure 6.7 shows the first mode shape 308(3, 1 1) of the cylinder supporting heavy mass. It is interesting to notice the similarity of this mode with the static deflection curves, Figure 6.1. Actually such similarity is expected since this mode is the most flexible one to be excited. Note also that this mode is close to the mode of "clamped-guided" boundary condition beam. Mathematically, this first mode may be expressed as:

$$u(x,\theta)=\Phi_1'(x)\{0.147[(1-x/L)\cos\theta+\cos\theta]+0.0327[(1-x/L)\cos2\theta+\cos\theta]+\text{---}\ \}$$

$$v(x,\theta)=\Phi_1(x)\{[(1-x/L)\sin\theta+\sin\theta]+0.806[(1-x/L)\sin2\theta+\sin\theta]+0.606[(1-x/L)\sin3\theta+\sin\theta]+0.434[(1-x/L)\sin4\theta+\sin\theta]+\text{---}\ \}$$

$$w(x,\theta)=-\Phi_1(x)\{[(1-x/L)\cos\theta+\cos\theta]+0.806[(1-x/L)\cos2\theta+\cos\theta]+0.606[(1-x/L)\cos3\theta+\cos\theta]+0.434[(1-x/L)\cos4\theta+\cos\theta]+\text{---}\ \}$$

The above expressions also show the degree of coupling between the different assumed modes of vibration. The neglected terms in these expressions have generalized coordinates of order 0.3 or less, compared with unity.

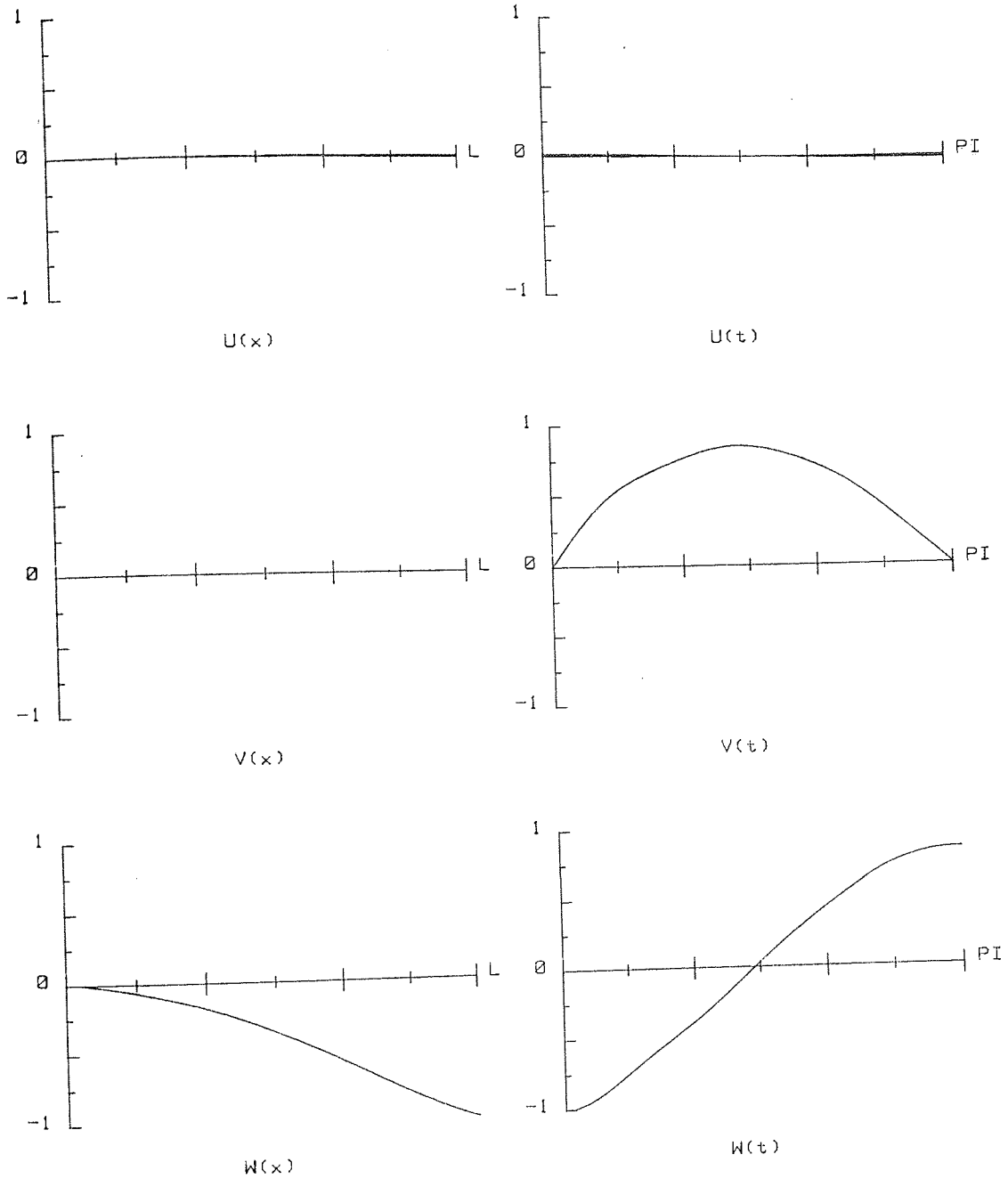

a) theta= 0°

b) x/L= .75

f= 308 Hz

Fig. 6.7 Fundamental Wave Forms of a Cylindrical Shell

Supporting Heavy Mass, Symmetric Mode

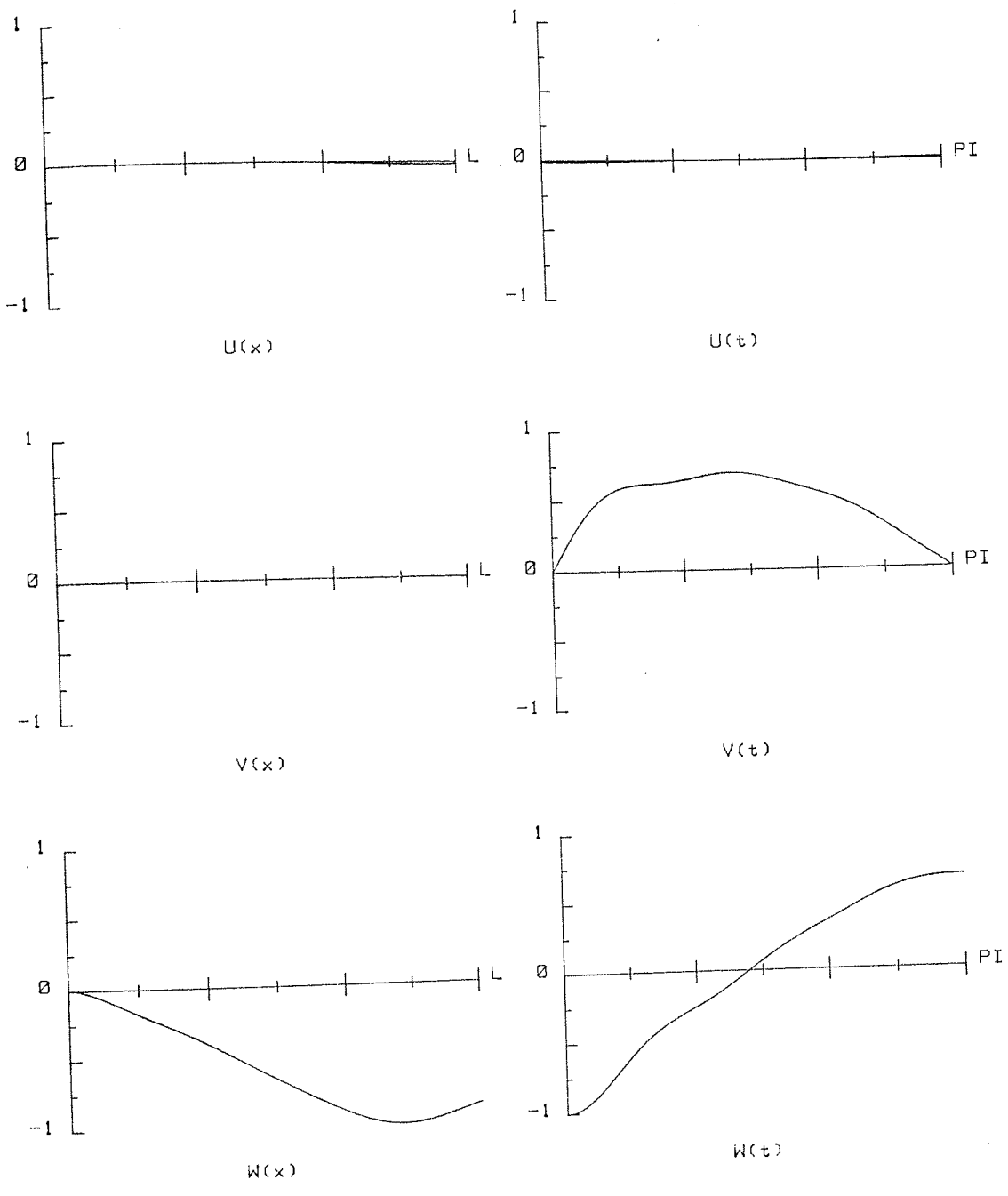

a) theta= 0^{0}

b) x/L= .75

f= 1258 Hz

Fig. 6.8 Third Symmetric Wave Forms of a Cylindrical Shell Supporting Heavy Mass

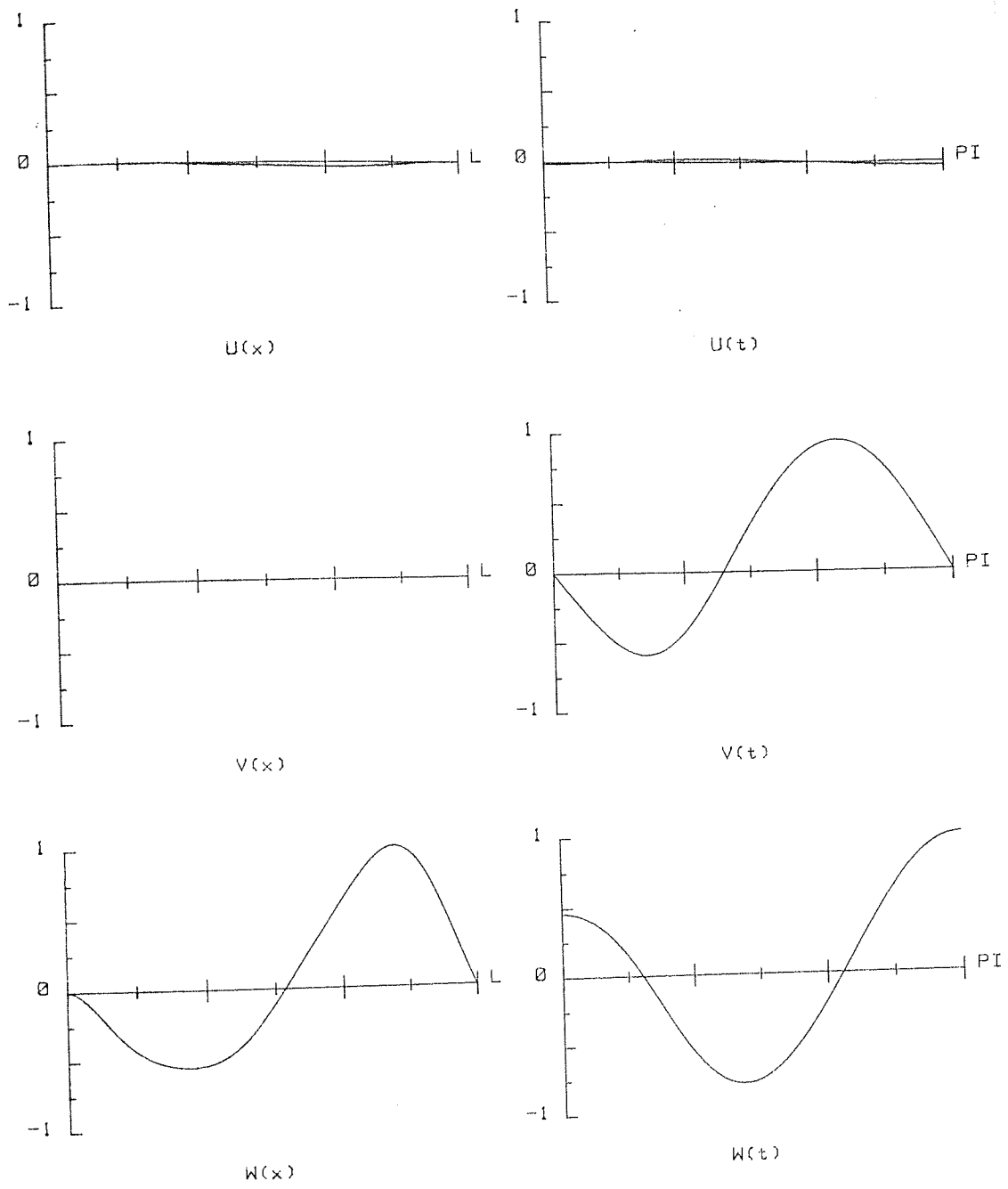

a) theta= 0^{o}

b) x/L= .75

f= 4057 Hz

Fig. 6.9 Fourth Symmetric Wave Forms of a Cylindrical Shell Supporting Heavy Mass

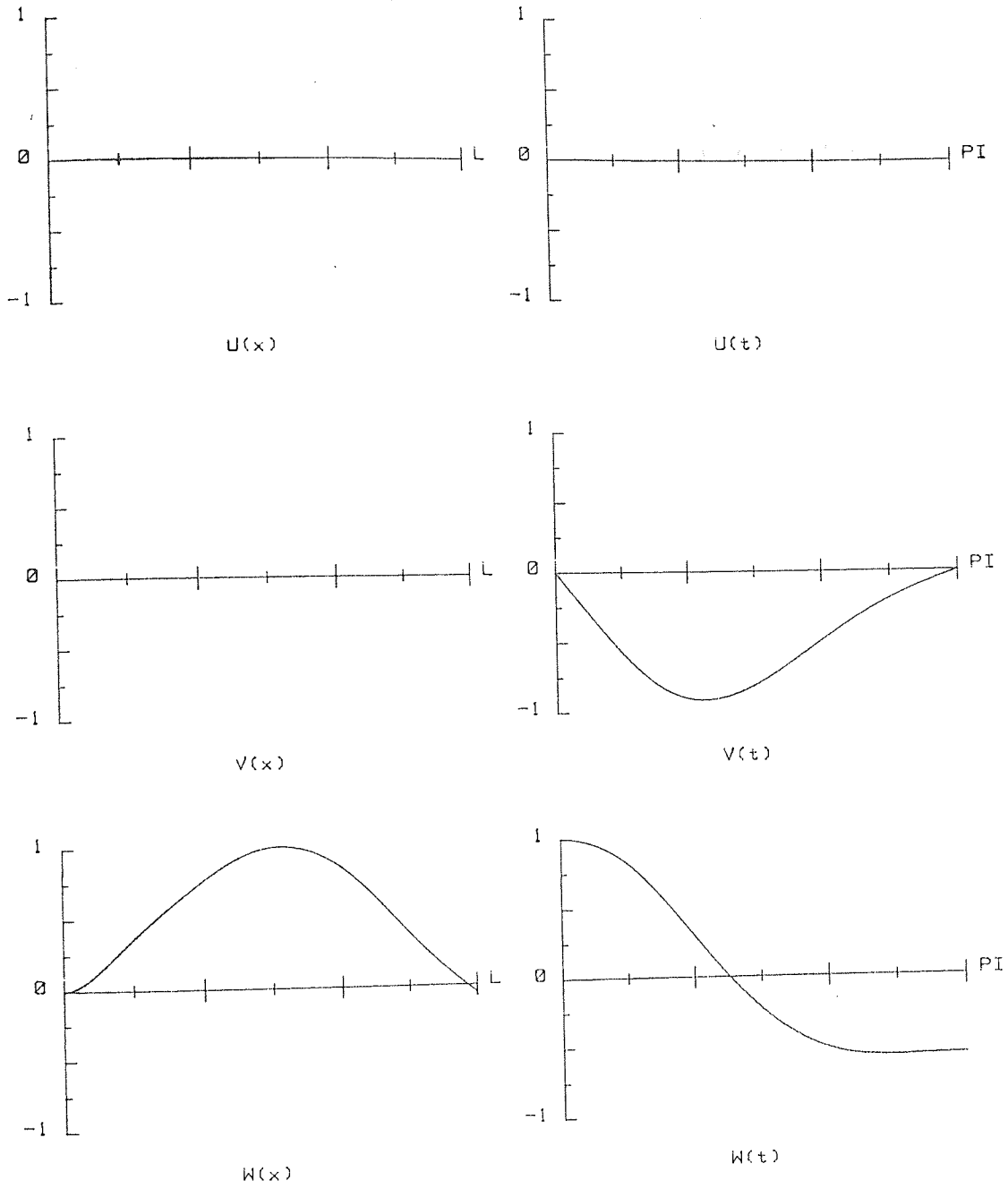

a) theta= 0^{0}

b) x/L= .75

f= 4604 Hz

Fig. 6.10 Fifth Symmetric Wave Forms of a Cylindrical Shell Supporting Heavy Mass

In this section, the static response and free vibration of cylindrical shell supporting heavy mass were examined. The phenomenon of coupled modes was also demostrated. The significance of this phenomenon in engineering applications will be discussed later. The accuracy of results obtained in this section satisfies practical engineering purpose, particularly for design practice.

6.5 Investigation of a Specific, Commercially Available Bell-housing:

In this section numerically and experimentally determined natural frequencies and associated mode shapes of a commercial bell-housing pump mounting are presented. The model consists of a circular cylindrical shell with two diameterally opposite cutouts, reinforced by two end circular rings and four longitudinal equally spaced stringers. Shell parameters are the same as those used in subsection 6.4.1. Dimensions details of rings, stringers and cutouts are given in Figure 5.1, Chapter five and listed below:

For rings: only the smaller ring details are given, since the other one was used for clamping the structure

$R_r = 0.105m$

$A_r = 9x10^{-4}m^2$

$I_{xx_r} = 2.7x10^{-7}m^4$

$I_{zz_r} = 1.687x10^{-8}m^4$

$J_r = 5.62x10^{-8}m^4$

For the stringer:

$A_s = 3.87 \times 10^{-4} m^2$ $\quad I_{yy_s} = 5.963 \times 10^{-8} m^4$

$I_{zz_s} = 2.6133 \times 10^{-9} m^4$ $\quad J_s = 8.3 \times 10^{-9} m^4$

$\bar{z}_s = 2.475 \times 10^{-2} m$

For cutouts:

x1 = 0.025 m $\quad$ x2 = 0.18 m

$\theta_{11} = -21.5^o$ $\quad \theta_{12} = 21.5^o$

6.5.1. Computer predicted results:

This subsection is concerned with the predicted natural frequencies and mode shapes of the model described above. The influence of various modifications to the structure is also shown. Table 6.14 gives results for the following different 5 cases:

1. plain clamped-free circular cylindrical shell
2. clamped-free longitudinally stiffened circular cylindrical shell
3. clamped-ring stiffened circular cylindrical shell
4. clamped-free circular cylindrical shell with 2 cutouts
5. clamped-ring stringer stiffened circular cylindrical shell with 2 cutouts.

For each of these 5 cases, the computer program

Plain Cylinder		Cylinder & Stringers		Cylinder & Ring	
Symmetric	Antisymmetric	Symmetric	Antisymmetric	Symmetric	Antisymmetric
816(3, 1 3)	816(3, 1 3)	860(3, 1 3)	860(3, 1 3)	1241(3, 1 1)	1241(3, 1 1)
876(3, 1 2)	876(3, 1 2)	869(3, 1 2)	1016(3, 1 2)	1780(3, 2 3)	1780(3, 2 3)
1294(3, 1 4)	1294(3, 1 4)	1188(3, 1 4)	1283(3, 1 4)	1888(3, 2 4)	1888(3, 2 4)
1714(3, 1 1)	1714(3, 1 1)	1649(3, 1 1)	1649(3, 1 1)	2167(3, 1 2)	2167(3, 1 2)
2024(3, 1 5)	2024(3, 1 5)	1837(3, 1 5)	1837(3, 1 5)		2403(2, 1 0)
2097(3, 2 4)	2097(3, 2 4)	2395(3, 2 3)	2169(3, 2 4)	2424(3, 2 5)	2424(3, 2 5)
2159(3, 2 3)	2159(3, 2 3)	2611(3, 1 6)	2395(3, 2 3)	2629(1, 1 0)	
2583(3, 2 5)	2583(3, 2 5)		2551(2, 1 0)	3252(3, 2 6)	3252(3, 2 6)
2938(3, 1 6)	2938(3, 1 6)	2928(3, 2 4)	2570(3, 1 6)	3459(3, 3 4)	3459(3, 3 4)
	2954(2, 1 0)	2976(3, 2 5)	3483(3, 1 7)	3580(3, 3 3)	3580(3, 3 3)
3405(3, 2 6)	3405(3, 2 6)	3243(3, 2 6)	3799(3, 2 6)	3722(3, 3 5)	3722(3, 3 5)
3733(3, 3 4)	3733(3, 3 4)	3483(3, 1 7)	3843(3, 3 4)	4299(3, 2 7)	4299(3, 2 7)

Table 6.14

Analytical Frequencies of an Actual Bell-housing (Hz.)

Cylinder with cutouts		All Structure	
Symmetric	Antisymmetric	Symmetric	Antisymmetric
753(3, 1 3)	692(3, 1 3)	1030(3, 1 1)	837(3, 1 1)
940(3, 1 2)	746(3, 1 2)	1250(3, 1 2)	1752(3, 1 2)
1345(3, 1 4)	1031(3, 1 1)	1950(3, 2 3)	1928(3, 2 4)
1452(3, 1 1)	1262(3, 1 4)	2163(3, 2 4)	1948(3, 2 3)
1916(3, 1 5)	1862(3, 2 3)		2277(2, 1 0)
2139(3, 2 3)	2010(3, 1 5)	2304(3, 2 1)	2574(3, 2 5)
2235(3, 2 1)	2012(3, 2 4)	2815(3, 2 6)	2865(1, 1 1)
2865(3, 1 6)	2571(3, 2 5)	3010(1, 1 0)	
	2615(2, 1 0)	3042(1, 1 1)	3113(3, 2 6)
2954(3, 3 4)	2918(3, 3 3)	3325(1, 1 2)	3348(3, 3 4)
3222(3, 2 5)	2961(3, 1 6)	3927(3, 3 6)	3502(3, 3 4)
3266(3, 2 6)	3382(3, 3 4)	5381(3, 3 1)	4179(3, 3 2)

Table 6.14 (Continued)

Analytical Frequencies of an Actual Bell-housing (Hz.)

was run 4 times, as follows:

a) for symmetric modes with even circumferential waves

b) for symmetric modes with odd circumferential waves

c) as (a) but for antisymmetric modes

d) as (b) but for antisymmetric modes

Each time, 90 degrees of freedom were used to describe the case. In other words each case was effectively modelled to have 360 degrees of freedom.

In the following discussion, the results for a plain cylinder will be taken as a reference for comparison. Also the mode shape identifier figures, the figures in brackets, have the same meanings as those in section 6.4.3; plain cylinder.

In the case of a plain cylinder, the structure is axisymmetric and there is no coupling between the different modes in the circumferential direction. The beam functions satisfy the "free" end condition for the shell in only an approximate manner; certain forces and moments are not zero as they should be. These conditions are to be satisfied, partially, in a limiting sense as a by-product of minimizing the action integral with respect to the finite generalized coordinates. So the actual "free" end is "partially" constrained in the analytical model. This leads to some degree of weak coupling in the axial modes of the

plain clamped-free cylinder. Figure 6.11 shows a typical antisymmetric mode shape for a plain cylinder. This is the 5th mode (3, 1 5) in the second column of Table 6.14. Mathematically this mode shape has the form:

$$u(x,\theta) = 0.19\ \Phi_1'(x)\ \sin 5\theta$$

$$v(x,\theta) = \{0.2\ \Phi_1(x) + 0.021\ \Phi_2(x)\}\ \cos 5\ \theta$$

$$w(x,\theta) = \{\Phi_1(x) + 0.11\ \Phi_2(x) + 0.028\ \Phi_3(x)\}\ \sin 5\ \theta$$

These expressions show that there is a weak coupling between u, v and the dominant radial, w, of the order of 0.2, and also a coupling in the axial mode functions of the order of 0.1.

Adding the stringers destroys the axisymmetry in the structure and results in a coupling of modes in the circumferential direction. This phenomenon may be seen in Figure 6.12 which represents a typical symmetric mode (3, 1 6) - mode 7 in the third column, Table 6.14. Mathematically, this mode shape has the form:

$$u(x,\theta) = -\Phi_1'(x)\ (0.13\ \cos 6\ \theta - 0.07\ \cos 2\ \theta)$$

$$v(x,\theta) = -\Phi_1(x)(0.165\sin 6\theta - 0.02\ \sin 2\theta) - 0.03\Phi_2(x)\sin 6\theta$$

$$w(x,\theta)=\Phi_1(x)(\cos 6\theta - 0.075\cos 2\theta - 0.06\cos 10\theta) + 0.19\Phi_2(x)\cos 6\theta$$

These expressions show the coupling of terms involving 2θ, 6θ, and 10θ. Second beam function appearance in the radial movement, w, may be due to the reason explained in the case of plain cylinder; i.e. the boundary condition

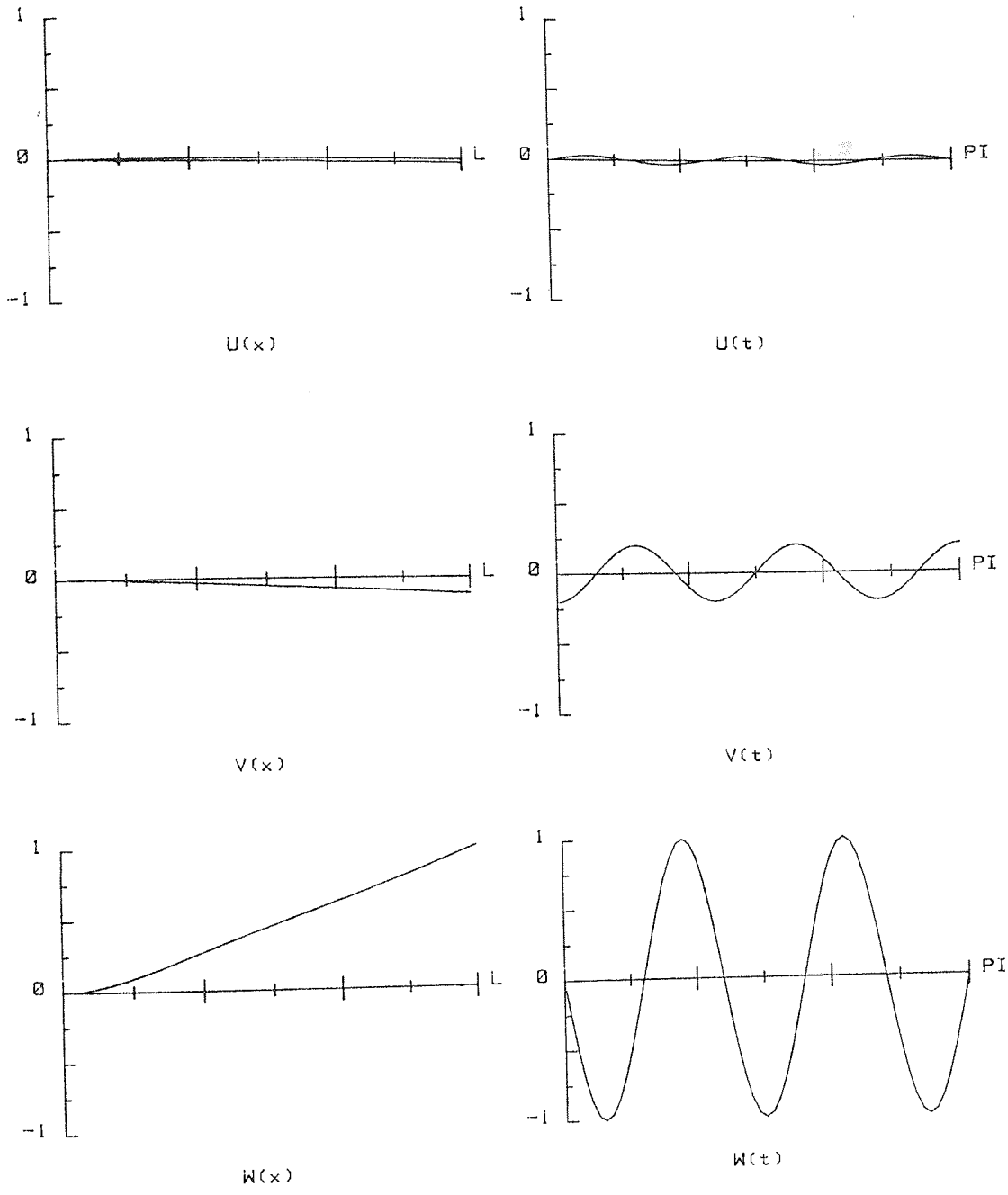

a) theta= 60^{0}

b) x/L=.75

f= 2024 Hz

Fig. 6.11 Wave Forms of a Plain Cylindrical

Shell ,Antisymmetric Mode

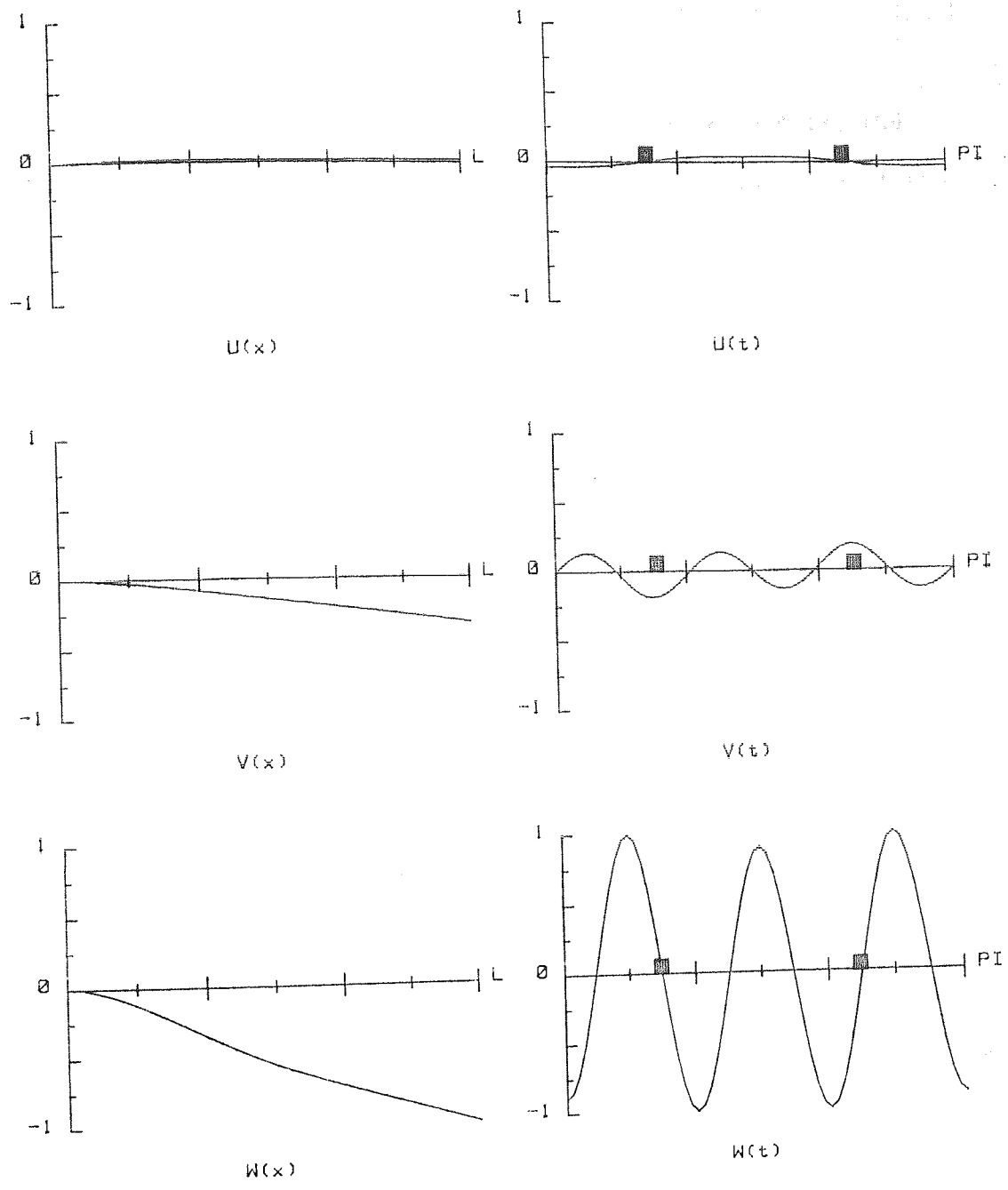

▩ Stringer Location

a) theta= 50^{0}

b) x/L=.75

f= 2611 Hz

Fig. 6.12 Wave Forms of a Stringer Stiffened

Cylindrical Shell ,Symmetric Mode

at the free end. As is evident from Table 6.14, the overall effect of adding stringers is a lowering of the frequencies. For example the first torsion frequency is reduced from 2954 Hz to 2551 Hz. Physically this means that the stringers contribute more to the kinetic energy than to the strain energy. But this is not true for all modes, for instance, the fundamental frequency was increased from 816 Hz to 860 Hz.

Adding the circular end ring to the plain cylinder preserves the axisymmetric shape of the structure, so there is no coupling in modes in the circumferential direction, but there is a strong axial modal coupling. This fact may be seen in Figure 6.13 which presents the antisymmetric mode (3, 1 2) - 4th mode in column 6, Table 6.14. Mathematically this mode shape has the form:

$$u(x,\theta) = \{-.21\Phi_2'(x) + .143\Phi_1'(x) + .014\Phi_3'(x)\} \sin 2\theta$$

$$v(x,\theta) = \{-.47\Phi_1(x) - .43\Phi_2(x) - .046\Phi_3(x)\} \cos 2\theta$$

$$w(x,\theta) = \{\Phi_1(x) + .95\Phi_2(x) + .119\Phi_3(x) + .055\Phi_5(x)\} \sin 2\theta$$

The strong coupling between the first and second axial modal functions in the radial movement, w, may be seen clearly in Figure 6.13. Such strong coupling suggested to Sharma and Johns, ref.(49, 52) that they should use a combination of clamped-free and clamped-simply-supported beam modal functions to describe the free vibration of clamped-ring stiffened cylinder. This

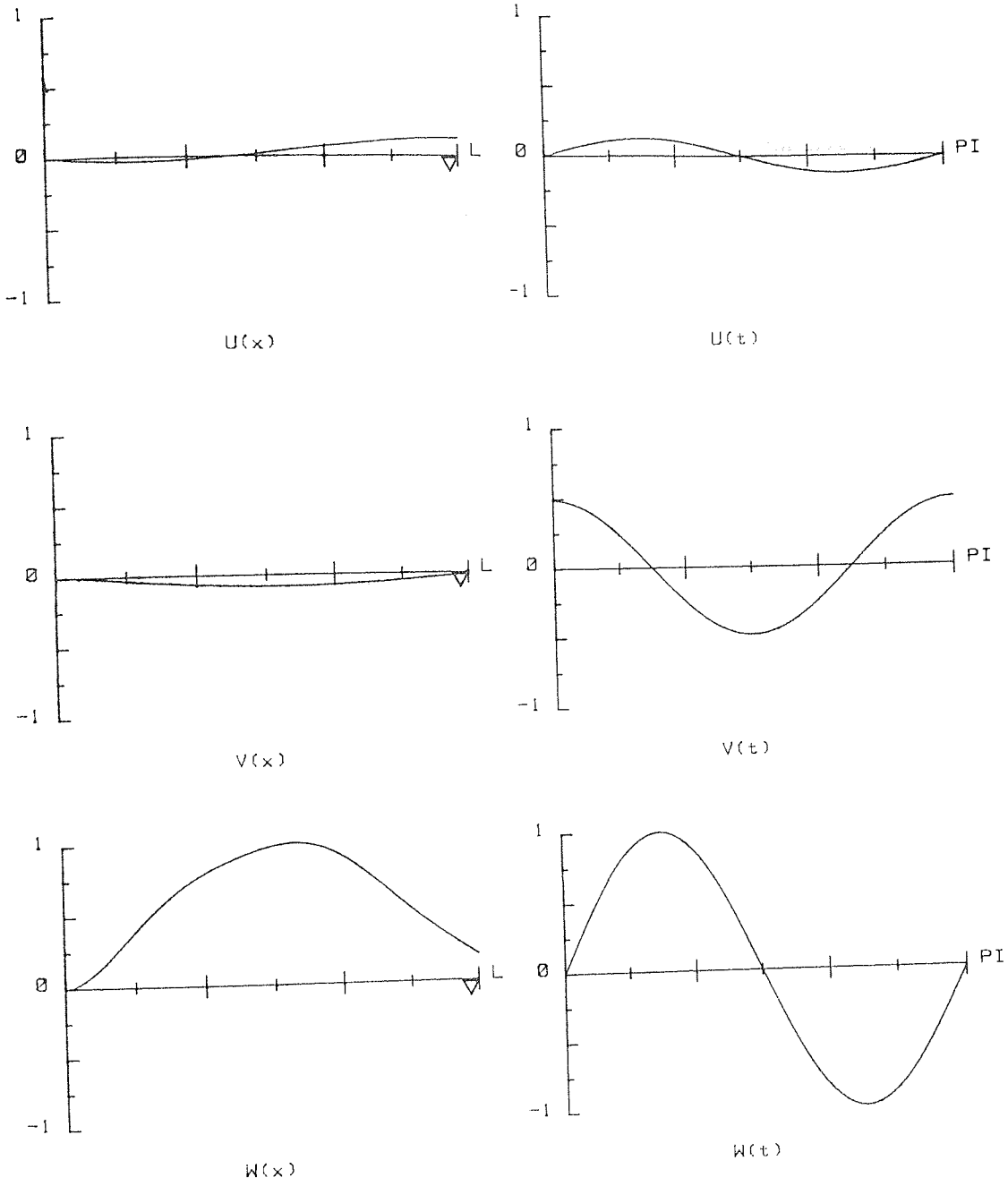

a) theta= 50°

b) x/L=.75

f= 2167 Hz

Fig. 6.13 Wave Forms of a Ring Stiffened

Cylindrical Shell ,Antisymmetric Mode

gave them a good result in comparison with the exact solution given by Forsberg,(51), but the elaborate integrations involved in their method makes it more difficult in comparison with the present method, particularly if the cutouts introduced into the structure.

Comparison of Figure 6.13 with Figure 6.7 - for clamped supporting heavy mass cylinder - shows a great similarity of the radial wave forms, in both graphs. Actually the effect of the heavy mass on the vibration of the shell is similar to the effect of the end ring, but in more exaggerated way. For example, while a reduction of the order of 80% was reported in the first torsion frequency in the former case, such reduction is only of order 18.6% in the case of end ring. In general, adding the ring increases most of the frequencies. This physically means that the ring contributes more to the strain energy than to the kinetic energy.

Compared with a stringer stiffened cylinder, the degree of coupling in axial modal functions due to the presence of the ring is much higher than the coupling in the circumferential modal functions due to the presence of stringers. In attempting to take this into account, 10 axial and 3 circumferential modal functions were used when comparing results of ring-stringer stiffened shell, see subsection 6.2.4.

The presence of cutouts coupled both axial and circumferential modal functions. This may be noticed in Figure 6.14 which presents the wave forms of the antisymmetric mode (3, 1 6) for the cylinder with 2 cutouts - this is mode number 11, column 8, Table 6.14. Mathematically this mode shape has the form:

$$u(x,\theta) = -\Phi_1'(x)\{-0.26 \sin 2\theta + 0.124 \sin 6\theta\}$$

$$v(x,\theta) = \Phi_1(x)\{-0.166\cos 6\theta + 0.031\} - 0.107\Phi_2(x)\cos 2\theta$$

$$w(x,\theta) = \Phi_1(x)\sin 6\theta + \Phi_2(x)\{0.24\sin 2\theta + 0.13\sin 4\theta + 0.077\sin 6\theta\}$$

For this cutout configuration, a reduction in most of the frequencies may be observed, particularly the fundamental and the first torsion which are reduced by 15% and 11.5% respectively. Also one might notice that the antisymmetric modes have lower frequencies than those of the corresponding symmetric modes. This means that the structure is more flexible in the antisymmetric case than in the symmetric one. But there are a few modes showing a reverse process.

The last two columns in Table 6.14 present the results for the whole structure; i.e. cylindrical shell stiffened with ring and stringers, with 2 cutouts. Comparing these results with the previous ones in Table 6.14 showed that the effect of the ring is the dominant one on most of the frequencies, but the effect of cutouts is pronounced in the lower modes, particularly

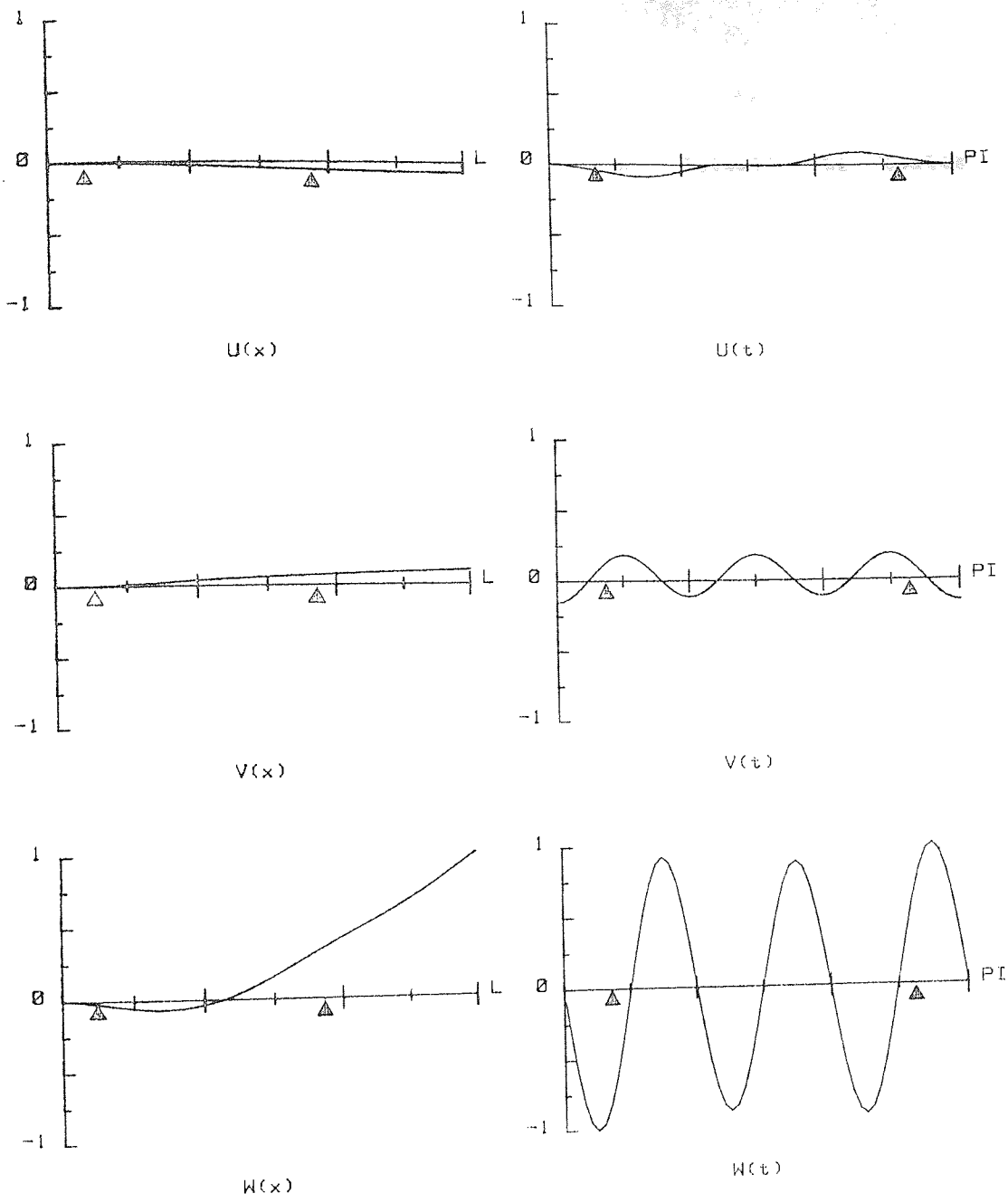

△ Cutout Location

a) theta= 40^{0}

b) x/L=.75

f= 2961 Hz

Fig. 6.14 Wave Forms of a Cylindricall Shell

With Cutout ,Antisymmetric Mode

the fundamental antisymmetric mode. Actually the results obtained for this case agree qualitatively with the trends obtained for a similar case, but with simply supported end conditions, in Ref.(55).

One might expect a strong coupling in both axial and circumferential wave forms in mode shapes. This is true and can be seen in Figure 6.15 which presents the wave forms of the symmetric mode (3, 2 3) - second mode in column 11, Table 6.14. Mathematically this mode has the form:

$$u(x,\theta)=\Phi_2'(x)\{-0.144\cos3\theta-0.095\cos\theta+0.069\cos 5\theta\}$$

$$v(x,\theta)=\Phi_2(x)\{-0.189\sin3\theta+0.137\sin5\theta\}+\Phi_1(x)\{-0.167\sin3\theta + 0.082\sin 5\theta\}$$

$$w(x,\theta)=\Phi_2(x)\{\cos3\theta+0.49\cos\theta-0.364\cos5\theta\}+\cos3\theta\{0.64\Phi_1(x) + 0.34\Phi_3(x)\}$$

Figure 6.15.a. shows this mode shape in planes away from the cutout regions while Figure 6.15.b. shows the same mode in planes passing through the cutout regions.

The interesting observation in Figure 6.15 is that the maximum amplitudes in the mode shape were noticed about the edges of cutouts.

In this structure configuration, the reduction in the first torsion frequency is of the order of 23%,

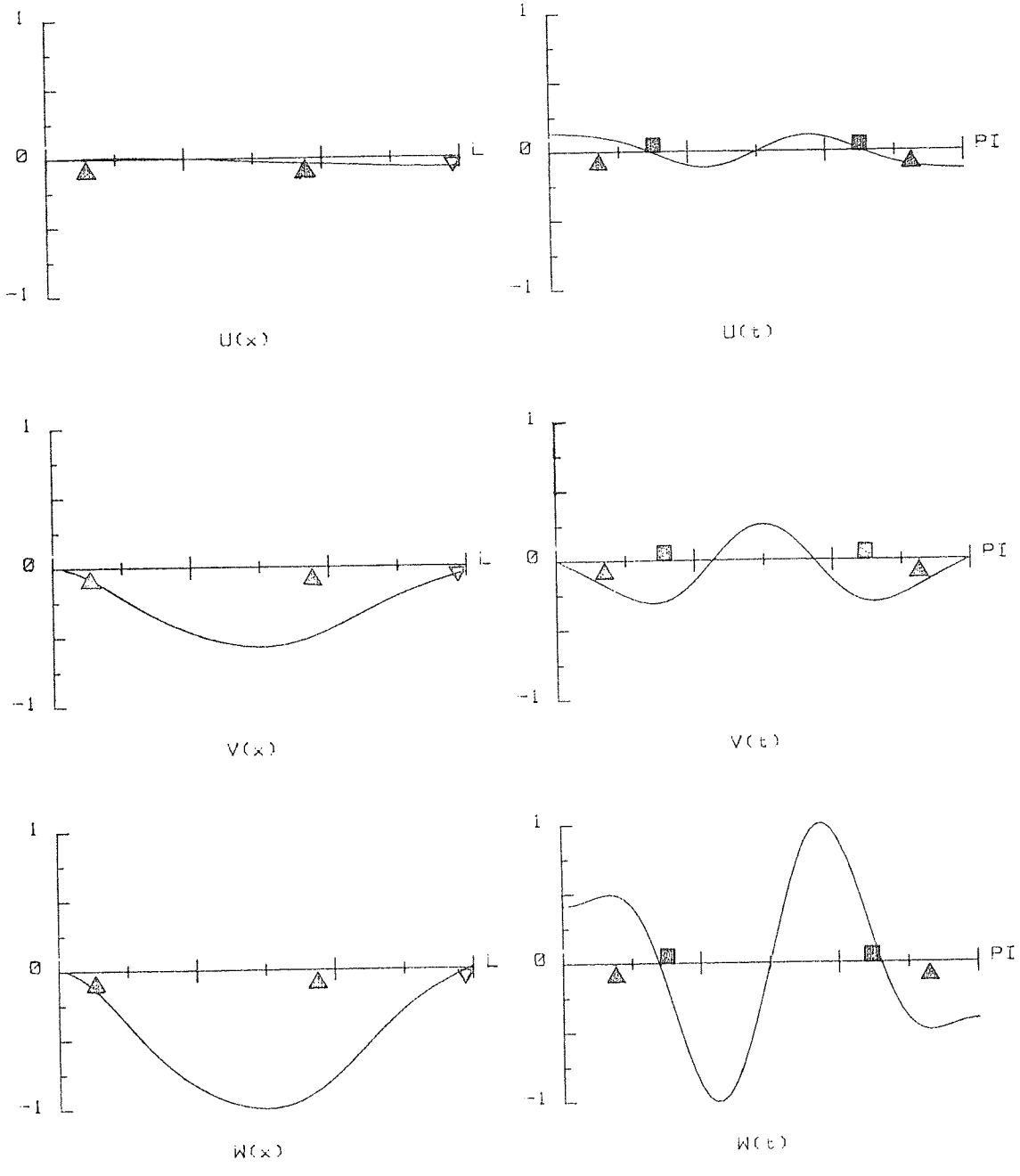

▽ Ring Location

▩ Stringer Location

△ Cutout Location

a) theta= 50^{0}

b) x/L=.75

f= 1950 Hz

Fig. 6.15a Wave Forms of a Ring-Stringer Stffened Cylindrical Shell With Cutouts ,Symmetric Mode

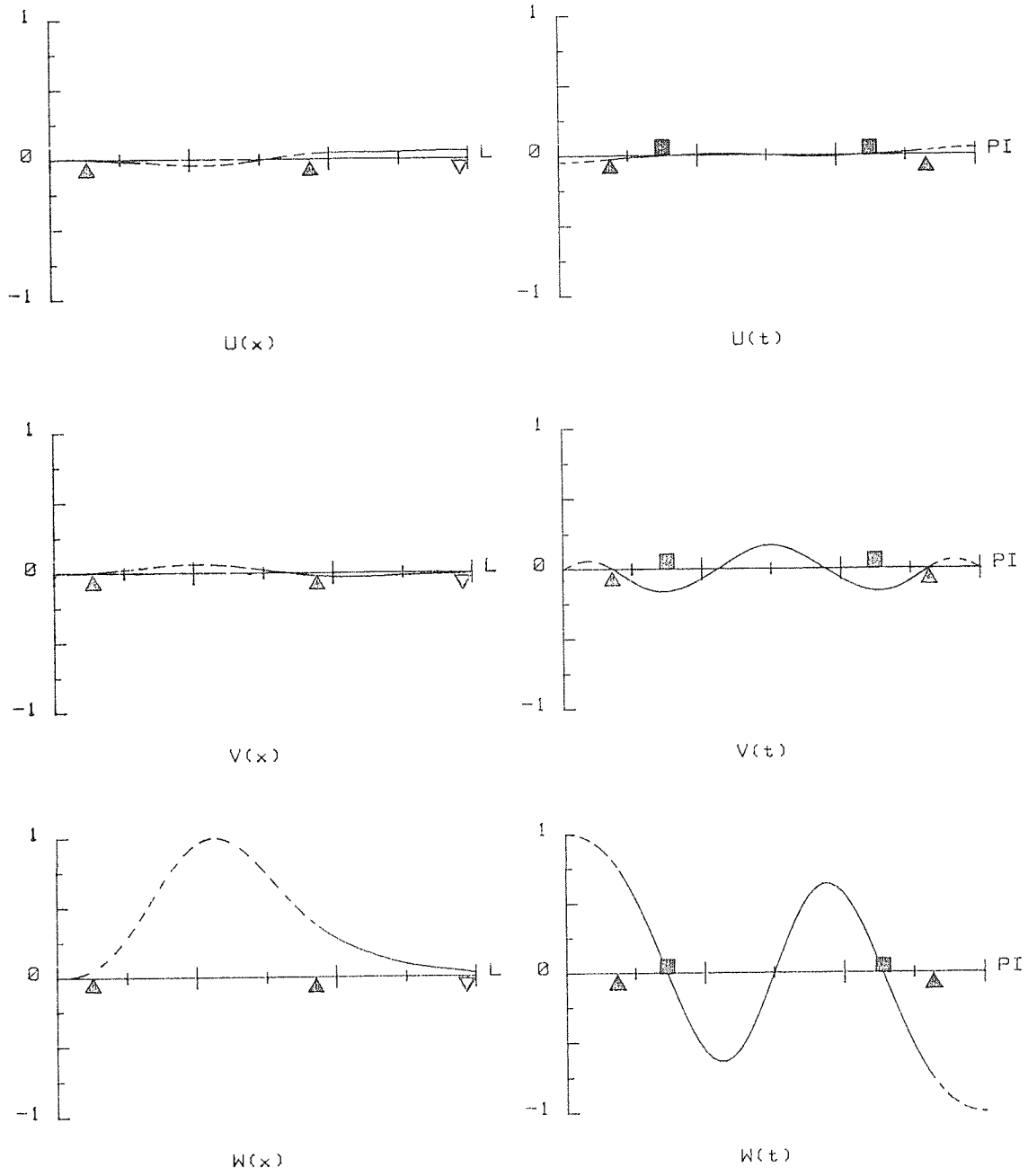

Fig. 6.15b Wave Forms of a Ring-Stringer Stffened Cylindrical Shell With Cutouts ,Symmetric Mode

the highest reduction obtained in this mode compared with the other previous configurations, presented in Table 6.14.

6.5.2. Comparison of Theoretical and Experimental Results:

This section presents a comparison of the theoretical and the experimental frequencies and mode shapes related to the model of configuration 5 in subsection 6.5.1. Table 6.15 shows such comparison. Letters S and A refer to symmetric and antisymmetric modes, respectively, and the other figures associated with mode shapes have the same meanings as those in section 6.5.1.

The correlation between the experimental and theoretical results is seen to be quite good, with average discrepancy of the order of 4.5%, and maximum discrepancy of the order of 8.3%. Such discrepancies between theory and experiment may be due to one or more of the following reasons:

1. Finite truncation of the series expressions for the mode shapes in the assumed displacement functions. Although increasing the number of terms in the series is found to improve the accuracy, the penalty is that more computing storage and longer executing time are required.

Mode Shape	Frequency		% Discrepancy
	Theory	Experiment	
3, 1 1 A	837	813	2.9
3, 1 1 S	1030	997	3.2
3, 1 2 S	1250	1348	7.8
3, 1 2 A	1752	-	-
3, 2 4 A	1928	1883	2.3
3, 2 3 A	1948	1985	1.9
3, 2 3 S	1950	-	-
3, 2 4 S	2163	2052	5.1
2, 1 0 A	2277	2202	8.3
3, 2 1 S	2304	2112	3.3
3, 2 5 A	2574	2436	5.3
3, 2 6 S	2815	2668	5.2
1, 1 1 A	2865	2757	3.8
1, 1 0 S	3010	2912	5.5
1, 1 1 S	3042	2873	3.25
3, 2 6 A	3113	2937	5.6

Table 6.15

Comparison of Theoretical and

Experimental Frequencies of an

Actual Bell-housing (Hz.)

2. Satisfaction of the assumed boundary conditions. It was assumed that the tested model had a clamped-free boundary condition. The absolute clamped end condition is extremely difficult to achieve experimentally, as explained in Ref.(53). Also using the beam functions in the axial direction satisfy the free end condition only in an approximate manner.

3. Slight differences in dimensions of both the theoretical and actual model.

4. Mechanical contact of both the vibrator and accelerometer with the tested model may ,slightly, alter its mechanical properties.

5. The shell is discontinuous at each point along the contour of the cutout; but the displacement functions are continuous in the whole region: $o \leqslant x \leqslant L$, $-\pi \leqslant \theta \leqslant \pi$. These displacement functions do not satisfy the kinetic boundary condition at the free edge of the cutout; but give displacements and stresses in this region. The kinetic boundary conditions are to be satisfied in a limiting sense as a by-product of minimizing the action integral with respect to the generalized coordinates. The success of this process depends to a certain extent on the number of terms employed in the displacement functions, since the truncation process opposes such success. This is an extreme situation for Rayleigh-Ritz method to handle.

6. It is assumed that each of the stiffening elements is attached to the shell through a single line, but in reality these elements were welded to the shell across their whole thicknesses. If the stiffener is not attached to the shell at a single line, then the stiffness of the shell, perpendicular to the stiffener's axis will be increased at the stiffener location. In this case the cross-stiffening effect given in Ref.(54) should be incorporated in the analysis, particularly if modes of vibration with wave length in order of magnitude of the stiffener thickness, are required more accurately.

7. Neglect of rotary inertia and shear deformation of the shell in the analysis.

Nevertheless, the agreement between measured and calculated frequencies is good and satisfactory within engineering limits, over a wide range of m and n.

6.6. Modal Coupling and Selection of Vibration Isolation Materials:

Now the significance of the coupled modes phenomenon is illustrated.

It has already been seen that the structure under consideration has a wide range of parameters which may be adjusted in order to alter its natural frequencies. This is a powerful means of shifting such frequencies

away from the pump exciting force frequencies imposed on the structure. But it may be desired to use vibration isolators, to reduce the magnitude of the force transmitted from the pump to its mounting. If this is the case, then the phenomenon of coupled modes has an important role to play in selecting the proper isolating material. By definition, the coupled modes are modes of vibration that are not independent, but which influence one another. This phenomenon may be found in some multi-degrees of freedom systems.

Some isolating materials function in a good manner to isolate transmitted forces in certain directions, but not in others. If such isolators are located at points where several modes of vibration are coupled and excited, then this may significantly affect their function. In other words, the contribution of the several coupled modes should be taken into account when a selection of isolating material is made. Further discussion of the subject may be found in Reference (61).

6.7. Closing Remarks:

In this Chapter, the evaluation of the numerical model and computer program has been investigated by comparing predictions with those given by some other approaches; theoretically and experimentally and a satisfactory conclusion was obtained in these comparisons of the results. Also the influence of some parameters, which have not been studied before, was examined from

the mechanical behaviour point of view of the bell-housing mount. Finally a comparison between theoretical and experimental results was carried out for a specific commercially available bell housing mount. Some relevant points about the discrepancies between theory and experiment were discussed to highlight the sources of errors that may be inherent either in the theory or the experimental work.

Total summary and conclusion of the whole study are the subject of the following Chapter, as well as some recommendations for further work which could usefully be done.

CHAPTER SEVEN

SUMMARY, CONCLUSION AND RECOMMENDATIONS FOR FURTHER WORK

7.1 Introduction:

Theoretical and experimental techniques have been developed to study the mechanical behaviour of bell-housing type pump mountings. The tested model consists of a thin circular cylindrical shell with rectangular cutouts, stiffened by longitudinal stringers (ribs) and rings (flanges). The Rayleigh-Ritz variational approach was used as a basis for formulating the mechanical problem utilizing the Love - Timoshenko theory for thin shells and Bernoulli theory of bending for the stiffeners. The analytical part of the study embraced the static response and the free vibration of the bell-housing. In the formulation; two boundary conditions for the shell were under investigation: "clamped-free" and "clamped-supporting heavy mass". Throughout the theoretical part, beam characteristic (axial) and trigonometric (circumferential) functions were used in the displacement model. The stiffeners were treated as discretely located.

The resulting equations of equilibrium in the static case were solved numerically by Cholesky decomposition

technique, while the eigen value problem in the free vibration case was solved by using an algorithm based on Householder and Sturm sequence techniques to obtain natural frequencies and mode shapes.

Theoretical analysis for static response and free vibration calculations have been implemented for digital computer solution with a capability of presenting the results in either graphical form and/or tables.

Experimental work was incorporated in the study for determinating natural frequencies and associated mode shapes of a specific unit. All the aims set forward in Chapter one have been fulfilled and this Chapter presents a summary, conclusion and recommendations for further work.

7.2. Summary:

The following results were obtained:

1. The results of the present analysis on free vibrations of stiffened and unstiffened circular cylindrical shells were compared with those obtained by other investigators, experimentally and theoretically; using other methods. The results of the present analysis showed a good agreement with those obtained from higher-order thin shell theories.
2. The influence of cutout size on natural frequencies and mode shapes of clamped-free shell was investigated.

3. The effect of cutout location on natural frequencies and mode shapes of clamped-free shell was illustrated.
4. The influence of cutout presence on natural frequencies and mode shapes of clamped-free shells with different thickness to radius ratios was studied.
5. The effect of cutouts on frequencies and mode shapes of clamped-free stringer-ring stiffened shells was investigated.
6. A study was made to determine the effect of the presence of a heavy mass-rigidly connected to a clamped-free shell at the "free" end - on natural frequencies and mode shapes of the shell.
7. The static response of the shell due to the presence of the heavy mass was given.
8. A comparison study between theoretical and experimental natural frequencies and mode shapes of a clamped-free stringer-ring stiffened shell with cutouts was held, and some reasons for slight discrepancies were mentioned.

From the results of this study, the following conclusions appear to be valid.

7.3 Conclusions:

The major observations and conclusions from this study may be listed as follows:

1. The numerical modelling developed for the study proved to be satisfactory for the static and free vibration

analysis of the pump mounting, bell-housing type. The computer program is well tested and reliable.

2. The desk top computers with suitable memory size are suitable for handling such complicated engineering problems.
3. Using digital computers as controller elements in the experimental rigs allow experimental work to be performed quickly and accurately.
4. Good agreement between theoretical and experimental results was obtained with average discrepancies of order 4.5%.
5. Elementary beam vibration functions are satisfactory approximations to the longitudinal components of the mode shapes of stiffened or unstiffened cylindrical shells, in the Rayleigh-Ritz process.
6. There is a weak circumferential modal coupling due to the presence of stringers, while there is a strong axial modal coupling due to the presence of rings.
7. Stringers tend to reduce the natural frequencies of a plain cylinder while rings tend to increase them. The influence due to the presence of rings is more than that of the stringers.
8. In general, the cutouts tend to decrease the frequencies. This effect increases with increase in the size of the cutout. But this phenomenon depends on the location of the cutouts; thus if they are

near to the free edge an increase in frequencies is obtained, where the shell behaves as "shorter" one.

9. Presence of cutouts has the effect of coupling the distinct axial and circumferential wave forms of the plain cylinder.

10. Maximum amplitudes in the mode shapes were reached at points near the edges of cutout, but in some modes were reached at some points away from these edges.

11. The effect of rings is the dominant one for shells with a cutout, stiffened by stringers and rings.

12. The presence of a heavy mass at the "free" end has similar effects to those due to rings, but in a more exaggerated manner, particularly in the torsion modes where the frequencies decrease more sharply.

13. The Rayleigh-Ritz method as applied to a shell with a cutout with no improvement in the displacement functions to handle discontinuities in the cutout region is a convenient analytical tool for estimating the overall behaviour of the shell.

14. There are many parameters that can be used to control the natural frequencies of the bell-housing pump mounting at the design stage in order to avoid resonant response to the excitation of the pump.

15. Since the interactive input and output of the computer program has been designed to be used easily by engineers with no computing experience, it would be possible to include the present software within a CAD package to provide a useful design tool for hydraulic pumps.

7.4 Recommendations for Further work :

The following recommendations for further study are made to improve the present results and to carry the present research forward:

1. The present analytical results should be compared with other results obtained by finite element and finite difference methods to evaluate the computational efficiencies.
2. Other experimental techniques may be employed to avoid the disadvantages of the present method, in particular the mechanical contact of the transducers with the tested model. For instance driving the shell by a pulsed magnetic field and measuring the response by a non-contacting probe (microphone).
3. Other displacement functions which allow the singular behaviour in the region of the cutouts may be sought and incorporated in the analysis. These functions, if found, will increase the capability of Rayleigh-Ritz method to deal with cutouts.

4. Assumption of treating the pump as a rigid mass is reasonable one as long as the natural frequencies of the pump casing are higher than those of the bell housing, otherwise the whole system should be treated as two elastically coupled systems.
5. The direct contribution of the bell-housing mount to the overall noise produced by the hydraulic system may be estimated experimentally.
6. Including damping in the present analysis would make it possible to perform a realistic modal analysis of the dynamic response of the bell-housing to identify the most excited modes under the running conditions. Then, using the present program can help in redesign of the structure to avoid the excitation of such modes.
7. Other types of pump mounting, like angle brackets or conical bell-housing mounts, may be investigated in view of their mechanical characteristics, which in turn affect their capability of transmitting mechanical vibration and noise radiation.
8. The computer program was written and implemented in general terms which makes it flexible to investigate the effect of cutouts on natural frequencies and mode shapes of cylindrical shells with other boundary conditions. This may be useful for other engineering applications.

APPENDIX A

Derivation of the Stiffener-Shell Compatibility Relations

According to the assumption set previously in sub section 3.2.1, Chapter three, the displacement vector of an arbitrary point in the ith stiffener cross-section, $\{q\}_i$, can be written as

$$\{q\}_i = \{q\}_{ci} + \begin{bmatrix} 0 & -\Phi_z & \Phi_\theta \\ \Phi_z & 0 & -\Phi_x \\ -\Phi_\theta & \Phi_x & 0 \end{bmatrix}_{i/ci} \times \{R\}_{i/ci} \qquad A.1$$

where i = $\begin{cases} s & \text{for stringer} \\ r & \text{for ring} \end{cases}$

C refer to the centroid of the cross-section

$\{q\}_{ci}$ the displacement vector of the cross-section's centroid with respect to the point of attachment on the middle surface of the shell ;

$(\Phi_x \quad \Phi_\theta \quad \Phi_z)_{i/ci}$ angles of rotation at an arbitrary point in the cross-section with respect to axes through the centroid of the stiffener

$\{R\}_{i/ci}$ the position vector of an arbitrary point in the cross-section relative to the centroid of the cross-section of the stiffener

$$\{R\}_{s/cs} = \begin{Bmatrix} 0 \\ y'_s \\ z'_s \end{Bmatrix} \quad \text{for stringer} \qquad \text{A.2}$$

$$\{R\}_{r/cr} = \begin{Bmatrix} x'_r \\ 0 \\ z'_r \end{Bmatrix} \quad \text{for ring}$$

The displacement vector of the centroid of the ith stiffener may be written as

$$\{q\}_{ci} = \{q\}_0 + \begin{bmatrix} 0 & -\Phi_z & \Phi_\theta \\ \Phi_z & 0 & \Phi_x \\ -\Phi_\theta & \Phi_x & 0 \end{bmatrix}_{ci/0} x \{R\}_{ci/0} \qquad \text{A.3}$$

where 0 refers to the middle surface of the shell;

$(\Phi_x, \Phi_\theta, \Phi_z)_{ci/0}$ angles of rotation of the centroid of the ith stiffener relative to the point of attachment on the shell middle surface ;

$\{R\}_{ci/0}$ the position vector of the centroid of the ith stiffener relative to the point of attachment

$$\{R\}_{cs/0} = \begin{Bmatrix} 0 \\ 0 \\ \bar{z}_s \end{Bmatrix} \quad \text{for stringer}$$

A.4

$$\{R\}_{cr/0} = \begin{Bmatrix} 0 \\ 0 \\ \bar{z}_r \end{Bmatrix} \quad \text{for ring}$$

Substituting equation A.3 into A.1, the following compatibility relation can be written as

$$\{q\}_i = \{q\}_0 + \begin{bmatrix} 0 & -\Phi_z & \Phi_\theta \\ \Phi_z & 0 & -\Phi_x \\ -\Phi_\theta & \Phi_x & 0 \end{bmatrix}_{ci/0} x \{R\}_{ci/0}$$

$$+ \begin{bmatrix} 0 & -\Phi_z & \Phi_\theta \\ \Phi_z & 0 & -\Phi_x \\ -\Phi_\theta & \Phi_x & 0 \end{bmatrix} x \{R\}_{i/ci} \qquad \text{A.5}$$

From the second assumption in subsection 3.2.1, Chapter three, it follows that:

$$\{\Phi\}_{ci/0} = \{\Phi\}_{i/ci} = \{\Phi\}_0 \qquad \text{A.6}$$

where

$\{\Phi\}_0$ is the angle of rotation vector of the middle surface of the shell at the point of attachment. This vector may be expanded as:

$$\{\Phi\}_0 = \begin{Bmatrix} \Phi_x \\ \Phi_\theta \\ \Phi_z \end{Bmatrix} \qquad \text{A.7}$$

where

$$\Phi_x = \frac{w,_\theta}{R} - \frac{v}{R}$$

$$\Phi_\theta = -w,_x$$

$$\Phi_z = \begin{cases} \dfrac{-u,_\theta}{R_c} + \dfrac{\bar{z}}{R_c} w,_{x\theta} & \text{for ring} \\ v,_x & \text{for stringer} \end{cases}$$

After equations A.2, A.4 and A.7 are substituted into equation A.5, the stringer compatibility relations can be written in terms of displacements of the shell middle surface as follows:

$$\{q\}_s = \begin{Bmatrix} u - (\bar{z}_s + z'_s)\, w,_x - y'_s\, v,_x \\ v - (\bar{z}_s + z'_s)\left(\dfrac{w,_\theta}{R} - \dfrac{v}{R}\right) \\ w - y'_s\left(\dfrac{w,_\theta}{R} - \dfrac{v}{R}\right) \end{Bmatrix} \qquad \text{A.8}$$

And the ring-shell compatibility relation has the form:

$$\{q\}_r = \begin{Bmatrix} u - (\bar{z}_r + z'_r)\, w,_x \\ v - x'_r \dfrac{u,_\theta}{R_c} - (\bar{z}_r + z'_r)\left(\dfrac{w,_\theta}{R} - \dfrac{v}{R}\right) + \dfrac{x'_r\, \bar{z}_r}{R_c} w,_{x\theta} \\ w + x'_r\, w,_x \end{Bmatrix} \qquad \text{A.9}$$

APPENDIX B

Strain Energy Expressions For Stringer and Ring Stiffeners

This Appendix presents the expanded forms of the strain energy expressions, previously deriven in Chapter three, section 3.5

a) Stringer strain energy:

$$U_s = \frac{1}{2}\int_0^L \Big[EA_s\, u_{,x}^2 - 2\,\bar{z}_s\, EA_s\, u_{,x}\, w_{,xx} + EI_{zz_s}\, v_{,xx}^2 + E(\bar{z}_s^2 A_s + I_{yy_s})\, w_{,xx}^2 + \frac{GJ_s}{R^2}\,(w_{,x\theta}^2 - 2\, w_{,x\theta}\, v_{,x} + v_{,x}^2)\Big]\Big|_{\theta=\theta_s} dx$$

b) Ring strain energy:

$$U_r = \frac{1}{2}\int_0^{2\pi}\Big[\frac{EA_r}{R_c}(v_{,\theta}^2 + 2wv_{,\theta} + w^2) + \frac{2EA_r\,\bar{z}_r}{R_c R}(v_{,\theta}^2 - w_{,\theta\theta}v_{,\theta} + wv_{,\theta} - ww_{,\theta\theta}) + \frac{EA_r\,\bar{z}_r^2}{R^2}(v_{,\theta}^2 - 2\,w_{,\theta\theta}v_{,\theta} + w_{,\theta\theta}^2) + \frac{EI_{xx_r}}{R_c R^2}(v_{,\theta}^2 - 2\,w_{,\theta\theta}v_{,\theta} + w_{,\theta\theta}^2) + \frac{EI_{zz_r}}{R_c}\Big(\frac{u_{,\theta\theta}^2}{R_c^2} - \frac{2\,w_{,x}\,u_{,\theta\theta}}{R_c} + w_{,x}^2\Big) + \frac{EI_{zz_r}\,\bar{z}_r}{R_c^2}\Big(w_{,x\theta\theta}\,w_{,x} - \frac{w_{,x\theta\theta}\,u_{,\theta\theta}}{R_c}\Big)$$

$$+\frac{EI_{zz_r}}{R_c^3}\,\bar{z}_r^2\,w^2_{,x\theta\theta}+\frac{GJ_r}{R_c}\left(\frac{u^2_{,\theta}}{R_c^2}+\frac{2w_{,x\theta}u_{,\theta}}{R_c}+w^2_{,x\theta}\right)$$

$$\left.-\frac{GJ_r\,\bar{z}_r}{R_c^2}\left(\frac{2w_{,x\theta}u_{,\theta}}{R_c}+2\,w^2_{,x\theta}\right)+\frac{GJ_r\,\bar{z}_r^2}{R_c^3}\,w^2_{,x\theta}\right]\Bigg|_{x=x_r}d\theta$$

APPENDIX C

Elements of the Mass and Stiffness Matrices For Clamped-Free End Condition

The matrix elements of equation 3.50, Chapter three are presented here. The characteristic mode function $\Phi_m(x)$ is as defined in equation 3.39, the prime superscript ($'$) denotes differentiation with respect to x.

C.1. Integrations and function values used in elements evaluation:

C.1.1. Complete cylinder longitudinal integrals

$$IX1 = \int_0^L \Phi_m'' \bar{\Phi}_m'' \, dx$$

$$IX2 = \int_0^L \Phi_m' \bar{\Phi}_m' \, dx$$

$$IX3 = \int_0^L \Phi_m'' \bar{\Phi}_m \, dx \qquad C.1$$

$$IX4 = \int_0^L \Phi_m \bar{\Phi}_m'' \, dx$$

$$IX5 = \int_0^L \Phi_m \bar{\Phi}_m \, dx$$

The exact integrals of these expressions are given in Appendix D.

C.1.2. Longitudinal cutout integrals:

With same notation used in subsection C.1.1., the longitudinal cutout integrals have the forms (for ith cutout):

$$IX1_c = \begin{cases} \frac{1}{4}\Big[3\Phi_m'' \Phi_m' + x(\Phi_m'')^2 - 2x\Phi_m' \Phi_m''' - \Phi_m \Phi_m''' \\ \qquad + x\beta_m^4 \Phi_m^2 \Big]_{x1i}^{x2i} & \text{for } m = \bar{m} \\ \frac{1}{\beta_{\bar{m}}^4 - \beta_m^4}\Big[\beta_{\bar{m}}^4 \Phi_{\bar{m}}' \Phi_m'' - \beta_m^4 \Phi_m' \Phi_{\bar{m}}'' - \beta_{\bar{m}}^4 \Phi_{\bar{m}} \Phi_m''' \\ \qquad + \beta_m^4 \Phi_m \Phi_{\bar{m}}''' \Big]_{x_{1i}}^{x_{2i}} & \text{for } m \neq \bar{m} \end{cases}$$

$$IX2_c = \begin{cases} \frac{1}{4}\Big[3\Phi_m \Phi_m' + x(\Phi_m')^2 - 2x\Phi_m \Phi_m'' - \frac{1}{\beta_m^4} \Phi_m'' \Phi_m''' \\ \qquad + \frac{x}{\beta_m^4} (\Phi_m''')^2 \Big]_{x_{1i}}^{x_{2i}} & \text{for } m = \bar{m} \\ \frac{1}{\beta_{\bar{m}}^4 - \beta_m^4}\Big[\beta_{\bar{m}}^4 \Phi_{\bar{m}} \Phi_m' - \beta_m^4 \Phi_m \Phi_{\bar{m}}' - \Phi_m'' \Phi_{\bar{m}}''' \\ \qquad + \Phi_{\bar{m}}'' \Phi_m''' \Big]_{x_{1i}}^{x_{2i}} & \text{for } m \neq \bar{m} \end{cases}$$

C.2

$$IX3_c = \begin{cases} \frac{1}{4}\left[\Phi_m \Phi_m' - x(\Phi_m')^2 + 2x\,\Phi_m \Phi_m'' + \frac{1}{\beta_m^4} \Phi_m'' \Phi_m''' \right. \\ \qquad \left. - \frac{x}{\beta_m^4} (\Phi_m''')^2 \right]_{x_{1i}}^{x_{2i}} & \text{for } m = \bar{m} \\ \frac{1}{\beta_{\bar{m}}^4 - \beta_m^4}\left[\beta_m^4 (\Phi_m \Phi_{\bar{m}}' - \Phi_{\bar{m}} \Phi_m') - \Phi_{\bar{m}}'' \Phi_m''' \right. \\ \qquad \left. + \Phi_m'' \Phi_{\bar{m}}''' \right]_{x_{1i}}^{x_{2i}} & \text{for } m \neq \bar{m} \end{cases}$$

$IX4_c = IX3_c$, but m should replace $\bar{m}$ and vice-versa

$$IX5_c = \begin{cases} \frac{1}{4}\left[\frac{3}{\beta_m^4} \Phi_m \Phi_m''' + x\Phi_m^2 - \frac{2x}{\beta_m^4} \Phi_m' \Phi_m''' \right. \\ \qquad \left. - \frac{1}{\beta_m^4} \Phi_m' \Phi_m'' + \frac{x}{\beta_m^4} (\Phi_m'')^2 \right]_{x_{1i}}^{x_{2i}} & \text{for } m = \bar{m} \\ \frac{1}{\beta_{\bar{m}}^4 - \beta_m^4}\left[\Phi_m \Phi_{\bar{m}}''' - \Phi_{\bar{m}} \Phi_m''' - \Phi_m' \Phi_{\bar{m}}'' + \Phi_{\bar{m}}' \Phi_m'' \right]_{x_{1i}}^{x_{2i}} \\ & \text{for } m \neq \bar{m} \end{cases}$$

C.1.3. Cutout circumferential integrals:

$$CCI1 = \int_{\theta_{1i}}^{\theta_{2i}} \cos n\theta \cos \bar{n}\theta \, d\theta \qquad C.3$$

$$CCI2 = \int_{\theta_{1i}}^{\theta_{2i}} \sin n\theta \sin \bar{n}\theta \, d\theta$$

C.1.4. Stringer circumferential functions

$$SCF1 = \cos n\theta \cos \bar{n}\theta$$
$$SCF2 = \sin n\theta \sin \bar{n}\theta \qquad \text{C.4}$$

Functions SCF1 and SCF2 are evaluated at each stringer circumferential coordinate, θ_s.

C.1.5. Ring longitudinal Functions

$$RLF1 = \Phi'_m \Phi'_{-m}$$
$$RLF2 = \Phi_m \Phi_{-m} \qquad \text{C.5}$$

Functions RLF1 and RLF2 are evaluated at each ring longitudinal coordinate, x_r.

C.2. Elements of the stiffness matrix

C.2.1. Contribution of the circular shell with typical cutout:

$$K11_{mn,\bar{m}\bar{n}} = \frac{12DR}{h^2}(\pi IX1 - CCI1.IX1_c) + \frac{Gh n\bar{n}}{R}(\pi IX2 - CCI2.IX2_c)$$

$$K12_{mn,\bar{m}\bar{n}} = \frac{12D\nu}{h^2} n(\pi IX4 - CCI1.IX4_c) - Gh\bar{n}(\pi IX2 - CCI2.IX2_c)$$

$$K13_{mn,\bar{m}\bar{n}} = \frac{12D\nu}{h^2}(\pi IX4 - CCI1.IX4_c)$$

$$K22_{mn,\bar{m}\bar{n}} = \frac{12D}{h^2R} n\bar{n}\ (\pi IX5\text{-}CCI1.IX5_c) + \frac{D}{R^3} n\bar{n}(\pi IX5\text{-}CCI1.IX5_c)$$

$$+GhR(\pi IX2\text{-}CCI2.IX2_c) + \frac{Gh^3}{12R}\ (\pi IX2\text{-}CCI2.IX2_c)$$

$$K23_{mn,\bar{m}\bar{n}} = \frac{12D}{h^2R} \bar{n}\ (\pi IX5\text{-}CCI1.IX5_c) + \frac{Dn^2\bar{n}}{R^3}\ (\pi IX5\text{-}CCI1.IX5_c)$$

$$-\frac{D\nu}{R} \bar{n}\ (\pi IX3\text{-}CCI1.IX3_c) + \frac{Gh^3}{6R}\ n\ (\pi IX2\text{-}CCI2.IX2_c)$$

$$K33_{mn,\bar{m}\bar{n}} = DR(\pi IX1\text{-}CCI1.IX1_c) + \frac{Gh^3}{3R}\ n\ \bar{n}\ (\pi IX2\text{-}CCI2.IX2_c)$$

$$-\frac{D\nu}{R} \bar{n}^2(\pi IX3\text{-}CCI1.IX3_c) - \frac{D\nu}{R}\ n^2(\pi IX4\text{-}CCI1.IX4_c)$$

$$+\frac{12D}{h^2R}\ (\pi IX5\text{-}CCI1.IX5_c) + \frac{D}{R^3}\ n^2\bar{n}^2(\pi IX5\text{-}CCI1.IX5_c)$$

C.2.2. Contribution of a typical stringer:

$$K11_{mn,\bar{m}\bar{n}} = EA_s\ SCF1.IX1$$

$$K12_{mn,\bar{m}\bar{n}} = 0$$

$$K13_{mn,\bar{m}\bar{n}} = -EA_s \bar{z}_s\ SCF1.IX1$$

$$K22_{mn,\bar{m}\bar{n}} = EI_{zz_s}\ SCF2IX1 + \frac{GJ_s}{R^2}\ SCF2.IX2$$

$$K23_{mn,\bar{m}\bar{n}} = \frac{GJ_s}{R^2}\ SCF2.IX2$$

$$K33_{mn,\bar{m}\bar{n}} = E(\bar{z}_s^2 A_s + I_{yy_s})\ SCF1.IX1 + \frac{GJ_s}{R^2}\ SCF2.IX2$$

C.2.3. Contribution of a typical ring:

$$K11_{mn,\bar{m}\bar{n}} = \frac{\pi}{R_c^3}\left\{EI_{zz_r}\, n^2\bar{n}^2 + GJ_r\, n\,\bar{n}\right\} RLF1$$

$$K12_{mn,\bar{m}\bar{n}} = 0$$

$$K13_{mn,\bar{m}\bar{n}} = \frac{\pi}{R_c^2}\left\{EI_{zz_r}\,\bar{n}^2 - EI_{zz_r}\,\frac{\bar{z}_r\, n^2\bar{n}^2}{R_c} + GJ_r\, n\,\bar{n}\right.$$

$$\left. - GJ_r\,\frac{\bar{z}_r\, n\,\bar{n}}{R_c}\right\} RLF1$$

$$K22_{mn,\bar{m}\bar{n}} = \frac{\pi}{R_c}\left\{EA_r\, n\,\bar{n} + 2\,\frac{EA_r\, z_r}{R}\, n\,\bar{n} + \frac{EA_r\, z_r^2\, n\,\bar{n}}{R^2}\right.$$

$$\left. + \frac{EI_{xx_r}\, n\,\bar{n}}{R^2}\right\} RLF2$$

$$K23_{mn,\bar{m}\bar{n}} = \frac{\pi}{R_c}\left\{EA_r\,\bar{n} + \frac{EA_r\,\bar{z}_r}{R}\,(n^2\bar{n} + \bar{n}) + \frac{EA_r\,\bar{z}_r^2 n^2\bar{n}}{R^2}\right.$$

$$\left. + \frac{EI_{xx_r}\, n^2\,\bar{n}}{R^2}\right\} RLF2$$

$$K33_{mn,\bar{m}\bar{n}} = \frac{\pi}{R_c}\left\{EA_r + \frac{EA_r\,\bar{z}_r}{R}\,(\bar{n}^2 + n^2) + \frac{EA_r\,\bar{z}_r^2}{R^2}\, n^2\bar{n}^2\right.$$

$$\left. + EI_{xx_r}\,\frac{n^2\bar{n}^2}{R^2}\right\} RLF2$$

$$+ \frac{\pi}{R_c}\left\{EI_{zz_r} - \frac{EI_{zz_r}\bar{z}_r}{R_c}\right.\quad (n^2+\bar{n}^2)+\frac{EI_{zz_r}\bar{z}^2_r}{R_c^2}\quad n^2\bar{n}^2$$

$$\left. + GJ_r\, n\,\bar{n} - GJ_r\,\bar{z}_r\,\frac{n\,\bar{n}}{R_c} + GJ_r\,\frac{\bar{z}^2_r}{R_c^2}\right\} RLF1$$

Note: The contributions of the complete shell and rings are zero if $n \neq \bar{n}$, but n and $\bar{n}$ were kept distinguishable for the sake of generality and checking of each expression.

C.3. Elements of the mass matrix:

C.3.1. Contribution of the circular shell with typical cutout:

$M11_{mn,\bar{m}\bar{n}} = \rho\, h\, R\, (\pi IX2\text{-}CCI1.IX2_c)$

$M22_{mn,\bar{m}\bar{n}} = \rho\, h\, R\, (\pi IX5\text{-}CCI2.IX5_c)$

$M33_{mn,\bar{m}\bar{n}} = \rho\, h\, R\, (\pi IX5\text{-}CCI1.IX5_c)$

C.3.2. Contribution of typical stringer:

$M11_{mn,\bar{m}\bar{n}} = \rho\, A_s\, SCF1.IX2$

$M12_{mn,\bar{m}\bar{n}} = 0$

$$M13_{mn,\overline{mn}} = -\rho A_s \bar{z}_s \quad SCF1.IX2$$

$$M22_{mn,\overline{mn}} = \rho\left\{A_s + 2A_s \frac{\bar{z}_s}{R} + \frac{I_{zz_s}}{R^2} + \frac{1}{R^2}(\bar{z}_s^2 A_s + I_{yy_s})\right\} SCF2.IX5$$

$$+ \rho I_{zz_s} \quad SCF2.IX2$$

$$M23_{mn,\overline{mn}} = \frac{\rho}{R^2}\left\{I_{zz_s} n + A_s \bar{z}_s R n + (\bar{z}_s^2 A_s + I_{yy_s}) n\right\} SCF2.IX5$$

$$M33_{mn,\overline{mn}} = \rho\left\{A_s SCF1 + \frac{I_{zz_s}}{R^2} n \bar{n}\, SCF2 + \frac{1}{R^2}(\bar{z}_s^2 A_s + I_{yy_s}) n \bar{n}\right.$$

$$\left. SCF2\left\{IX5 + \rho(\bar{z}_s^2 A_s + I_{yy_s})\right.\right. \quad SCF1.IX2$$

C.3.3. Contribution of typical ring:

$$M11_{mn,\overline{mn}} = \pi\rho R_c\left\{A_r + \frac{I_{zz_r}}{R^2} n \bar{n}\right\} RLF1$$

$$M12_{mn,\overline{mn}} = 0$$

$$M13_{mn,\overline{mn}} = -\pi\rho A_r \bar{z}_r R_c \quad RLF1$$

$$M22_{mn,\overline{mn}} = \pi\rho R_c\left\{A_r + \frac{2A_r \bar{z}_r}{R} + \frac{1}{R^2}(\bar{z}_r^2 A_r + I_{xx_r})\right\} RLF2$$

$$M23_{mn,\overline{mn}} = \pi\rho R_c \left\{ \frac{A_r \bar{z}_r}{R} + \frac{n}{R^2} \left(\bar{z}_r^2 A_r + I_{xx_r} \right) \right\} RLF2$$

$$M33_{mn,\overline{mn}} = \pi\rho R_c \left(I_{zz_r} + \bar{z}_r^2 A_r + I_{xx_r} \right) RLF1 +$$

$$\pi\rho R_c \left(A_r + \frac{n\,\bar{n}}{R^2} \left(\bar{z}_r^2 A_r + I_{xx_r} \right) \right) RLF2$$

Note: The contributions of the complete shell and rings are zero if $\bar{n} \neq n$.

The expressions so far expanded are those for the symmetric modes of the clamped-free end condition. The corresponding expressions for antisymmetric modes can be obtained by making the following substitutions:

$\cos n\theta \rightarrow \sin n\theta$

$\sin n\theta \rightarrow -\cos n\theta$

APPENDIX D

Elements of the Mass and Stiffness Matrices of Clamped-Supporting a Heavy Mass Condition

The matrix elements of the clamped-supporting heavy mass end condition are presented here. These expressions are different than those expressed in Appendix C due to the restraint condition imposed on the shell at the "free" end due to the presence of the rigid mass. The function $\Phi_m(x)$ has the same meaning as in Appendix C.

D.1. Cylinder longitudinal integrals:

$$IX1 = \int_0^L \Phi_m' \Phi_n' \, dx = \frac{4\beta_m\beta_n}{\beta_n^4-\beta_m^4}\left[(-1)^{m+n}(\alpha_m\beta_n^3 - \alpha_n\beta_m^3 - \beta_m\beta_n(\alpha_n\beta_n - \alpha_m\beta_m)\right] \qquad \text{for } m \neq n$$

$$= \alpha_n\beta_n(2 + \alpha_n\beta_n L) \qquad \text{for } m = n$$

$$IX2 = \int_0^L (1-x/L)\,\Phi_m' \Phi_n' \, dx = \frac{4\beta_m^2\beta_n^2}{\beta_n^4-\beta_m^4}\left[\beta_m\alpha_m - \beta_n\alpha_n\right] + \frac{8\beta_n^2\beta_m^2\left[(-1)^m\beta_m^2 - (-1)^n\beta_n^2\right]^2}{L(\beta_n^4-\beta_m^4)^2} \qquad \text{for } m \neq n$$

$$= \frac{1}{2}\alpha_n\beta_n\,(1 + \alpha_n\beta_n L) + \frac{2}{L} \qquad \text{for } m = n$$

$$IX3 = \int_0^L (1-x/L)^2\,\Phi_m'\,\Phi_n'\,dx = \frac{4\beta_n^2\beta_m^2}{\beta_n^4-\beta_m^4}\left[\alpha_m\beta_m - \alpha_n\beta_n\right] +$$

$$\frac{16\beta_n^2\beta_m^2}{L(\beta_n^4-\beta_m^4)^2}\left[\beta_n^4 + \beta_m^4\right] \qquad \text{for } m \neq n$$

$$= \frac{3}{2L} + \frac{\alpha_n\beta_n}{3}\,(6 + \alpha_n\beta_n L) \qquad \text{for } m = n$$

$$IX4 = \int_0^L \Phi_m\,\Phi_n\,dx = 0 \qquad \text{for } m \neq n$$

$$= L \qquad \text{for } m = n$$

$$IX5 = \int_0^L (1-x/L)\,\Phi_m\,\Phi_n\,dx = \frac{8\alpha_n\alpha_m\beta_n\beta_m}{L(\beta_n^4 - \beta_m^4)^2}\left[2\,\beta_n^2\,\beta_m^2\right.$$

$$\left.-(-1)^{m+n}(\beta_n^4 + \beta_m^4)\right] \qquad \text{for } m \neq n$$

$$= \frac{L}{2} - \frac{2\alpha_n^2}{L\beta_n^2} \qquad \text{for } m = n$$

$$IX6 = \int_0^L (1-x/L)^2\,\Phi_m\,\Phi_n\,dx = \frac{32\alpha_n\alpha_m\beta_n^3\beta_m^3}{L(\beta_n^4 - \beta_m^4)^2} + \frac{8}{L^2(\beta_n^4\,\beta_m^4)^3}\left[\right.$$

$$(-1)^{m+n}\alpha_n\beta_n\,(\beta_n^8 + 12\,\beta_n^4\beta_m^4 + 3\,\beta_m^8) -$$

$$(-1)^{m+n}\ \alpha_m\beta_m\ (3\beta_n^8 + 12\beta_n^4\beta_m^4 + \beta_m^8) -$$

$$(10\beta_n^4 + 6\beta_m^4)\alpha_m\beta_n^2\beta_m^3 + (6\beta_n^4 + 10\beta_m^4)\alpha_n\beta_n^3\beta_m^2\Big]$$

for $m \neq n$

$$= \frac{L}{3} - \frac{5\alpha_n^2}{2\beta_n^2 L} + \frac{\alpha_n}{\beta_n^3 L^2} \qquad \text{for } m = n$$

$$IX7 = \int_0^L \Phi_m \Phi_n'' \, dx = \frac{4\beta_n^2(\alpha_n\beta_m\alpha_m\beta_n - \alpha_n\beta_n)}{\beta_m^4 - \beta_n^4}\Big[(-1)^{m+n}\beta_n^2 + \beta_m^2$$

for $m \neq n$

$$= \alpha_n\beta_n\ (2 - \alpha_n\beta_n L)\Big] \qquad \text{for } m = n$$

$$IX8 = \int_0^L (1-x/L)\ \Phi_m \Phi_n'' \, dx = \frac{4\beta_n^2\beta_m^2}{\beta_n^4 - \beta_m^4}\Big[\alpha_n\beta_n - \alpha_m\beta_m\Big]$$

$$+ \frac{4\beta_n^2}{L(\beta_n^4 - \beta_m^4)^2}\Big[(-1)^{m+n}\ \beta_n^2(\beta_n^4 + 3\beta_m^4)$$

$$- \beta_m^2(3\beta_n^4 + \beta_m^4)\Big] \qquad \text{for } m \neq n$$

$$= \frac{\alpha_n\beta_n}{2}\ (2 - \alpha_n\beta_n L) \qquad \text{for } m = n$$

$$IX9 = \int_0^L (1-x/L)^2 \, \Phi_m \Phi_n'' \, dx = \frac{4\beta_n^2\beta_m^2}{\beta_n^4 - \beta_m^4}\left[\alpha_n\beta_n - \alpha_m\beta_m\right]$$

$$\frac{-8\beta_n^2\beta_m^2}{L(\beta_n^4 - \beta_m^4)^2}\left[3\beta_n^4 - \beta_m^4\right] \qquad \text{for } m \neq n$$

$$= -\frac{1}{2L} + \frac{\alpha_n\beta_n}{3}(3 - \alpha_n\beta_n L) \qquad \text{for } m = n$$

$$IX10 = \int_0^L \Phi_m' \, \Phi_n'' \, dx = \frac{4\beta_n^3\beta_m\alpha_n\alpha_m}{\beta_m^4 - \beta_n^4}\left[\beta_m^2 - (-1)^{m+n}\beta_n^2\right]$$

$$\text{for } m \neq n$$

$$= 2\alpha_n^2\beta_n^2 \qquad \text{for } m = n$$

$$IX11 = \int_0^L (1-x/L) \, \Phi_m' \, \Phi_n' \, dx = \frac{-4\alpha_n\alpha_m\beta_n^3\beta_m^3}{\beta_n^4 - \beta_m^4} +$$

$$\frac{4\beta_m\beta_n}{L(\beta_n^4 - \beta_m^4)^2}\Big[(-1)^{m+n}(\beta_n^4 + 3\beta_m^4)\,\beta_n^3\alpha_m$$

$$-(-1)^{m+n}\,4\,\beta_n^4\beta_m^3\alpha_n +$$

$$\beta_n\beta_m^2\,\alpha_m(3\beta_n^4 + \beta_m^4) - 2\,\beta_m\beta_n^2\,\alpha_n(\beta_n^4 + \beta_m^4)\Big]$$

$$\text{for } m \neq n$$

$$= \alpha_n\beta_n\left(\frac{\alpha_n\beta_n}{2} + \frac{1}{L}\right) \qquad \text{for } m = n$$

$$IX12 = \int_0^L \Phi_m'' \Phi_n'' \, dx = 0 \qquad \text{for } m \neq n$$

$$= \beta_n^4 L \qquad \text{for } m = n$$

$$IX13 = \int_0^L (1-x/L) \, \Phi_m'' \Phi_n'' \, dx = \frac{8\alpha_m \alpha_n \beta_m^3 \beta_n^3}{L)\beta_n^4 - \beta_m^4)^2}$$

$$\left[(-1)^n \beta_n^2 - (-1)^m \beta_m^2 \right]^2 \qquad \text{for } m \neq n$$

$$= \beta_n^2 \left(\frac{\beta_n^2 L}{2} + \frac{2\alpha_n^2}{L} \right) \qquad \text{for } m = n$$

$$IX14 = \int_0^L (1-x/L)^2 \, \Phi_m'' \Phi_n'' \, dx = \frac{16 \alpha_m \alpha_n \beta_m^3 \beta_n^3}{L(\beta_n^4 - \beta_m^4)^2} \left[\beta_n^4 + \beta_n^4 \right] +$$

$$\frac{8\beta_m^2 \beta_n^2}{L^2(\beta_n^4 - \beta_m^4)^3} \left[(-1)^{m+n} \alpha_n \beta_n^3 \beta_m^2 (6\beta_n^4 + 10\beta_m^4) \right.$$

$$- (-1)^{m+n} \alpha_m \beta_n^2 \beta_m^3 (6\beta_m^4 + 10\beta_n^4) + \alpha_n \beta_n ($$

$$\beta_n^8 + 12\beta_n^4 \beta_m^4 + 3\beta_m^8) - \alpha_m \beta_m (3\beta_n^8 + 12$$

$$\left. \beta_n^4 \beta_m^4 + \beta_m^8) \right] \qquad \text{for } m \neq n$$

$$= \frac{\alpha_n \beta_n}{L^2} + \frac{\beta_n^4 L}{3} + \frac{3}{2} \frac{\alpha_n^2 \beta_n^2}{L} \qquad \text{for } m = n$$

$$IX15 = \int_0^L \Phi_m \Phi_n' \, dx = \frac{-4\beta_n^2}{\beta_n^4 - \beta_m^4} \left[\beta_m^2 - (-1)^{m+n} \beta_n^2 \right]$$

for $m \neq n$

$$= 2$$

for $m = n$

$$IX16 = \int_0^L (1-x/L) \, \Phi_m \Phi_n' \, dx = \frac{-4\beta_n^2 \beta_m^2}{\beta_n^4 - \beta_m^4}$$

for $m \neq n$

$$= \frac{1}{2}$$

for $m = n$

Note: The subscript n should be replaced by $\bar{m}$, but it is kept for the sake of clarity.

D.2. Cylinder circumferential integrals:

$$A1 = \int_0^{\pi} \cos n\theta \cos \bar{n}\theta \, d\theta$$

$$A2 = \int_0^{\pi} \cos n\theta \cos \theta d\theta$$

$$A3 = \int_0^{\pi} \cos \bar{n}\theta \cos \theta d\theta$$

$$A4 = \int_0^{\pi} \cos^2 \theta \, d\theta = \frac{\pi}{2}$$

$$A5 \int_0^{\pi} \sin n\theta \sin \bar{n}\theta \, d\theta$$

$$A6 = \int_0^{\pi} \sin n\theta \sin \theta d\theta$$

$$A7 = \int_0^{\pi} \sin \bar{n}\theta \sin \theta d\theta$$

$$A8 = \int_0^{\pi} \sin^2 \theta \, d\theta = \frac{\pi}{2}$$

$$A9 = \pi$$

$$A1 = A5 = 0 \quad \text{if} \quad n \neq \bar{n}$$

$$= \frac{\pi}{2} \quad \text{if} \quad n = \bar{n}$$

$$A2 = A6 = 0 \quad \text{if} \quad n \neq 1$$

$$= \frac{\pi}{2} \quad \text{if} \quad n = 1$$

$$A3 = A7 = 0 \quad \text{if} \quad \bar{n} \neq 1$$

$$= \frac{\pi}{2} \quad \text{if} \quad \bar{n} = 1$$

The following functions will be required to calculate the mass and stiffness matrices:

$$B1 = A1(IX14-IX11_a/L-IX11/L+IX1/L^2)+A2(IX13-IX10/L)$$
$$+A3(IX13-IX10_a/L) + A4\ IX12$$

$$B2 = n\bar{n}\ A5IX3 + nA6IX2 + \bar{n}\ A7IX2 + A8IX1$$

$$B3 = A9IX12$$

$$B4 = \bar{n}\ A1(IX9_a - IX16_a/L) + A2(IX8_a - IX15_a/L)$$
$$+ \bar{n}\ A3IX8_a + A4IX7_a$$

$$B5 = -\{nA5(IX3 - IX16_a/L) + A7(IX2 - IX15_a/L) + nA6IX2 + A8\,IX1\}$$

$$B6 = -\{nA1(IX9 - 2IX16/L) + A3(IX8 - 2IX15/L) + nA2IX8 + A4IX7\}$$

$$B7 = n\,\bar{n}^2\,A1IX6 + \bar{n}^2\,A31X5 + nA2IX5 + A4IX4$$

$$B8 = \bar{n}\,A5(IX3 - IX16/L - IX16_a/L + IX4/L^2) + \bar{n}\,A7(IX2 - IX15_a/L) + A6\,(IX2 - IX15/L) + A8IX1$$

$$B9 = A1IX6 + A2\,IX5 + A3\,IX5 + A4\,IX4$$

$$B10 = A1(IX14 - 2\,IX11_a/L - 2IX11/L + 4IX1/L^2) + A3(IX13 - 2IX10_a/L) + A2(IX13 - 2IX10/L) + A4\,IX12$$

$$B11 = -\{\bar{n}^2A1(IX9_a - 2IX16_a/L) + A2(IX8_a - 2IX15_a/L) + \bar{n}^2\,A3IX8_a + A4\,IX7_a\}$$

$$B12 = -\{n^2A1(IX9 - 2IX16/L) + A3(IX8 - 2IX15/L) + n^2\,A2IX8 + A4\,IX7\}$$

$$B13 = n^2\bar{n}^2A1\,IX6 + n^2A2\,IX5 + \bar{n}^2A3\,IX5 + A4\,IX4$$

$$B14 = n\,\bar{n}\,A5(IX3 - IX16_a/L - IX16/L + IX4/L^2) + nA6(IX2 - IX15/L) + \bar{n}\,A7(IX2 - IX15_a/L) + A8\,IX1$$

$$B15 = -\{A1(IX9_a - IX16_a/L) + A2(IX8_a - IX15_a/L) + A3\,IX8_a + A4\,IX7_a\}$$

$$B16 = n\,\bar{n}\,A1\,IX6 + nA2\,IX5 + \bar{n}\,A3\,IX5 + A4\,IX4$$

$$B17 = A5(IX3 - IX16_a/L - IX16/L + IX4/L^2) + A6(IX2 - IX15/L) + A7(IX2 - IX15_a/L) + A8\,IX1$$

$$B18 = -\{n\,A1\,IX6 + A3\,IX5 + nA2\,IX5 + A4\,IX4\}$$

$$B19 = A1\,IX3 + A2\,IX2 + A3\,IX2 + A4\,IX1$$

$$B20 = A9\,IX1$$

$$B21 = A5\,IX6 + A6\,IX5 + A7\,IX5 + A8\,IX4$$

$$B22 = -\{\bar{n}\,A1\,IX6 + A2\,IX5 + \bar{n}\,A3\,IX5 + A4\,IX4\}$$

$$B23 = -\{\bar{n}\,A1(IX9_a - 2\,IX16_a/L) + A2\,(IX8_a - 2IX15_a/L) + \bar{n}\,A3\,IX8_a + A4\,IX7_a\}$$

$$B24 = n^2\,\bar{n}\,A1\,IX6 + n^2\,A2\,IX5 + \bar{n}\,A3\,IX5 + A4\,IX4$$

$$B25 = nA5(IX3 - IX16_a/L - IX16/L + IX4/L^2) + nA6\,(IX2 - IX15/L) + A7\,(IX2 - IX15_a/L) + A8\,IX1$$

$$B26 = A9\,IX4$$

Note: The subscript "a" associated with the longitudinal integrals in the B's expression means interchanging m with n and vice-versus in the corresponding integral, i.e.:

$$IX9_a = \int_0^L (1-x/L)^2\,\Phi_m''\,\Phi_n\,dx$$

D.3. Symmetric case:

D.3.1. Stiffness matrix elements:

$$K11_{mn,\bar{m}\bar{n}} = 2R\left[\frac{Eh}{1-\nu^2}\,B1 + \frac{Gh}{R^2}\,B2\right]$$

$$K12_{mn,\bar{m}} = 0$$

$$K13_{mn,\bar{m}\bar{n}} = 2\left[\frac{Eh}{1-\nu^2}\,\nu(B4 + B15) + Gh\,B5\right]$$

$$K22_{m,\bar{m}} = 2R\,\frac{Eh}{1-\nu^2}\,B3$$

$$K23_{m,\bar{m}\bar{n}} = 0$$

$$K33_{mn,\bar{m}\bar{n}} = 2R\{\frac{Eh}{1-\nu^2}\,\frac{1}{R^2}\,(B9 + B16 + B18 + B22) + Gh\,B17$$

$$+ \frac{Eh^3}{12(1-\nu^2)}\left[B10 + \frac{\nu}{R^2}\,(B11 - B6 - B23 + B12)\right.$$

$$\left. + \frac{1}{R^4}\,(B16 - B7 - B24 + B13)\right]$$

$$+ \frac{Gh^3}{12R^2}\left[B17 - 2(B8 + B25) + 4\,B14\right]\}$$

D.3.2. Mass matrix elements:

$$M11_{mn,\bar{m}\bar{n}} = 2\rho RhB19 + \frac{(-1)^{m+\bar{m}}}{R^2}\,4\alpha_m\beta_m\alpha_{\bar{m}}\beta_{\bar{m}}\,(M_p l^2 + I_{YY_p})$$

$$M12_{mn,\bar{m}} = 0$$

$$M13_{mn,\bar{m}\bar{n}} = (-1)^{m+\bar{m}} \; 4\alpha_m \beta_m \frac{M_p}{R}$$

$$M22_{m,\bar{m}} = 2\rho Rh \; B20 + (-1)^{m+\bar{m}} \; 4\alpha_m \beta_m \alpha_{-}\beta_{-} M_p$$

$$M23_{m,\bar{m}\bar{n}} = 0$$

$$M33_{mn,\bar{m}\bar{n}} = 2\rho Rh \; (B21 + B9) + (-1)^{m+\bar{m}} \; 4 \; M_p$$

D.4. Antisymmetric case:

D.4.1. Stiffness matrix elements:

$$K11_{mn,\bar{m}\bar{n}} = 2R\left[\frac{Eh}{1-\nu^2} \; B1 + \frac{Gh}{R^2} \; B2\right]$$

$$K12_{mn,\bar{m}} = 0$$

$$K13_{mn,\bar{m}\bar{n}} = 2\left[\frac{Eh}{1-\nu^2} \; \nu(B4 - B15) - GhB5\right]$$

$$K22_{m,\bar{m}} = 2RGh \; B20 \; (1 + \frac{h^2}{12R^2})$$

$$K23_{m,\bar{m}\bar{n}} = 0$$

$$K33_{mn,\bar{m}\bar{n}} = 2R\{\frac{Eh}{1-\nu^2} \; \frac{1}{R^2} \; (B18 + B9 + B16 + B22)$$

$$+Gh \; B17 + \frac{Eh^3}{12(1-\nu^2)}\left[B10 + \frac{\nu}{R^2} \; (B11 - B6\right.$$

$$\left. - B23 + B12) + \frac{1}{R^4} \; (B16 - B7 - B24 + B13)\right]$$

$$+ \frac{Gh^3}{12R^2}\left[B17 - 2(B8 + B25) + 4 \; B14\right]\}$$

D.4.2. Mass matrix elements:

$$M11_{mn,\bar{m}\bar{n}} = 2\rho hR\, B19 + \frac{(-1)^{m+\bar{m}}\, 4\alpha_m \beta_m \alpha_{\bar{m}} \beta_{\bar{m}}}{R^2} (M_p l^2 + I_{ZZ_p})$$

$$M12_{mn,\bar{m}} = 0$$

$$M13_{mn,\bar{m}\bar{n}} = (-1)^{m+\bar{m}}\, 4\alpha_m \beta_m \frac{M_p l}{R}$$

$$M22_{m,\bar{m}} = 2\rho hRB26 + (-1)^{m+\bar{m}} \frac{4\, I_{XX_p}}{R^2}$$

$$M23_{m,\bar{m}\bar{n}} = 0$$

$$M33_{mn,\bar{m}\bar{n}} = 2\rho hR\,(B9 + B21) + (-1)^{m+\bar{m}}\, 4\, M_p$$

APPENDIX E

Elements of The Force Vector

This Appendix presents the expanded form of the generalized force vector, $\{Q\}$, previously given in equation 3.57 Chapter three.

$$Q_{mn}^{us} = (-1)^{m+1} \, 2 \, \alpha_m \beta_m \, \frac{M_p \, g \, l}{R}$$

$$Q_m^{uA} = 0$$

$$Q_{mn}^{sc} = (-1)^{m+1} \, 2 \, M_p \, g$$

where g is the gravitational acceleration.

REFERENCES

1. Rayleigh, Lord. — The Theory of Sound. Dover Publications, 1945

2. Morse, P.M. — Vibration and Sound. 2nd ed. McGraw-Hill Book Company, New York, 1948

3. Kinsler, L.E. and Frey, A.R. — Fundamentals of Acoustics John Wiley & Sons, New York, 1962

4. Harris, C.M.(Ed.) — Handbook of Noise Control. McGraw-Hill Book Company, New York, 1957

5. Beranek, L.C. — Noise Reduction. McGraw-Hill Book Company, New York, 1960

6. Crook, A. and Heron, R.A. — "Air Borne Noise From Hydraulic Lines due to Liquid Borne Noise". Research Project Seminar on Quiet Oil Hydraulic System. The Inst. of Mech. Eng., London, Nov. 1977.

7. Henderson, A.R. — "Measuring the Performance of Fluid Borne Noise Attenuations". Research Project Seminar on Quiet Oil Hydraulic System. The Inst. of Mech. Eng., London, Nov. 1977.

8. Foster, K. and Hannan, D.M. — "Fundamental Fluid Borne and Air Borne Noise Generation of Axial Piston Pumps" Research Project Seminar on Quiet Oil Hydraulic System. The Inst. of Mech. Eng., London, Nov. 1977.

9. Heron, R.A. and Hansford, I. — "Air Borne Noise due to Structural Borne Vibrations Transmitted Through Pump Mountings and Along Circuits" Research Project Seminar on Quiet Oil Hydraulic System. The Inst. of Mech. Eng., London, Nov. 1977.

10. Richards, T.H. — Energy Methods in Stress Analysis. Ellis-Horwood Series in Engineering Science, London, 1977.

11. Meirovitch, L. — Analytical Methods in Vibration. McGraw-Hill Book Company, New York, 1970.

12. Timoshenko, S.P. and Woinowsky-Krieger, S. — Theory of Plates and Shells. 2nd ed., McGraw-Hill Book Company New York, 1959.

13. Timoshenko S.P. and Goodier, J.N. — Theory of Elasticity. 3rd ed., McGraw-Hill Book Company, New York, 1970.

14. Fung, Y.C. and Sechler, E.E.(Ed.) — Thin-Shell Structures. Theory, Experiment and Design. Prentice Hall, Inc. Englewood Cliffs, 1974

15. Love, A.E.H. — A Treatise on The Mathematical Theory of Elasticity. 4th ed., Dover Publications, 1944.

16. Donnell, L.H. — "A Discussion of Thin Shell Theory" Proc. Fifth Intern.Congr.Appl.Mech., 1938

17. Mushtari, Kh.M. — "Certain Generalizations of the Theory of Thin Shell". Izv. Fiz.Mat. ob-va. pri kaz.un-te., Vol.11 No.8. 1938.

18. Flugge, W. — Stresses in Shells. Springer-Verlag (Berlin), 1962.

19. Novozhilov,V.V. — The Theory of Thin Elastic Shells. P.Noordhoff Ltd (Groningen,The Netherland), 1964.

20. Sanders, J.L.,Jr. — "An Improved First Approximation Theory For Thin Shells" NASA TR-R24, 1959

21. Naghdi, P.M., and Berry, J.G. — "On the Equations of Motion of Cylindrical Shells", J. Appl.Mech., Vol.21, No.2, pp.160-166, June 1964.

22. Reissner, E. — "A New Derivation of the Equations of the Deformed Elastic Shells". Amer.J.Math.,Vol.63, No.1, pp.177-184 Jan. 1941.

23. Vlasov, V.Z. — Obshchaya teoriya obolchek; yeye prilozheniya v tekhnike Gos.Izd. Tekn-Teor.Lit., Moscow-Leningrad, 1949. (English transl.NASA TTF-99 General Theory of Shells and Its Applications in Engineering, Apr. 1964)

24. Kadi, A.S. "A Study and Comparison of the Equations of Thin Shell Theories" Ph.D. Dissertation, Ohio State University, 1970.

25. Reismann, H. "Forced Motion of Cylindrical Shells". Rept. No.9, School of Engineering, New York State University at Buffalo, Dec. 1965.

26. Warburton, G.B. "Comments on Vibration Studies of a Ring-Stiffened Circular Cylindrical Shell" J.Sound and Vibration, Vol.9, No.2, pp.349-353, 1969.

27. Forsberg, K. "Influence of boundary conditions on the modal characteristics of Thin Cylindrical Shells" AIAA Journal, Vol.2, No.12, pp.2150-2157, Dec.1964.

28. Resnick, B.S., and Dugundji, J. "Effects of Orthotropicity, Boundary Conditions, and Eccentricity on the Vibrations of Cylindrical Shells". AFOSR Sci, Rept. AFOSF 66-2821, ASRL TR 134-2 (AD648077), Nov. 1966.

29. Ramamurti, V. and Pattabirama, J. "Free Vibrations of circular cylindrical shells". J.Sound and Vibration, Vol. 48(1), pp 137-154, 1976.

30. Mikulas, M.M. and McElman, J.A. "On Free Vibrations of Eccentrically Stiffened Cylindrical Shells and Plates" NASA - TN - D - 3010, Sept.1965.

31. Egle, D.M. and Sewall, J.L. "An Analysis of Free Vibration of Orthogonally Stiffened Cylindrical Shells with Stiffeners Treated as Discrete Elements" A.I.A.A. Journal. Vol.6, No.3, pp 518-526, March 1968

32. Wah, T. and Hu, C.L. "Vibration Analysis of Stiffened Cylinders including Inter-Ring Motion". J.Acou.Soc. of Amer. Vol.43, No.5, pp 1005-1016, 1968.

33. Pattabiraman, J. Ramamurti, V. and Reddy, D.V. "Static and Dynamics of Elastic Shells with cutouts - A Review". Jou. of Ship Research, Vol.18, No.2 pp 113-126 June 1974.

34. Forsberg, K., Brogan, F. and Smith, S. "Experimental and Analytical Investigation of the Dynamic Behaviour of a Cylinder with a Cutout". AIAA/ASME 9th Structures, Structural Dynamics and Materials Conference Palm Springs, Calif., April, 1968.

35. Olson, M.D. and Lindberg, G.M. "Vibration Analysis of Cantilivered Curved Plates Using a New Cylindrical Shell Finite Element". Conf. on Matrix Methods in Structural Mechanics, Wright-Patterson Air Force Base, Dayton, Ohio, AFFDL-TR-68-150, 1968.

36. Holmes, W.T. "Axisymmetric Vibrations of a Conical Shell Supporting a Mass". J.Acou.Soc. of Amer., Vol.34 No.4. pp 458-461, April, 1962.

37. Young, D. and Felgar, R.P.Jr. "Tables of Characteristic Functions Representing Normal Modes of Vibration of a Beam". Publ. No.4913, Eng.Res., No.44, Bur.Eng. Res., University of Texas, July, 1949.

38. Felgar, R.P.Jr. "Formulas For Integrals Containing Characteristic Functions of Vibrating Beam" Cir.No.14, Bur.Eng.Res., University of Texas, 1950.

39. Huffington, N.J.Jr. and Schumacher,R.N. "Flexure of Parallel Stiffened Plates" RR-59, Research Dept.,Martin Co., Baltimore, Md., Jan.1965.

40. Tang. S.C. "Response of a Finite Tube to Moving Pressure" J.Eng.Mech. Div.,Proc.Amer. Soc.Civil Engrs., Vol.93 EM3, pp 239-256. June 1967.

41. Reismann, H. and Medige, J. "Forced Motion of Cylindrical Shells" Proc. of Amer.Soc. Civil Engrs., EM5, pp 1167-1182, Oct.1968.

42. Wilkinson, J.H. The Alegebraic Eigen value Problem. Oxford Clarendon Press, P.337, 1965.

43. Nyholm, G.E. "Computer Solution of the Eigen value Problem in Vibration Analysis" M.Sc. Thesis, The University of Aston in Birmingham, Nov. 1979.

44. Sewall, J.L. and Pusey, C.G. "Vibration Study of Clamped-Free Elliptical Cylindrical Shells" AIAA Jour. pp 1004-1011, June 1971.

45. Park, A.C. et al "Dynamics of Shell-Like Lifting Bodies, Part II. The Experimental Investigation" Tech.Rept. AFFDL-TR-65-17 Part II, Wright-Patterson AFB, Ohio, June 1965.

46. Boyd, D.E. and Rao. C.P. "A Theoretical Analysis of the Free Vibration of Ring and/or Stringer-Stiffened Elliptical Cylinders With Arbitrary End Conditions" NASA CR-2151, Feb.1973.

47. Ucmaklioglu, A. "Vibration of Shells with Application to Hollow Blanding". Ph.D. Thesis, Dept. of Engineering Science, University of Durham, Sep. 1978

48. Gill, P.A.T. "Vibrations of Clamped-Free Circular Cylindrical Shells" J.Sound and Vibration, Vol.25(3) pp 5o1-5o3, 1972.

49. Sharma, C.B. and Johns, D.H. "Vibration Characteristics of Clamped-Free and Clamped-Ring Stiffened Circular Cylindrical Shell" J.Sound and Vibration, Vol.14, pp 459-474, 1971.

50. Sewall, J.L. Clary, R.R. and Leadbetter, S.A. "An Experimental and Analytical Vibration Study of a Ring-Stiffened Cylindrical Shell Structure with Various Support Conditions" NASA TN D-2398 Aug. 1964.

51. Forsberg, K. "Exact Solution for Natural Frequencies of Ring Stiffened Cylinders". AIAA/ASME 10th Structures, Structural Dynamics and Material Conference, New Orleans, Louisiana, April, 1969.

52. Sharma, C.B. and Johns, D.J. "Vibration Characteristics of Clamped-free and Clamped-Ring Stiffened Circular Cylindrical Shells: A Theoretical Analysis" TT 7001, Dept. of Transport Technology, Loughborough University of Tech., Jan. 1970.

53. Sewall, J.L. and Naumann, E.C. "An Experimental and Analytical Vibration Study of Thin Cylindrical Shells with and without longitudinal stiffeners" NASA TN D-4705, Sep. 1968.

54. Egle, D.M. and Soder, K.E. "Theoretical Analysis of the Free Vibration of Discretely Stiffened Cylindrical Shell with Arbitary End Conditions" NASA CR - 1316, June 1969.

55. Mahabaliraja and Boyd, D.E. "Vibrations of Stiffened Cylinders with Cutouts" J.Sound and Vibration, Vol.52(1) pp 65-78, 1977.

56. Toda, S. and Komotsu, K. "Vibrations of Circular Cylindrical Shells with Cutouts" J.Sound and Vibration Vol.52(4) pp 497-510, 1977.

57. Ramamurti, V. and Pattabiraman, J. "Dynamic Behaviour of a Cylindrical Shell with a Cutout" J.Sound and Vibration, Vol.52(2), pp 193-200, 1977.

58. Brogan, F., Forsberg, K. and Smith, S. "Dynamic Behaviour of a Cylinder with a Cutout" AIAA, Vol.7, pp 903-911, 1969.

59. Mirsky, I. and Herrmann, G. "Axially Symmetric Motions of Thick Cylindrical Shells" J.Appl.Mech., Vol.25, No.1. pp 97-103, Mar. 1958.

60. Meriam, J. Dynamics. 2nd ed. John Wiley & Sons Inc., 1977.

61. Harris, C.M. and Crede, C.E.(Ed.) Shock & Vibration Handbook. 2nd ed. McGraw-Hill Book Company, New York, 1976.

62. Private Communication Dr. R. Taylor
Department Mech.Eng. University of Aston in Birmingham.